National Technical University of Athens

School of Naval Architecture and Marine Engineering
Laboratory of Marine Engineering

Diploma Thesis

Development of a Semi-Empirical Combustion Model for a Dual Fuel Four-Stroke Diesel-Methanol Marine Engine

Theofilopoulos Panagiotis

Supervisor: Assistant Prof. George Papalambrou

Committee Member: Prof. L. Kaiktsis
Committee Member: Assistant Prof. C.I. Papadopoulos

Athens, July 2021

Acknowledgments

This diploma thesis has been carried out at the Laboratory of Marine Engineering (LME) at the School of Naval Architecture and Marine Engineering of the National Technical University of Athens, under the supervision of Assistant Professor George Papalambrou.

First of all, I would like to thank Assistant Professor George Papalambrou who accepted me to conduct this thesis at the LME and gave me the chance to work in a very interesting topic. I would also want to thank him for his patience, understanding, support and his knowledge that shared with me.

I also want to thank Doctoral Student Vasileios Karystinos for his immediate responses, patience and understanding that showed to me. I also thank him for his motivation, assistance and support during the diploma thesis development and I am very grateful for this cooperation.

I am also sincerely grateful to Professor Lambros Kaiktsis and Assistant Professor Christos (I.) Papadopoulos for evaluating my work and being a member of my supervisors committee.

I would like to express my gratitude to my family, for the encouragement, support, motivation and understanding throughout my studies and my diploma thesis.

I finally am grateful to each and everyone who support me and contributed with its own way to accomplish this work. Thank you.

Abstract

In recent years, the environmental pollution has become a major issue and efforts are being made to find a solution.

In this respect, Dual fuel engines have been evolving in recent years with the aim of reducing pollutant emissions and meeting the demand of the upcoming emissions regulations.

In this thesis was developed a combustion model in order to estimate the Heat Release Rate and the In-Cylinder Pressure of a Dual-Fuel Internal Combustion Marine Engine fueled by Methanol in combination with Pilot Injection of Diesel.

Based on data from papers and experiments taken from bibliography, firstly an Ignition Delay model was investigated to predict the Start of Combustion.

Subsequently, in order to estimate the Heat Release Rate, was selected a zero-dimensional and semi-empirical approach. Triple Wiebe functions were investigated, whose parameters were fitted using the experimental data. Furthermore, polynomial fit was applied in order to develop models for the Wiebe Parameters.

The Heat Release Rate Model mentioned above was validated through data from bibliography that wasn't used in the model development, in order to verify its prediction capability.

Ultimately, the in-cylinder Pressure was predicted using the Heat Release Rate Model and the first law of Thermodynamics and was validated from experimental data.

List of Figures

List of Tables

Contents

Chapter 1

Introduction

1.1 Thesis Objective

In recent years, the environmental pollution and the energy security have come to the foreground. The heavy usage of non-renewable resources and especially petroleum and fuels, for the production of electricity, thermal heat or for the movement of people and goods, has caused mitigation of energy sources stocks, creating a big concern about the imminent future. In addition, the way of using these resources is not so efficient, especially in the past few years. With dwindling of oil resources, the energy crisis is getting worse, especially in the countries with limited oil resources like China [6]. Moreover, diesel and gasoline engines, that are in use nowadays, produce harmful emissions for the environment and the atmosphere, contributing to the greenhouse effect.

Consequently, the saving of non-renewable resources, the development of the methods of using these resources in order to be more efficient and generally the protection of the planet, has become a topic of research. In this respect, this thesis participates in the work of finding alternative methods to produce the power that ships need to sail, through the examination of the combustion that take place inside a dual-fuel diesel-methanol marine engine.

In this diploma thesis, a semi-empirical combustion model is examined in order to estimate the Heat Release Rate and the in-cylinder Pressure of a Dual-Fuel Four Stroke Marine Engine, fueled by Methanol with Pilot Injection of Diesel.

1.2 Shipping Sector and Environment

Marine sector and merchant shipping specialize in the transportation of goods in large quantities, keeping the operational cost low. However is one of the main contributor in air pollution because of the Nitrogen Oxides (NOx), Sulfur Oxides (SOx) and Particulate Matters (PM) emissions, both in the open sea and in the port. Recent reviews have indicated that 50% of the NOx emissions in ports and coastal regions comes from marine diesel engines and that ocean-going vessels produce approximately 20 million tonnes of NOx, 10 million tonnes of SOx and 1 million tonnes of PM annually [7]. As for the greenhouse gases (GHG), it is mentioned that 15% of NOx , 4-9% of Sulfur Dioxide (SO_2) and 2.7% of Carbon Dioxide (CO_2) of the global atmospheric pollution are emitted by marine diesel engines [8].

NOx emissions contribute in the formation of smog and acid rain and SOx emissions cause acid rain as well, and are harmful for the health of humans and trees[9].

Due to the high necessity of a low cost and low quality fuel for shipping activities, Heavy Fuel Oil (HFO) is used in large quantities causing the consumption of 60 million barrels of crude oil every year [7].

The air pollution is a major issue and has concerned the International Maritime Organization (IMO) and governments around the globe. In this respect, MARPOL has set legislation for NOx emissions (according to MARPOL Annex VI) and more specifically has published Tier I (after 2000), Tier II (after 2011) and Tier III (after 2016). Additionally specific areas have been appointed as Emission Control Areas (ECA) where there are strict limitations and regulations in SOx or NOx emissions. It is worth mentioning that Tier I and II limits are global unlike Tier III that apply only to NOx ECA [7]. The sulfur content limit of marine fuels in SOx emission control areas (SECAs) decreased from 1.5% to 1% and to 0.1% in 2015, and the maximum value globally declined from 4.5% to 3.5% and to 0.5% in 2020 [7]. As SECAs have been already designated the Baltic Sea, the North Sea and the English Channel and it is expected to be designated the Mediterranean Sea as well [8]. Additionally have been made mandatory the Energy Efficiency Design Index (EEDI) for the new vessels and the Ship Energy Efficiency Management Plan (SEEMP) for all ships[10]. The EEDI provides a specific figure for an individual ship design, expressed in grams of carbon dioxide (CO2) per ship's capacity-mile (the smaller the EEDI the more energy efficient ship design) [9].The general aim of IMO is to reduce the total annual GHG emissions from shipping by at least 50% by 2050 compared to 2008 levels[10].

As a result, because of the strict legislation for the ships emissions and

due to the mitigation of fossil fuels and non-renewable resources, it is under investigation some alternative ways for the propulsion of ships in order to be more efficient and more friendly for the environment. These includes modifications and new designs in the components of engines, differentiation in the combustion process and research about alternative fuels as a substitute of conventional fuels with a view to their more ecological production and the less pollutant emissions during their combustion. Some of the most promising alternative solutions as fuels for marine engines are Hydrogen, Bio-diesel, LNG and Methanol.

1.3 Methanol as an Alternative Fuel

As mentioned before, one of the most promising alternative fuel for use in shipping industry is Methanol. It is among the top traded chemicals around the world and it is used for production of adhesives, paints, LCD screens, silicones, pharmaceuticals, and also used by the wood and automotive industry [11]

In other words, there is already large scale production and infrastructure. More specifically, 70 million metric tons produced in 2015 and a global production capacity of about 110 million metric tons [11]. Moreover, there is a 20 million tons annual production of methanol as fuel or fuel blend [11] and as a result an investigation for conventional fuels replacement by methanol is ongoing.

From an economic view, on July 2021 methanol costs 410 Euro/MT (484 USD/MT) in Europe, 420 USD/MT in Asia Pacific and 542 USD/MT in North America [12]. On the other hand, on July 2021, Very Low Sulfur Fuel Oil (VLSFO) costs 527.5 USD/MT in Rotterdam, 577.5 USD/MT in Asia Pacific and 612 USD/MT in America [13]. As a result, Methanol is cheaper than VLSFO.

1.3.1 Existing Methods of using Methanol as Fuel

The use of methanol as fuel for power production is not something new. In Motor Racing had been realized its performance-enhancing attributes and had been used blends of methanol and benzene in Grand Prix cars as a method to maximize the engine performance [11].

Aviation also had used methanol as knock suppressant but only on take-off and to an extent when maximum power was required [11].

The vehicle technology was developed as well, since the M85 (85% Methanol and 15% gasoline by volume) had been used by 15000 vehicles, buses and

trucks in the California methanol fuel trial in the 1980s and 1990s which was driven primarily by air quality considerations. Methanol caused significantly lower unburned hydrocarbons (UHC) and oxides of nitrogen (NOx) emissions than typical gasolines in use at the time [11].

1.3.2 Production of Methanol

Methanol can be produced both with conventional and renewable methods by coal, natural gas[14], coke-oven gas or waste biomass such as crop residues, forage, grass, crops, wood resources, forest residues, short rotation wood energy crops and lignocellulosic components of municipal wastes [15]. Methanol was traditionally made from wood, hence one of its common names, 'wood alcohol'[11]. In fact, methanol can be made from any material that can be decomposed into hydrogen and carbon monoxide (CO) or carbon dioxide (CO_2) [14].

The current production of methanol consists of three steps. The first is the production of synthesis gas (syn-gas), a mixture of CO, H2 and CO2. The most common syn-gas production is by reforming of natural gas, but it can also be obtained from other carbon-based materials. The second step is the conversion of the syn-gas to methanol and the final step is distillation[11].

1.3.3 Methanol Characteristics

Methanol, is a simple oxygenated hydrocarbon [11] whose molecule is:

$$CH_3OH$$

and it's density is $791.3 kg/m^3$ at 20 ^oC [16]. It contains oxygen atom and has no carbon–carbon double bond, thus resulting in less PM formation when an engine fuels with methanol fuel [15]. Methanol has high specific energy ratio (i.e. energy per unit of fuel-air mixture),high flame speed, high molar expansion ratio (Ratio of number of moles of products to the reactants) and low combustion temperature. High latent heat of evaporation is one of the characteristics of Methanol. In particular,it has 3.5 times higher than that of diesel [14].Thus, can reduce the intake air temperature, and the in-cylinder combustion could be influenced especially at low engine speed and load [6]. Methanol is a low-reactivity fuel due to its low cetane number and due to its 50% contamination of oxygen in its molecule can reduce the NOx and smoke emissions [14]. Thus special measures are needed to enable the use of methanol in compression ignition (CI) engines [11]. The oxygen content, amounting to half of methanol's molecular mass, leads to

a low (mass-based) stoichiometric air requirement (air/fuel ratio, AFR) and the fraction of methanol in a stoichiometric mixture is high [11]. It is worth mentioning that the high heat of vaporization, combined with low stoichiometric air/fuel ratio, leads to high degrees of intake charge cooling as the fuel evaporates [11]. Methanol is characterized by high hydrogen-to-carbon ratio and the fact that it is higher than that of gasoline, methanol has 7% lower specific CO2 emissions compared to gasoline.

One of the most important and useful characteristics of methanol is that is liquid at standard temperature and pressure conditions (STP) [11] due to the hydrogen bonding which gives rise to the formation of quasi-super molecules, or cyclic tetramers [11]. As a result, the storage, transportation, distribution, and application of methanol are similar to those of traditional gasoline and diesel fuels as a liquid [17]. Methanol (such as ethanol) is simply biodegradable and as a result doesn't cause environmental issues [11]. Methanol's density is higher than that of gasoline and has a heating value less than half that of gasoline. Thus the volumetric energy content is half that of gasoline and consequently injection duration need to be twice as long in order to introduce the same energy into the engine. This also implies larger fuel tanks are needed for a similar range [11]. Methanol's polarity also causes a low vapor pressure causing more difficult a cold start [11]. When methanol is introduced in the engine's intake port, this can lead to very low temperatures caused from methanol's evaporation [11]. Methanol-air mixtures have a higher laminar burning velocity than gasoline[11]. Having a single carbon atom it cannot easily form the carbonaceous particulate matter common from long-chain hydrocarbons [11]. Methanol is a polar molecule as is water, hence its infinitely miscibility with water and that it can also absorb water from atmosphere [11].

However, the use of methanol as an alternative fuel in internal combustion engines , has some drawbacks that are worth to be mentioned. Initially,the foremost drawback for the utilization of methanol in diesel engines is probably its low cetane number, which, depending on the measurement method, typically ranges from 2 to 12 [17]. The much high latent heat of vaporization also weakens its auto-ignition ability [17]. Methanol and diesel are two fuels with different reactivity, and there is interaction between the two fuels especially under low temperature oxidation. So the ratio between methanol and diesel might have a huge impact on the ignition and combustion process [14].

1.3.4 Methanol's Health and Safety Concerns

Methanol is one dangerous and toxic substance, as this is true for all fuels being considered as gasoline and diesel substitutes. The major issue of alcohols - and especially methanol - is the toxicity in ingestion, skin, eye contact or inhalation. Although it is readily metabolized in small amounts by the human body, on account of it being found naturally in fruit and vegetables and therefore not rejected by the body as an alien substance, methanol toxicity arises as a result of overloading the digestive system. When this occurs, the concentration of the toxic intermediary products formaldehyde and formic acid becomes too high, and this is what causes damage. Reported fatal doses when untreated are between 1 and 2 ml per kg body weight. This would correspond to 60-240 ml for a typical range of body weights[11].

Methanol is not readily ignitable below 10 ^oC.

Although, methanol flames are practically invisible in sunlight, pure methanol fires can be extinguished with water[11].

The rapid biodegradation property of methanol also makes it attractive as marine fuel, since any spill quickly disperses due to its infinite solubility in water, and then biodegrades simply [11].

1.3.5 Methanol in Internal Combustion Engines

Methanol as a possible alternative fuel is under investigation for use in internal combustion engines.

There are three methods that methanol could be used as fuel: as blend, neat methanol (pure methanol) or in dual fuel mode [17]. The blending of methanol with diesel fuel requires additives for stabilizing the mixed fuel and there is a limitation on the amount of methanol that can be premixed with diesel fuel for stable operation. Actually, the diesel–methanol blending has been made possible only by the addition of surfactants in order to form micro-emulsions, rather than real solutions. The use of neat methanol in diesel engines usually requires the addition of relatively large amount of expensive ignition improving compounds and very high compression ratios. Dual fuel combustion seems to be the most feasible solution due to its excellent performance and ultra-low emissions compared to conventional diesel combustion. In dual fuel combustion is used a high cetane number fuel such as diesel or biodiesel to ignite a low cetane number fuel such as methanol [17].

As mentioned above, the most promising way to use methanol as fuel is in diesel methanol dual fuel (DMDF) mode in one of the following methods: separate fuels direct injection, dual fuel injection or fumigation method.

The use of two separate fuels injection system is more complicated because it involves significant engine modifications as the methanol injector is placed at the top of combustion chamber[17]. Methanol can be injected directly in the combustion chambers, similar to the diesel injection. The diesel injection then serves as a pilot fuel for igniting the methanol. This concept is a commercial reality today, used by MAN for low-speed two-stroke engines and Wärtsilä for medium-speed four-stroke engines. In the case of the Wärtsilä medium-speed engine, injectors are used with a central diesel nozzle and 3 methanol nozzles equally positioned around the diesel nozzle, within the same injector body. Methanol is injected at 600 bar. The MAN two-stroke engine uses separate injectors for diesel and methanol, adding 2 methanol injectors that inject methanol at around 500 bar. In both engines, a separate hydraulic oil circuit is used to actuate the methanol injectors and high pressure methanol pumps are needed, which are expensive due to methanol's low lubricity and high corrosivity[11].

Using only one injector to inject two fuels in an engine is only reported by the system developed by Westport Corp., called HPDI[17]. This has the advantage that only one injector is needed and the engine conversion is relatively straightforward. However methanol's low lubricity compared to diesel might necessitate lubricating additives[11].

In this regard, fumigation is favored currently, because it requires a minimum of modification to the engine since methanol injectors is placed at the intake manifold[17] and a low pressure methanol fueling system and port fuel injectors are necessary [11]. However methanol fumigation is unfavorable for cold start and low load operation [17]. With the method of fumigation has been developed a diesel/methanol compound combustion (DMCC) system where at cold start and low speed conditions, the engine operates on diesel alone to ensure cold starting capability and to avoid aldehydes production under these conditions. At medium to high loads, the engine operates on diesel methanol dual fuel (DMDF) mode, of which methanol is fumigated into intake manifold and the homogeneous air/methanol mixture is ignited by the diesel directly injected. As a result, there is no difficulty in cold start and in case of lacking methanol fuel supply, this engine still runs according to the diesel cycle by switching from dual fuel mode to pure-diesel mode [17]. Methanol fumigation seems to be a promising method for the application of methanol on diesel engine [15]. Diesel methanol dual fuel (DMDF) led to an increase in HC and CO emissions, while the NOx and PM emissions reduced simultaneously [15].

Methanol does produce hydrocarbon emissions at a similar level to gasoline and its combustion characteristics and single-carbon-molecule nature mean that its emissions of oxides of nitrogen and particulate matter are sig-

nificantly lower than for complex hydrocarbon fuels [11]

Alcohols such as methanol have also been used in diesel applications but CI Engines require more significant modifications than SI Engines [11].

Furthermore, the material compatibility need to be taken into account. Methanol and generally light alcohols are more corrosive to both ferrous and non-ferrous metals than gasoline. They can be extremely aggressive toward magnesium, aluminum and copper but steel and other ferrous metals are usually only slightly affected. Methanol is electrically conductive and tanks, pumps, lines and spigots should be alcohol-compatible [11].

1.3.6 Methanol in Shipping Industry

Due to the high contribution of marine industry in air pollution and the emission legislations, methanol is investigated to replace conventional fuels such as diesel and HFO [11].

Initially, the focus was mostly on liquified natural gas (LNG). However, as it will be mentioned later in this thesis, LNG storage system is more complicated and methanol, as it is liquid at STP conditions, is an easier fuel to handle and store. Furthermore, its safety characteristics and its emissions compared to the bunker fuel or heavy fuel oils that large ships currently generally use, favor the use of methanol[11].

However, one of the most important reasons that makes methanol a very strong candidate alternative fuel, is its miscibility in water. Thus, double hull vessels, such as tankers and carriers that transport hydrocarbons (as they are not mix with water), could be modified and store the methanol fuel for combustion in void spaces because in case of a leak or breach there is no hazard for environmental pollution as methanol dilutes so rapidly that dangerous concentrations are never reached[11].

1.3.7 LNG vs Methanol

Recent technical report from the EU's Joint Research Centre concluded that LNG and methanol seem to be the most promising alternative fuels for shipping at the moment. This is partly based on methanol's availability in most large ports[11].

Another reason that LNG is a promising alternative fuel is because of the evaporation of LNG in LNG Carriers and because it is efficient to use the evaporated LNG somehow. As a result, LNG DF engines have been developed for LNG Tankers. However, making provisions for a liquified gas storage system has substantial effects on ship design or retrofits[11].

On the other hand, methanol is much safer in use than LNG because it is a liquid at STP and the (net) volumetric LHV is approximately 23% lower (15.9 vs. 20.5 MJ/l)[11]. Moreover, methanol is more easily stored aboard a vessel without the attendant storage complications arising from cryogenic storage of a gas. The flash point of methanol is much lower than that of LNG and the flammability index of methanol is in fact much closer to that of diesel. Finally, in case of a pool fire methanol is more safe than either gases or liquid hydrocarbons[11]

1.4 Dual Fuel Engines

1.4.1 History of Dual Fuel Engines

Dual Fuel (DF) engines have been evolving in recent years with the aim of reducing pollutant emissions and meeting the demand of the upcoming emissions regulations in shipping sector.

However, this method of power production and generally the use of gas as fuel in internal combustion engines has been invented many years ago and before 19th century. The first successful attempt to use gaseous fuels in engines was by the Belgian Engineer Étienne Lenoir in 1860. After that, researches have been made in 1867 by two German engineers, Nikolaus August Otto and Eugen Langen, in order to evolve this concept. These engineers investigated the use of gas and air mixture and its ignition using a pilot flame burning. Some years later the German engineer Rudolf Christian Karl Diesel investigated the injection of the pilot fuel into the compressed gas and air mixture. In this way, he could achieve immediate ignition of fuel and as a result he introduced the concept of using a high reactive fuel to ignite a low reactive one. As it can be easily understood, the complexity of such an engine was too high, hence the difficulty for commercial use. One of the first use of DF engines and their use for marine propulsion was in world war two. After that, DF engines are under investigation and due to the imminent legislation about the air pollution seem to be more and more attractive [9].

1.4.2 Existing Use of Dual Fuel Engines

Dual Fuel engines have already found their use in many applications. There are stationary installations where DF engines are used for power production, co-generation, compression of gases and pumping duties. In transportation there are a few applications in trucks, buses, vans and taxis. Finally, Agricultural Industry and Marine transportation has already some applications of DF engines in cargo ships, ferries and fishing vessels [5].

1.4.3 Dual Fuel Technologies

The name "Dual Fuel" engines implies that there is use of two fuels for the combustion of an engine. This is the main idea of the DF concept. A DF engine, from mechanical view, is a conventional diesel compression-ignition engine, whose total heat release comes from two separate sources - the two fuels.

It needs to be mentioned that bi-fuel applications differ from dual fuel engines [5]. In these applications, the engine have the ability to combust two different fuels but only one at a time. In other words, these engines have two separate ways to produce power, with different fuels.

There are two predominant Dual Fuel Technologies. The first one and the most common used is the injection of a small quantity of diesel liquid fuel to create the friendly conditions for the ignition of the main fuel or a mixture of a gaseous fuel in the air. The injection of a small quantity of fuel is called "pilot injection" and is used to ignite a mixture with weak auto-ignition ability [5].

The other DF technology includes a fully operational diesel engine with diesel as the main fuel. The second fuel is injected in the combustion chamber with the primary fuel, at the same time, in order to provide more energy, hence the production of additional power. This means that the second fuel acts supplementary in case of more power needs. This DF technology necessitates little or no modifications to the existing injection system and it is very flexible. It is mentioned that at light load conditions, the second fuel is not used and this explains more its supplement role [5].

1.4.4 Four-Stroke Dual Fuel Engines

As the name implies, in these type of engine the combustion cycle last four strokes or two crankshaft revolutions. Four stroke engines are usually run in higher rotational speed and they are smaller in size compared with two-stroke engines.

Dual Fuel configuration is possible in four stroke engines. The primary fuel is injected in the intake manifold and mixes with air before the combustion chamber. In case of methanol use, during its injection, methanol from liquid phase (at STP) goes to gas phase and as a result the mixture that is inserted in the combustion chamber at the intake valve open is a gas-air mixture. Inside the combustion chamber there is a fuel injector which injects a small amount of pilot fuel (diesel in most cases) to accomplish the ignition of a low reactivity mixture. After the combustion ending, the exhaust valve opens and the products of the combustion leaves the combustion chamber.

Investments in dual-fuel four-stroke engines have been made from big engine manufacturers. A Four-Stroke Wärtsilä Dual-Fuel Engine is presented in the following figure.

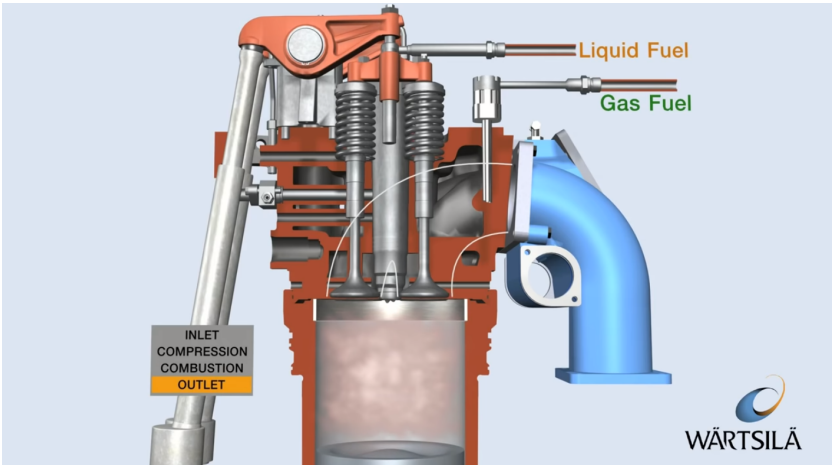

Figure 1.1: Wärtsilä Four-Stroke Dual-Fuel Engine [1]

1.4.5 Two-Stroke Dual Fuel Engines

The other common type of engines are the two-stroke engines. These engines need the half strokes for a comblete combustion cycle and in other words the cycle last one crankshaft revolution. They are big in size, usually run up to 100 RPM which means their speed range are lower than the four-stroke engines, and they are commonly used in marine industry for ocean-going vessel's propulsion.

There are two approaches for two-stroke DF engines by two engine manufacturers, MAN B&W and WinGD.

In MAN B&W's DF engines the gas is injected into the compressed air near the Top Dead Center where the in-cylinder pressure exceed 150 bar, hence the 300 bar gas injection pressure. To increase the heat and turbulence and to accelerate the combustion, a small amount of diesel pilot fuel is also injected via a micro-pilot fuel injector. Diffusion combustion is took place and as a result CO_2 and CO emissions are low and there is no problem of knocking phenomena. However, the required diesel pilot fuel quantity ranges between 5-10% of the total fuel energy and so Tier III compliance can be met only by installing exhaust gas after-treatment or recirculation systems [9].

On the other hand, WinGD has developed a different concept of DF engine in 2013. In X-DF engines the gas is injected into the chamber at the start of compression where the in-cylinder pressure is low (up to 16 bar [9]). This is the main difference compared with MAN B&W's concept. When the piston reaches the Top Dead Center, pilot fuel is injected to ignite the in-cylinder mixture. It is worth to be mentioned that pilot fuel is injected in a pre-chamber causing immediate increase of temperature and pressure after

its ignition and due to that fact the gas is ignited in the main chamber. In this concept, there is no need for extra equipment for compliance with Tier III legislation because of the small of amount of pilot injected diesel, the high speed of combustion and the low maximum temperature that cause low NOx emissions. Knocking phenomena are not appeared in this DF concept and the investment cost for these engines is lower. However at high load conditions there is a possibility for misfiring phenomena[9].

1.4.6 Dual Fuel Engines in Marine Industry

Dual Fuel engines are a topic of research in shipping industry in order to meet the upcoming emission legislations. It is not a secret that LNG Carriers and their inevitable cargo evaporation are one of the main reasons for the development of DF engines, aiming to make advantage of the "lost" cargo. However, the DF researchers examines more alternative fuels such as methanol.

In general, Compression-Ignition (CI) engines are more attractive by researchers compared with Spark-Ignition (SI) engines due to their better fuel economy, the high compression ratio and no throttling loss [17]. The main goal is to reduce the emissions and the crude oil usage in order to protect the environment and its energy resources. To accomplish that, the combustion and efficiency have to be improved.

The majority of ocean-going vessels are using conventional diesel engines for their propulsion. Thus, in order to meet the upcoming legislations and due to the fact that little hardware modifications are required [9], they could convert their engines into DF and use as fuel an alternative one with less harmful. emissions.

Furthermore, there is no difficulty in cold start, in light load conditions or even in case of primary fuel lack, as the engine will still be fully operational running according to the diesel cycle by switching from dual fuel mode to pure-diesel mode [17]. As a result, there would be no dangerous issues by the engine due to its effectiveness.

1.5 Thesis Structure

In Chapter 2, the theoretical knowledge used in this thesis is presented. Chapter 3 contains the design of the model and the steps of its development. In Chapter 4 the results and the validation of the combustion model are displayed and finally in Chapter 5 is proposed future work and are comented some conclusions of this work.

Chapter 2

Theoretical Background

In this chapter, the theoretical knowledge and the theorems that used in this work are presented. In particular, in order to make calculations with physical consequence, theorems and equations from thermodynamics, internal combustion engines books and chemical equilibrium functions have been used and are presented in this chapter.

2.1 Modeling Approaches

In order to model the combustion phenomenon of a DF diesel methanol engine, some assumptions have to be made some and the approach method of the Heat Release Rate and the in-cylinder Pressure has to be selected. The modeling approaches are presented below [18] and the model that finally selected is referred in chapter 3.

Zero-Dimensional model or Single Zone Model is the easiest way to approach the combustion process without investigating the precise physical background. It uses empirical or semi-empirical mathematical expressions that often give the Heat Release Rate and describe the combustion phenomenon from some parameters that need to be calibrated with experimental data and operating conditions. From a thermodynamic view, in the cylinder there is uniformity which means the different zones of the cylinder volume are not taken into account and for instance the Pressure and the Temperature are the same in the combustion chamber. The advantage of this method of approach is the low necessity of computational power and the fast results making it suitable for applications that need fast predictions without many precision requirements. Furthermore, Zero-Dimensional models can be easily incorporated in the Electronic Control Unit (ECU) of an engine and based on their predictions, several parameters, such as fuel consumption, could be

determined. However, in most cases there is poor estimations outside the calibration region. A single zone cylinder model is presented in the following figure.

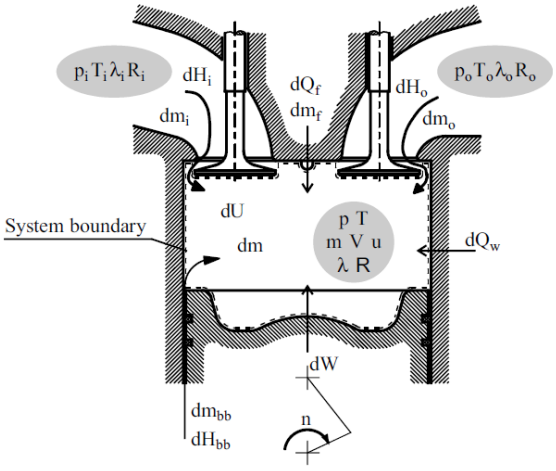

Figure 2.1: Single Zone Cylinder Model [2]

One more accurate approach is the use of Quasi-Dimensional Models. They take into account the physics and chemistry behind the combustion process by solving energy and mass equations and it is not assumed uniformity inside the cylinder. Moreover the injection profile needs to be determined and can predict precisely the emissions composition. Although the necessity for computational power and the mathematical complexity are significantly more, quasi-dimensional models are faster than multi-dimensional models, making them suitable for applications with good precision necessity in the results and with an acceptable computational time.

Multi-dimensional CFD (Computational Fluid Dynamics) models are the most accurate methods to describe the combustion process. They solve mass and momentum equations and have complete physical and chemical consequence. CFD models need high computational effort due to their mathematical complexity and their accuracy depend strongly on the initial boundary conditions. Thus, advanced technology need to be used and the computational time is high. Usually, multi-dimensional simulations are used in the investigation of certain engine-related processes in detail [11]. CFD models are often used for mechanical design where the precision of the estimations has to be in high levels.

2.2 Engine Operating Parameters

2.2.1 In-Cylinder Geometrical Relationships

In order to model the in-cylinder combustion, several geometrical parameters have to be calculated. In this respect, the geometrical relationships for internal combustion engines according to [3],which will be used in this work, are presented.

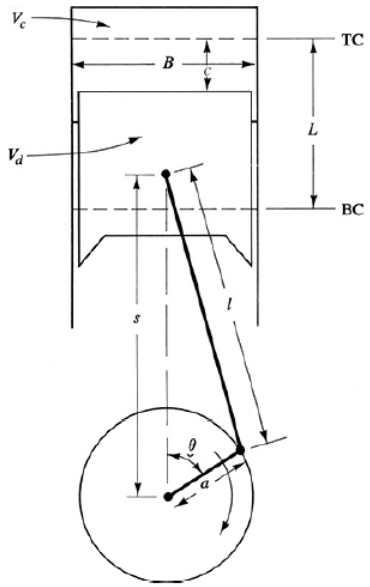

Figure 2.2: In-Cylinder Geometrical Relationships [3]

Initially, is exhibited the Compression Ratio (symbolized by ε or r_c) which is the ratio between the maximum cylinder volume and the minimum cylinder volume. In other words, it is the ratio between the combustion chamber volume when the piston is at Bottom Dead Center (BDC) and the volume when the piston is at the Top Dead Center (TDC). It is one of the most important characteristics of an engine and is calculated based on the following expression.

$$\varepsilon = \frac{Vc + Vd}{Vc} \tag{2.1}$$

In the above equation, as Vc is symbolized the Clearance Volume of the cylinder (when piston is at TDC) and Vd is the displaced volume by the movement of piston.

The in-cylinder volume at any crank position θ is given by the following expression:

$$V = Vc + \frac{\pi B^2}{4} c \tag{2.2}$$

where Vc is the clearance volume, B is the engine's bore and c is:

$$c = \frac{S}{2}[R + 1 - cos\theta - (R^2 - sin^2\theta)^{1/2}] \tag{2.3}$$

where S is the engine's stroke, θ is the crank angle and R is the ratio between the Connecting Rod Length l and the Crank Radius α:

$$R = \frac{l}{\alpha} \tag{2.4}$$

It is also mentioned that the Crank Radius is is the half of the engine's stroke.

Finally, the volume of the cylinder in an angle θ in degrees is calculated by the following equation:

$$V(\theta) = \frac{\pi B^2 S}{4} \left[\frac{1}{\varepsilon - 1} + \frac{1}{2} \left(R + 1 - cos(\theta \frac{\pi}{180}) - \sqrt{R^2 - sin^2(\theta \frac{\pi}{180})} \right) \right] \tag{2.5}$$

The above expression, when $\theta = 0$ *degrees*, gives the Clearance Volume V_c of the cylinder.

In addition, the derivative of the in-cylinder volume is.

$$\frac{dV(\theta)}{d\theta} = \frac{\pi^2 B^2 S}{8 \cdot 180} \left[\frac{cos(\theta \frac{\pi}{180}) sin(\theta \frac{\pi}{180})}{\sqrt{R^2 - sin^2(\theta \frac{\pi}{180})}} + sin(\theta \frac{\pi}{180}) \right] \tag{2.6}$$

The cylinder wall area A_w in crank angle θ is calculated as follows:

$$A_w = A_{ch} + A_p + \frac{\pi B S}{2} \left[R + 1 - cos(\theta \frac{\pi}{180}) - \sqrt{R^2 - sin^2(\theta \frac{\pi}{180})} \right] \tag{2.7}$$

where A_{ch} is the cylinder head surface area, A_p is the piston crown surface area, R is the rod length to crank radius ratio, B and S are the engine's bore and stroke. It is assumed that:

$$A_{ch} = A_p = \frac{\pi B^2}{4} \tag{2.8}$$

2.2.2 Number of Operation Cycles in One Second

The number of cycles per one second and is calculated based on the following equation [19]:

$$v = \frac{n}{30K} \tag{2.9}$$

where as n is symbolized the rotational speed in RPM and K takes value depending on the strokes of the engine.

2.2.3 Fuel Consumption per Cycle and Cylinder

In order to be calculated the fuel consumption in one cylinder and in one cycle, is used the following expression [19]:

$$b = \frac{\dot{m_B}}{z \cdot v} \tag{2.10}$$

In the above equation, b is the fuel quantity per cycle, $\dot{m_B}$ is the fuel consumption, z is the engine's cylinder number and v is the number of operation cycles per one second and is calculated by the equation 2.9.

2.2.4 Fuel Heating Value

The fuel heating value is an important parameter of the engine's operation.

The released combustion heat in one operation cycle and in one cylinder is given by the following expression [19]:

$$Q_B = b \cdot LHV \tag{2.11}$$

where b is the fuel consumption per cycle and cylinder and LVH is the Lower Heating Value of the fuel.

The engine's total Fuel Heating Value Q_{HV} is [19]:

$$Q_{HV} = \dot{m_B} \cdot LHV \tag{2.12}$$

where $\dot{m_B}$ is the engine's fuel consumption.

2.2.5 Brake Mean Effective Pressure

The Brake Mean Effective Pressure is calculated dividing the work per cycle by the cylinder volume displaced per cycle and it is a relative engine performance measure [3].

In particular the Brake Mean Effective Pressure is calculated with the following expression in SI units:

$$bmep\ [kPa] = \frac{P[kW] \cdot K \cdot 10^3}{2 \cdot Vd[dm^3] \cdot N[RPS]} \tag{2.13}$$

where P is the engine's power given by:

$$P\ [kW] = 2\pi \cdot N[RPS] \cdot T[Nm] \cdot 10^{-}3 \tag{2.14}$$

N is the engine's rotational speed, T is the Torque exported from the engine, K is the number of engine's strokes (K=4 for Four-Stroke engines) an Vd is the displaced volume.

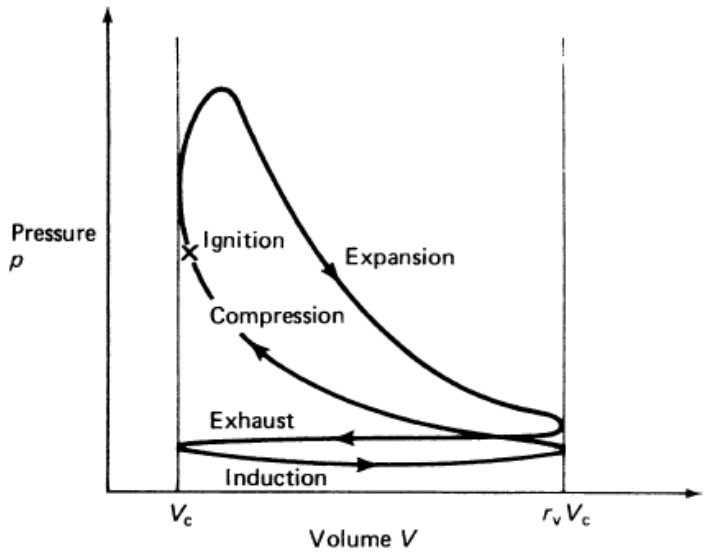

Figure 2.3: Indicator Diagram for Four-Stroke Engine [4]

2.2.6 Equation of State of Ideal Gas

In this work, the in-cylinder temperature is calculated by the Equation of State of Ideal Gas:

$$pV = n\bar{R}T \tag{2.15}$$

where p is the Pressure, V is the Volume, n are the total moles of mixture, T is the Temperature and $\bar{R}$ is the Universal Gas Constant.

The universal Gas Constant has a constant value and it is [3]:

$$\bar{R} = 8.3143 \, \frac{J}{mol \cdot K}$$

In many cases it is used the alternative form of the Equation of State which is:

$$pV = mRT \tag{2.16}$$

In this occasion m is the mass of mixture and

$$R = \frac{\bar{R}}{MW} \tag{2.17}$$

where MW is the molecular weight and m is the mass of the gas[3].

2.3 Compression-Ignition Engines Combustion

2.3.1 Heat Release Rate Analysis

In CI internal combustion engines, the in-cylinder pressure and the heat release rate are two important and useful values for the engine's behavior.

The Heat Release Rate until an angle ϕ is:

$$\frac{dQ(\phi)}{dt} = \frac{dx_b(\phi)}{dt} \cdot m_{fuel} \cdot LHV \cdot \eta_{comb} \tag{2.18}$$

where m_{fuel} is the total mass of fuel, LHV is the lower heating value of the fuel and $dx_b(\phi)/dt$ is the burnt mass fraction rate until angle ϕ

When two fuels are used, the equivalent LHV is:

$$LHV = \frac{m_{f1} \cdot LHV_{f1} + m_{f2} \cdot LHV_{f2}}{m_{f1} + m_{f2}} \tag{2.19}$$

According to [3], the net heat release rate dQ_n/dt is calculated by the First Thermodynamic Law:

$$\frac{dQ_n}{dt} = \frac{dQ_{ch}}{dt} - \frac{dQ_{ht}}{dt} \tag{2.20}$$

where dQ_{ch}/dt is the gross heat release rate and dQ_{ht}/dt is the heat transfer rate to the cylinder walls. In other words, the net heat release rate is the difference between the work on the piston and the rate of change of lost internal energy by the cylinder walls [3].

If it is assumed that the content in the combustion chamber is an ideal gas, the equation 2.20 can be transformed into:

$$\frac{dQ_n}{dt} = \frac{\gamma}{\gamma - 1} p \frac{dV}{dt} - \frac{1}{\gamma - 1} V \frac{dp}{dt} \tag{2.21}$$

In the above equation, γ is the ratio of specific heats, p in-cylinder pressure, V is in-cylinder volume and dp/dt and dV/dt are the rate of change of in-cylinder pressure and volume respectively.

According to the ratio of specific heats γ, it is mentioned that [3]:

$$\gamma = \frac{C_P}{C_V} \tag{2.22}$$

For diesel heat release rate analysis, γ has values between 1.3 and 1.35. In this work, it is assumed that γ has a constant value [20]and more specifically:

$$\gamma = 1.35$$

The equation 2.21 connects the in-cylinder pressure rate of change with the net heat release rate and it will be used to estimate the in-cylinder pressure by the heat release rate model, which will be described later in this work.

2.3.2 Heat Loss Rate

The Heat Loss Rate is the heat that is transferred between the cylinder walls and the in-cylinder gases through convection and radiation. However, in Homogeneous Charge Compression Ignition (HCCI) engines the radiation effect is neglected [21]. In this work it is assumed that radiation effect is neglected in dual fuel mode as well. As a result, the heat transfer is caused only from convection and the convective heat transfer rate using the Newton's Law of cooling is given by the following equation [21]:

$$\frac{dQ_h}{dt} = h_c A_w (T - T_w) \tag{2.23}$$

In the above expression, h_c is the heat transfer coefficient, A_w is the cylinder wall area, T is the in-cylinder temperature and T_w is the wall temperature.

As heat transfer coefficient it is selected the Woschni method and it is calculated as follows [22]:

$$h_c = 3.26 \cdot B^{-0.2} \cdot p^{0.8} \cdot T^{-0.55} \cdot v_c^{0.8} \tag{2.24}$$

where B is the engine's stroke, p and T are the in-cylinder pressure and temperature respectively, and v_c is the characteristic velocity which is calculated as follows [22]:

$$v_c = 2.28 \cdot \bar{S_p} + 0.00324 \frac{V_d \cdot T_r}{p_r \cdot V_r}(p - p_m) \tag{2.25}$$

In the above expression, $\bar{S_p}$ is the mean piston speed given by the equation, V_d is the displaced volume, p_r , V_r , T_r are the in-cylinder pressure, volume, and temperature respectively at some reference state, and p_m is the motored cylinder pressure at the same crank angle as the in-cylinder pressure p. The reference state, it is assumed that it is the inlet valve close. Moreover, it is selected the wall temperature to be equal to 100^oC [4].

The mean piston speed $\bar{S_p}$ is calculated with the following equation [3]:

$$\bar{S_p} = 2SN \tag{2.26}$$

where S is the engine's stroke and N is the rotational speed.

Furthermore, the motored pressure p_m is calculated using the polytropic process expression. As a result [23]:

$$p = p_r \cdot \left(\frac{V_r}{V}\right)^{\gamma} \tag{2.27}$$

2.4 Thermochemistry Expressions

2.4.1 Dual-Fuel Mode and Pure-Diesel Mode Combustion

In this work, it is examined a dual fuel engine fueled by methanol with pilot injection of diesel fuel. In this respect, inside the cylinder is taken place the combustion of diesel and methanol with the air. Thus, the overall chemical equation in stoichiometric composition is:

$$1\ C_{12}H_{23} + 1\ CH_3OH + \frac{77}{4}\ \left(O_2 + \frac{79}{21}\ N_2\right) \longrightarrow 13\ CO_2 + \frac{27}{2}\ H_2O + \frac{869}{12}\ N_2$$

Nonetheless, in DF engines, as it is mentioned in the introduction, there is capability to run the engine only with diesel fuel for power production. In addition, pure-diesel mode is used in low load levels. As a result, in this work it is also examined the pure-diesel mode combustion. The overall chemical equation in stoichiometric composition is:

$$1\ C_{12}H_{23} + \frac{3}{2}\ \left(O_2 + \frac{79}{21}\ N_2\right) \longrightarrow 12\ CO_2 + 2\ H_2O + \frac{79}{14}\ N_2$$

2.4.2 Number of Moles and Mole Fraction of a Substance

The Number of Moles of a substance can be found if they are known the molecular weight MW and the mass m of this substance. In particular:

$$n = \frac{m}{MW} \tag{2.28}$$

In addition, the mole fraction x_i of the substance i can be found by the following expression:

$$x_i = \frac{n_i}{n_{total}} \tag{2.29}$$

where n_i is the moles of the investigated substance and n_{total} is the total moles of the mixture. In other words, the mole fraction gives the ratio of the moles of a substance in the total moles of a mixture.

2.4.3 Equivalence Ratio and Relative Air to Fuel Ratio

Initially is presented the Air to Fuel Ratio (A/F) which is the ratio between the mass of air of a mixture and the mass of fuel of a mixture. With A is

symbolized the Air Mass and with F is symbolized the Fuel Mass.

The Equivalence Ratio shows if a mixture stoichiometric and if not how it declines from stoichiometric composition. In particular, the equivalence ratio is the the fuel and oxidizer ratio divided by the stoichiometric fuel and oxidizer ratio [24]. In other words[3]:

$$\phi = \frac{(F/A)_{actual}}{(F/A)_{stoich}} \tag{2.30}$$

The inverse of the Equivalence ratio is the Relative Air/Fuel Ratio, is symbolized with λ and is calculated by the following expression [3]:

$$\lambda = \frac{(A/F)_{actual}}{(A/F)_{stoich}} \tag{2.31}$$

Taken these parameters into account, it can be understood the mixture composition and its declination from the stoichiometric one. In particular, for fuel-lean mixtures $\phi < 1 \& \lambda > 1$, for fuel-rich mixtures $\phi > 1 \& \lambda < 1$ and for stoichiometric mixtures $\phi = \lambda = 1$ [3].

2.4.4 Relative Oxygen Concentration

The Relative Oxygen Concentration is the ratio between the oxygen concentration of dual-fuel mode combustion and the oxygen concentration of pure-diesel mode combustion [25]:

$$r = \frac{w_{dualfuel}(O)}{w_{purediesel}(O)} \tag{2.32}$$

In order to find the oxygen concentration, the following equation is used [25], [26]:

$$w(O) = \frac{x_a}{4.76(x_a + x_m + x_{exh})} \tag{2.33}$$

where x_a is the mole fraction of air, x_m is the mole fraction of mixture and x_{exh} is the mole fraction of exhaust gases. In this work it is assumed that there are no exhaust gases in the mixture, hence $x_{exh} = 0$.

According to the Relative Oxygen Concentration, r decreases according to that of conventional diesel, due to the methanol evaporation effect.

2.5 Combustion Modeling

2.5.1 Ignition Delay Modelling

In the first stage of this work, an Ignition Delay Model was used in order to estimate the interval between the injection time of diesel and the time that the mixture is ignited, i.e. the Start of Combustion (SOC). Particularly, the SOC is the crank angle that the mixture is ignited and it will be used in the Wiebe function, which will be described later in this work.

Ignition of a mixture takes place where large hydrocarbon molecules crack to smaller molecules. It varies depending on the fuel, whose ignition quality is defined by the cetane number, and the cylinder charge pressure and temperature. When the cetane number of a fuel is low and the ignition delay is long, most of the fuel has been injected when the ignition takes place and as a result there are rapid burning rates and high rates of pressure rise, producing knocking sound. On the other hand, when the cetane number is higher, the ignition delay is shorter and due to the fact that a smaller quantity of fuel has been injected in the cylinder, the engine operation is smother [3].

Several semi-empirical approaches exist in bibliography, which are based on the Arrhenius equation:

$$\tau_{id} = A \cdot p^{-n} \cdot exp\left(\frac{E_A}{\bar{R} \cdot T}\right) \tag{2.34}$$

The ignition delay is usually given in time units. To convert the delay from crank angle units to time units, is used the following equation:

$$\tau_{id}\,[ms] = \frac{\tau_{id}\,[CA]}{0.006 \cdot N\,[RPM]} \tag{2.35}$$

where $N\,[RPM]$ is the engine speed.

After having been estimated the ignition delay, the Start of Combustion can be easily calculated:

$$(Start\ of\ Combustion) = (Injection\ Time) + (Ignition\ Delay) \tag{2.36}$$

as the Injection Time is known in most cases.

2.5.2 Wiebe Function

The Heat Release Rate is highly correlated with the Burned Mass Fraction Rate (BMF Rate) as shows the equation 2.18. Thus, in order to find the

BMF Rate, Wiebe Functions were used. In particular, Wiebe Functions give the fraction of the burned fuel until a specific angle i.e. the Burned Mass Fraction (BMF) and as a result, their derivative give the BMF Rate.

Wiebe function was introduced by a Russian engineer and scientist Ivan Ivanovich Wiebe in 1962. It is a derivative of the normal distribution of a continuous random variable and it is based on chemical kinetics and chain reactions theory. [9].

The Single Wiebe function and it's derivative are presented below [19]:

$$x_b(\theta) = 1 - exp\left[-a\left(\frac{\theta - \theta_{ign}}{\Delta\theta}\right)^{m+1}\right] \tag{2.37}$$

$$\frac{dx_b}{d\theta}(\theta) = \left(\frac{a\,(m+1)}{\Delta\theta}\right)\left(\frac{\theta - \theta_{ign}}{\Delta\theta}\right)^{m} exp\left[-\alpha\left(\frac{\theta - \theta_{ign}}{\Delta\theta}\right)^{m+1}\right] \tag{2.38}$$

In these two above expressions, $x_b(\theta)$ is the fuel mass fraction burnt until crank angle θ, θ_{ign} is the crank angle in crank angle degrees (CAD) in which the combustion starts (SOC), $\Delta\theta$ is the combustion duration in CAD [19], a is the efficiency parameter and m is the shape factor.

The below figure show how the efficiency parameter and the shape factor affect the Burned Mass Fraction.

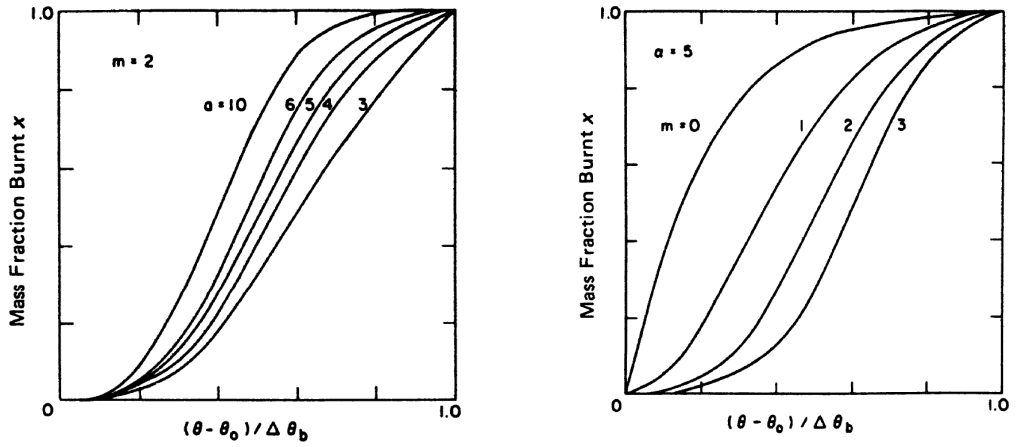

(a) Efficiency Parameter, α (b) Shape Factor, m

Figure 2.4: Effect of α and m parameters on Burned Mass Fraction [4]

The efficiency parameter a is a function of the burnt fuel mass fraction by the end of combustion x_d and it can be calculated by the following equation [9]:

$$a = -ln(1 - x_d) \tag{2.39}$$

In most cases, it is assumed that $x_d = 0.999$, which means that almost all the fuel burnt during the combustion and as a result $a = 6.908$.

The double and triple wiebe functions is nothing different but the combination of two and three single wiebe functions respectively. They are used to describe different phases of combustion and can predict with accepted precision the heat release rate of the a dual fuel engine. However, in these occasions it is added an Amplitude Correction Factor λ_i that represents the contribution of each combustion stage to the heat release [9] and it is a fact that:

$$\sum_{i=1}^{n} \lambda_i = 1 \tag{2.40}$$

where n is the degree of Wiebe function that is used. For instance, if Double Wiebe is used $n = 2$ and if Triple wiebe is used then $n = 3$.

In particular, Multiple Wiebe function and its derivative are presented below:

$$x_b(\theta) = \sum_{i=1}^{n} \lambda_i \left(1 - exp \left[-a \left(\frac{\theta - \theta_{ign}}{\Delta\theta_i} \right)^{m_i+1} \right] \right) \tag{2.41}$$

$$\frac{dx_b}{d\theta}(\theta) = \sum_{i=1}^{n} \lambda_i \left(\left(\frac{a\ (m_i + 1)}{\Delta\theta_i} \right) \left(\frac{\theta - \theta_{ign}}{\Delta\theta_i} \right)^{m_i} exp \left[-\alpha \left(\frac{\theta - \theta_{ign}}{\Delta\theta_i} \right)^{m_i+1} \right] \right) \tag{2.42}$$

where n is the degree of Wiebe Function.

There are a lot of variations for the multiple Wiebe Functions. However in this work, the Miyamoto approach was investigated [27]. The main characteristic of this approach is that all branches start from the crank angle of start of combustion.

Therefore, having determined the coefficients of these functions, it can be found the Heat Release and the Heat Release Rate throughout the combustion and subsequently the in-cylinder pressure of an engine.

The triple wiebe can model three phases of the combustion of a dual-fuel engine and the three wiebe branches are presented in the following figure.

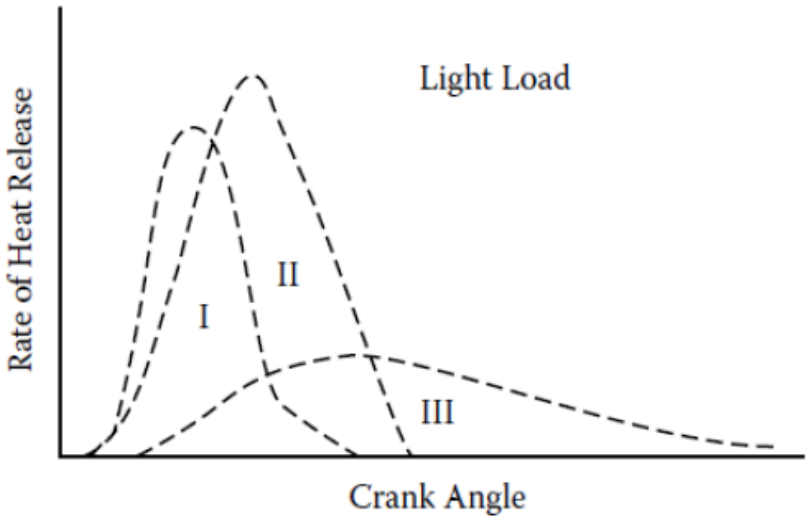

Figure 2.5: Dual Fuel CI Engines - Combustion Phases [5]

When methanol ratio is low, the first stage is premixed combustion of both methanol and diesel while the other two phases is diffusion combustion of diesel. In cases of methanol as main fuel, the combustion characteristics are different. The first stage also represent premixed combustion of methanol and diesel but the other two describe the methanol flame propagation through the cylinder and auto ignition of methanol through the rest of the cylinder [28].

2.5.3 Premixed Combustion Phase Modeling

The premixed phase is the first phase of the combustion and investigations have been made to determine the premixed fraction β which gives the ratio of the mass of fuel burned in premixed phase of combustion to the total mass fuel. The premixed fraction could be estimated by the following expression [29]:

$$\beta = 1 - \frac{a_w \cdot \phi^{b_w}}{\tau_{id}^{c_w}} \tag{2.43}$$

where a_w, b_w, c_w are coefficients that need to be determined, ϕ is the equivalence ratio and τ_{id} is the ignition delay in time units.

This premixed fraction is the Amplitude Correction Factor of Premixed

Phase of Combustion λ_{31}, which is used in Wiebe Function. Thus, the equation 2.43 can be used to estimate the Wiebe Parameter λ_{31} of the equation 2.41.

2.6 Regression Tools

Regression Analysis is a method of statistical modeling and a very useful tool for engineers and researchers. It is used to be estimated the relationship between some dependent variable often some experimental result) and some independent variables (often some variables of a condition such as the engine running conditions) [9]. In other words, Regression Analysis gives a method to estimate and predict an experimental result by some known independent variables and it is achieved by finding the curve that fits better the results according to specific functions [9].

Lasso Regression or L1 Regularization is a very similar method to Linear Regression (using Mean Squared Error) or Ridge Regression (L2 Regularization). Nevertheless, Lasso Regression adds a penalty equal to the absolute value of the coefficients and the error that needs to be minimized is based on the following expression [30]:

$$error = \sum_{i=1}^{n}(y_i - \sum_{j=1}^{p} x_{i,j}\beta_j)^2 + \lambda \sum_{j=1}^{p} |\beta_j| \tag{2.44}$$

The utility of Lasso Regression is due to the fact that some coefficients can become zero, hence the more convenience of the model [30].

In the above expression, λ is a tuning parameter and controls the strength of L1 penalty. When $\lambda = 0$ then the estimation is equal to Linear Regression and the error to be minimized is the Mean Squared Error. As λ takes higher values, more coefficients are forced to be zero but the accuracy of the model decreases [30].

This method is used in some stages of this work in order to estimate the value of some parameters according to some condition parameters. However, as it will be mentioned in the following chapter, in order to use the Lasso Regression, it is used a prefabricated package of a programming language that does exactly this work, i.e. finding the coefficients of a function minimizing the Lasso Regression error (equation 2.44)

Chapter 3

Combustion Model Development

In this chapter the design procedure and the development of this work are presented. The approach of the selected model and the assumptions that were made for the combustion model are also presented here

3.1 Experimental Data

For the calibration and the validation of the combustion model some experimental data were used. Some experimental data were used which were taken from a Dual-Fuel Compression Ignition Marine Engine, fueled by Methanol with pilot injection of Diesel. In this engine, Methanol is injected in the intake manifold and the pilot diesel is injected directly to the cylinder.

The experiments were conducted in three different speeds: 1000 RPM, 1100 RPM and 1300 RPM. However, for the model development, were used only the 1000 and 1300 RPM data and the 1100 RPM data were used for the model validation.

Several operating conditions and in particular it was tested the quantity of methanol and diesel, the injection time, the load and speed at which the engine runs. Thus, for each test, the known condition parameters are the load, speed, injection time, diesel, methanol and air consumption. The results that were obtained are the crank angle history (in crank angle degrees) of Gross Heat Release Rate in J/CA units and of in-cylinder Pressure in MPa.

The experimental apparatus, from which the experimental data were taken,

is a Four-Stroke Diesel-Methanol Dual Fuel Engine, whose characteristics are presented in the following table.

Engine Specifications	
Bore [mm]	108
Stroke [mm]	130
nR [-]	2
Cylinders [-]	6
Power [kW]	192
Displacment [L]	7.1455
Compression Ratio	18
Conn. Rod Length [mm]	210
Intake Valve Close [deg ATDC]	-125.5

Table 3.1: Engine Specifications

The conditions of the experiments that have been taken [6],[28] are presented in the following tables.

Wiebe Parameters of 1000 RPM Experiments							
Test Name	1000-235-709	1000-537-0	1000-431-235	1000-334-417	1000-235-709	1000-875-0	1000-603-552	1000-476-770
BMEP [Mpa]	0.35	0.35	0.35	0.35	0.35	0.662	0.662	0.662
Speed [RPM]	1000	1000	1000	1000	1000	1000	1000	1000
Torque [Nm]	198.86	198.86	198.86	198.86	198.86	381.97	381.97	381.97
Power [kW]	20.83	20.83	20.83	20.83	20.83	40.00	40.00	40.00
Diesel Consumption [kg/h]	2.35	5.37	4.31	3.34	2.35	8.7444	6.03	4.76
Methanol Consumption [kg/h]	7.09	0	2.35	4.17	7.09	0	5.52	7.695
Air Consumption [kg/h]	266	266	266	266	266	287.9	287.9	287.9
Injection Time [CAD]	-10	-10	-10	-10	-10	-10	-10	-10
Φ Diesel	0.13	0.30	0.24	0.18	0.13	0.45	0.31	0.24
Φ Methanol	0.17	0.00	0.06	0.10	0.17	0.00	0.12	0.17
Fuel Consumption [kg/h]	9.44	5.37	6.66	7.51	9.44	8.74	11.55	12.46

Table 3.2: Wiebe Parameters of 1000 RPM Experiments

Wiebe Parameters of 1300 RPM Experiments							
Test Name	1300-351-369	1300-351-738	1300-351-1580	1300-772-0	1300-772-441	1300-772-659	1300-772-866
BMEP [Mpa]	0.142	0.258	0.569	0.285	0.45	0.540869764	0.6
Speed [RPM]	1300	1300	1300	1300	1300	1300	1300
Torque [Nm]	80.74	146.70	323.55	162.06	255.88	307.55	341.17
Power [kW]	10.99	19.97	44.05	22.06	34.83	41.87	46.45
Diesel Consumption [kg/h]	3.51	3.51	3.51	7.72	7.72	7.72	7.72
Methanol Consumption [kg/h]	3.69	7.38	15.8	0	4.41	6.59	8.66
Air Consumption [kg/h]	307	316	341	338	352	361	362
Injection Time [CAD]	-5.4	-5.4	-5.4	-3.3	-3.3	-3.3	-3.3
Φ Diesel	0.17	0.16	0.15	0.34	0.32	0.31	0.31
Φ Methanol	0.08	0.15	0.30	0.00	0.08	0.12	0.15
Fuel Consumption [kg/h]	7.20	10.89	19.31	7.72	12.13	14.31	16.38

Table 3.3: Wiebe Parameters of 1300 RPM Experiments

Wiebe Parameters of 1100 RPM Experiments					
Test Name	1100-233-730	1100-317-538	1100-367-438	1100-620-0	1100-657-152
BMEP [Mpa]	0.477	0.477	0.477	0.477	0.477
Speed [RPM]	1100	1100	1100	1100	1100
Torque [Nm]	542	542	542	542	542
Power [kW]	41.05	55.85	64.66	109.24	115.75
Diesel Consumption [kg/h]	2.33	3.17	3.67	6.2	6.57
Methanol Consumption [kg/h]	7.3	5.38	4.38	0	1.52
Air Consumption [kg/h]	276	279	282	289	285
Injection Time [CAD]	-6	-6	-6	-6	-6
Φ Diesel	0.12	0.17	0.19	0.32	0.34
Φ Methanol	0.17	0.12	0.10	0.00	0.03
Fuel Consumption [kg/h]	9.63	8.55	8.05	6.20	8.09

Table 3.4: Wiebe Parameters of 1100 RPM Experiments

3.2 Selected Modeling Approach and Basic Assumptions

In this thesis, it was selected a Zero-Dimensional (Single Zone Model) and semi-empirical approach. The values that are examined are the Heat Release Rate and in continuation the in-cylinder Pressure. It is assumed that there is uniformity inside the combustion chamber and as a result the pressure the temperature are supposed to be the same at all zones of combustion.

Furthermore, it is assumed that there is no mass exchange at the time between the intake valve close (IVC) and the exhaust valve open (EVO). During this interval, the number of molecules that are present in the combustion chamber it is supposed to be constant and in particular is the sum of the air molecules that comes from the compressor, the diesel molecules that are injected to the combustion chamber and the number of methanol molecules that are injected into the intake manifold.

The combustion model is semi-empirical. This means that there is a physical consequence but the model doesn't follow the physical laws absolutely. As a result, there is not only one correct solution and method to predict the Heat Release Rate and the in-cylinder Pressure.

It is referred that the interval of combustion that is investigated in this work is after the Start of Combustion. Phenomena that take place in the combustion chamber and in the intake manifold, like the evaporation of methanol, are neglected.

As the approach that selected is a Zero-Dimensional Model, it is assumed that there is uniformity inside the combustion chamber and different spatial conditions are not considered. In other words, Pressure and Temperature are the same at all points of the cylinder volume.

Furthermore, it is assumed that the Pressure at Intake Valve Close (IVC) is input in the combustion model. The IVC is:

$$IVC = 125^o \; ATDC$$

and as a result the Pressure at this point is considered to be known.

In this work, it is assumed that the Ratio of Specific Heats, γ has a con-

stant value and more specifically:

$$\gamma = 1.35$$

3.3 Schematic Presentation of Combustion Model Construction

The stages of the construction of the Combustion Model that were followed in this work, are presented in the following figures. The rounded box with orange color represent the Experimental Data which is the Start of the procedure. The rounded boxes with blue color indicates data, either experimental or predicted. The oval shape with gray color represent procedures e.g. curve fitting and the green rectangle represent a constructed and calibrated model.

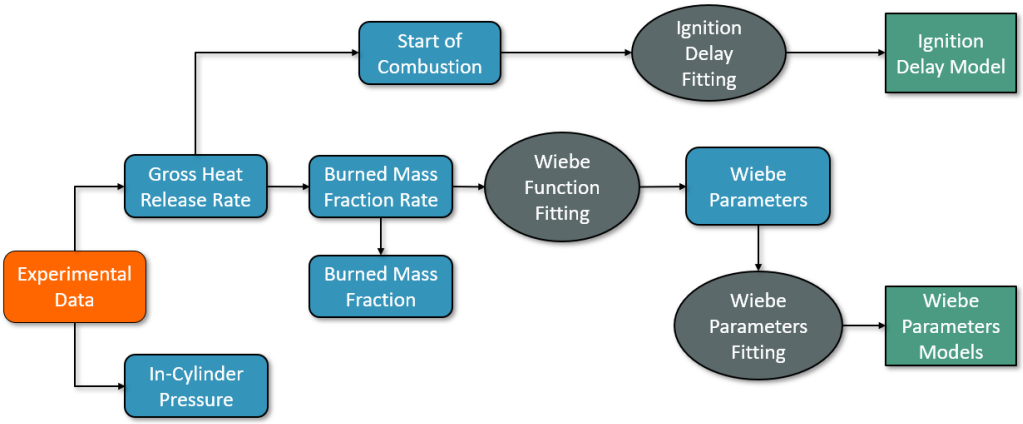

Figure 3.1: Construction of the Combustion Model - Part 1

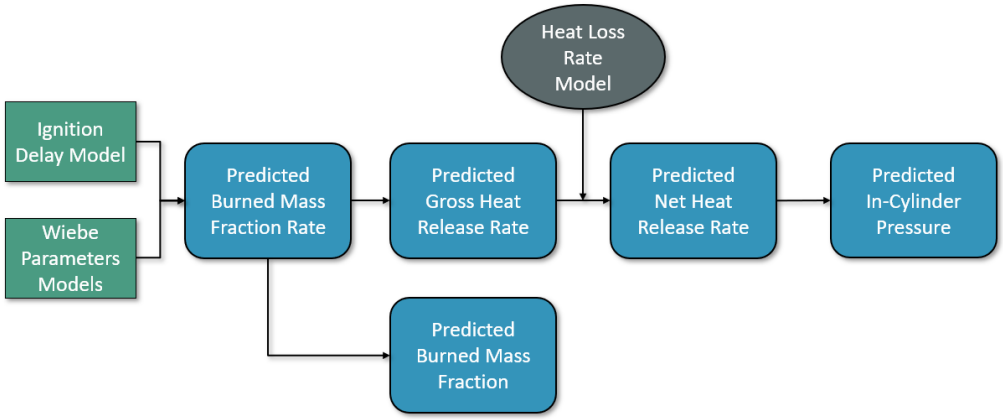

Figure 3.2: Construction of the Combustion Model - Part 2

3.4 Tools and Programs

In this work, the programming language Julia was used in order to make calculations, to process data and to create figures.

In particular Pluto Notebooks and Jupyter Notebooks were used. In addition, they were used several prefabricated packages in order to make standard procedures. In particular, "LsqFit" was used for curve fitting, "Optim" was used for optimization of an objective function and "ScikitLearn" was used for Machine Learning and Lasso Regression.

Apart from Julia, Microsoft Excel was used for collecting the experimental data, for simple calculations and for data monitoring.

3.5 In-Cylinder Temperature Calculation

In several stages of this work the calculation of the in-cylinder temperature is required. When the pressure is known, the in-cylinder temperature can be calculated using the Equation of State (equation 2.15).

$$pV = n\bar{R}T$$

The in-cylinder pressure is obtained either from the experimental data or from polytropic compression expression (equation 2.27):

$$p = p_0 \cdot \left(\frac{V_0}{V}\right)^{\gamma} \tag{3.1}$$

and the in-cylinder volume can be calculated using the equation 2.5.

$$V(\theta) = \frac{\pi B^2 S}{4}\left(\frac{1}{\varepsilon - 1} + \frac{1}{2}\left(R + 1 - cos(\theta\frac{\pi}{180}) - \sqrt{R^2 - sin^2(\theta\frac{\pi}{180})}\right)\right)$$

From the diesel, methanol and air consumption, using the equations 2.9 and 2.10 can be found the mass of diesel, methanol and air in one cycle and one cylinder.

$$v = \frac{n}{30K} \qquad m_{cyl} = \frac{\dot{m_B}}{z \cdot v}$$

These values, dividing them with their molecular weight (equation 2.28), give the number of moles of each substance. Finally, summing up the number of moles of diesel, methanol and air, can be calculated the total in-cylinder number of moles in one operating cycle.

$$n_{cyl} = \frac{m_{diesel,cyl}}{MW_{diesel}} + \frac{m_{methanol,cyl}}{MW_{methanol}} + \frac{m_{air,cyl}}{MW_{air}}$$

As a result, the equation of state (equation 2.15) can give the in-cylinder temperature.

3.6 Ignition Delay Model

The first stage of the combustion model development is to create a method to estimate the Ignition Delay. According to some researches that have been made, was chosen the ignition delay model that was described in chapter 3. The basic idea is to find a method to estimate the ignition delay based on the operating conditions. There are tested and compared two predominant Ignition Delay Models which are based on the equation.

3.6.1 Start of Combustion of Experimental Data

From the experimental data and for all tests has to be determined the Start of Combustion. The Start of Combustion (SOC) is after the Injection Time and is the crank angle where the Heat Release Rate takes the first positive

value. Another way to estimate the SOC is to be found the crank angle after the Injection Time where the second derivative of the in-cylinder pressure changes from negative to zero. A third method is to calculate the SOC is to find the zero of Heat Release Rate Derivative which means to find the point of changing the slope of the Heat Release Rate. The first method was finally selected due to better results and the SOC is the crank angle where HRR becomes positive after the Injection Time.

3.6.2 1st Ignition Delay Model

The first ignition delay model that was examined, was suggested by Zou et al. [25]. According to them, the ignition delay is:

$$\phi_{i,Zou}\,[CAD] = A \cdot C_f \cdot r^k \cdot exp(E \cdot M + Q^{0.63}) \tag{3.2}$$

In the above equation:

$$A = 0.36 + 0.22 \cdot \bar{S}_p \tag{3.3}$$

$$E = \frac{618840}{C_N + 25} \tag{3.4}$$

$$M = \frac{1}{\bar{R}T} - \frac{1}{17190} \tag{3.5}$$

$$Q = \frac{21.2}{p - 12.4} \tag{3.6}$$

where $\bar{S}_p$ $[m/s]$ is the mean piston speed, C_N is the Cetane Number of Methanol, $\bar{R}$ $[J/(mol \cdot K)]$ is the universal gas constant, T $[K]$ is the temperature and p $[bar]$ is the pressure at Top Dead Center (TDC). Moreover, C_f and k are coefficients that are needed to be calibrated based on the engine's characteristics and its running conditions.

Initially, one variable that needs to be determined is the Relative Oxygen Concentration, r. This variable is the ratio between the oxygen concentration in dual-fuel mode and the oxygen concentration in pure-diesel mode. From the definition can be understood that when the engine operates in pure-diesel mode:

$$r \;=\; 1$$

.

First, is found the oxygen concentration of the two modes separately using the equation 2.33. Regarding the dual-fuel mode, the mole fractions of air and methanol can be found using the equation 2.29.

$$x_i = \frac{n_i}{n_{total}} \qquad w(O) = \frac{x_a}{4.76(x_a + x_{meth} + x_{exh})}$$

It is assumed that there are no exhaust gases in the cylinder, hence:

$$x_{exh} = 0$$

As far as the pure-diesel mode concerned, the charge mixture contains only air because no methanol fuel is injected.

It is also assumed, that equal quantity of air is inserted in the cylinder both in dual-fuel and in pure-diesel mode. Thus, the consumption of mass in the equivalent pure-diesel mode is found. Subsequently, with the same method that used in dual-fuel mode, the mass of diesel and air in one cylinder per cycle can be calculated, the number of moles and the mole fractions as well. Finally, can be found the oxygen concentration in the equivalent pure-diesel mode.

Therefore, by the equation 2.32

$$r = \frac{w_{dualfuel}(O)}{w_{purediesel}(O)}$$

the Relative Oxygen Concentration can be found.

It is worth to be mentioned that according to bibliography, when gas is inducted, the concentration of oxygen in the mixture falls, which will lead to an increase in the ignition delay period of the pilot fuel [26].

The in-cylinder pressure at top dead center is calculated based on the polytropic compression expression (equation 2.27) as the pressure at Intake Valve Close is known and the temperature is calculated based on the method mentioned in section 3.5.

The two coefficients, Cf and k are variables that have to be determined through fitting of ignition delay function with the experimental data. The result of the fit of this model is presented below.

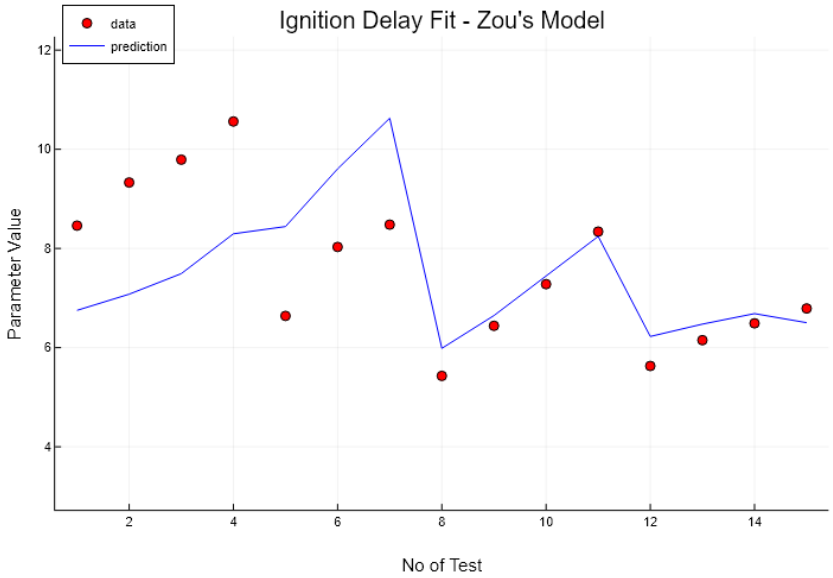

(a) Model Validation

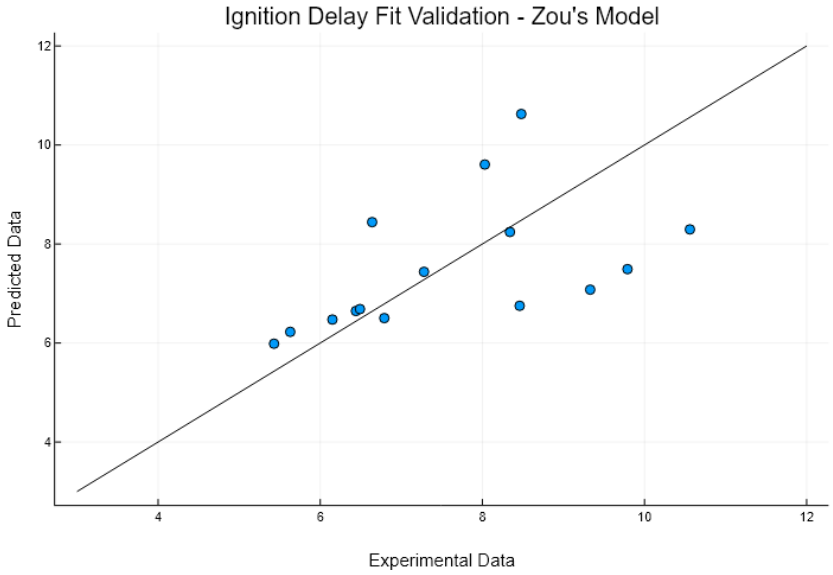

(b) Calculated vs. Experimental Data

Figure 3.3: Zou et al. Ignition Delay Model Validation

3.6.3 2nd Ignition Delay Model

The second ignition delay model that was investigated, was suggested by Assanis et al. [31]. According to them, the ignition delay in time units is

given by the following expression.

$$\tau_{id,Assanis} = A \cdot \phi^k \cdot p^n \cdot exp\left(\frac{E_A}{\bar{R} \cdot T}\right) \tag{3.7}$$

where ϕ is the equivalence ratio of diesel, p and T are the pressure and temperature at Injection Time, $\bar{R}$ is the universal gas constant and E_A is the activation energy of diesel which is:

$$E_A = \frac{618840}{C_{N,diesel} + 25} \tag{3.8}$$

Finally, A, k and n are parameters that have to be calibrated based on the experimental data.

However, according to [29], the diesel fuel is pilot injected in the combustion chamber in a mixture of air an methanol. Thus, the equivalence ratio of diesel have to be corrected. The method that suggested in this paper is to define a pseudo-diesel equivalence ratio which is the ratio of the diesel to oxygen relative to the stoichiometric diesel to oxygen ratio. This expression implies that the pilot diesel has access to all the oxygen in the cylinder charge.

$$\phi_{pD} = \frac{\frac{m_{diesel}}{m_{O_2}}}{\left(\frac{m_{diesel}}{m_{O_2}}\right)_{stoich}} \tag{3.9}$$

In order to convert the ignition delay from time units to crank angle units, it is used the equation 2.35

This ignition delay model, was modified slightly in order to give better results and is presented below.

$$\phi_{id,Assanis} = A \cdot \phi_{pD}^k \cdot p^n \cdot exp\left(\frac{E_A}{\bar{R} \cdot T}\right) \cdot (6 \cdot N)^s \cdot (-t_{inj})^i \tag{3.10}$$

The results of this model fitting are presented below.

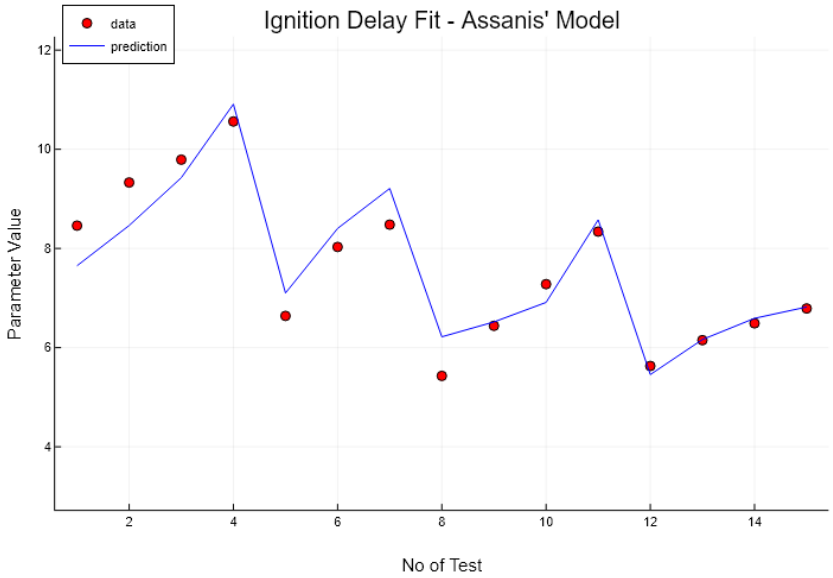

(a) Model Validation

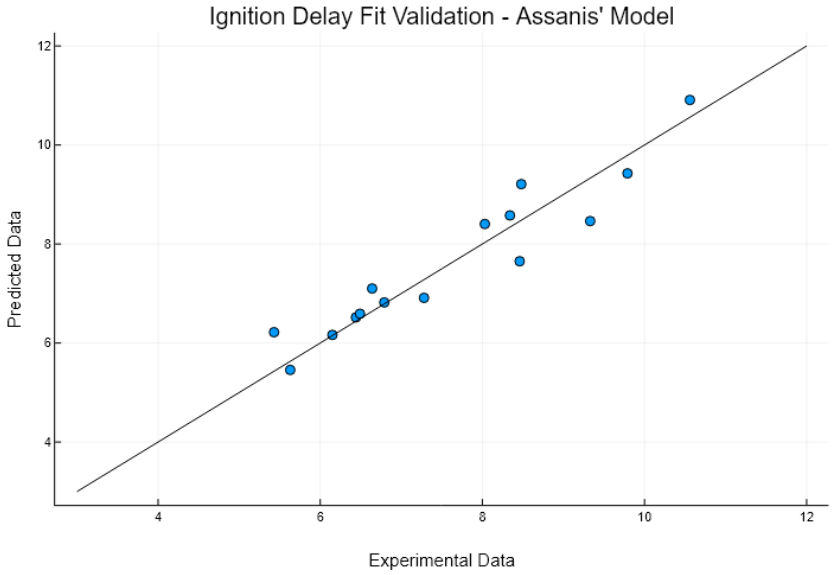

(b) Calculated vs. Experimental Data

Figure 3.4: Assanis et al. Ignition Delay Model Validation

3.6.4 Selected Ignition Delay Model

The ignition delay models comparison is presented below.

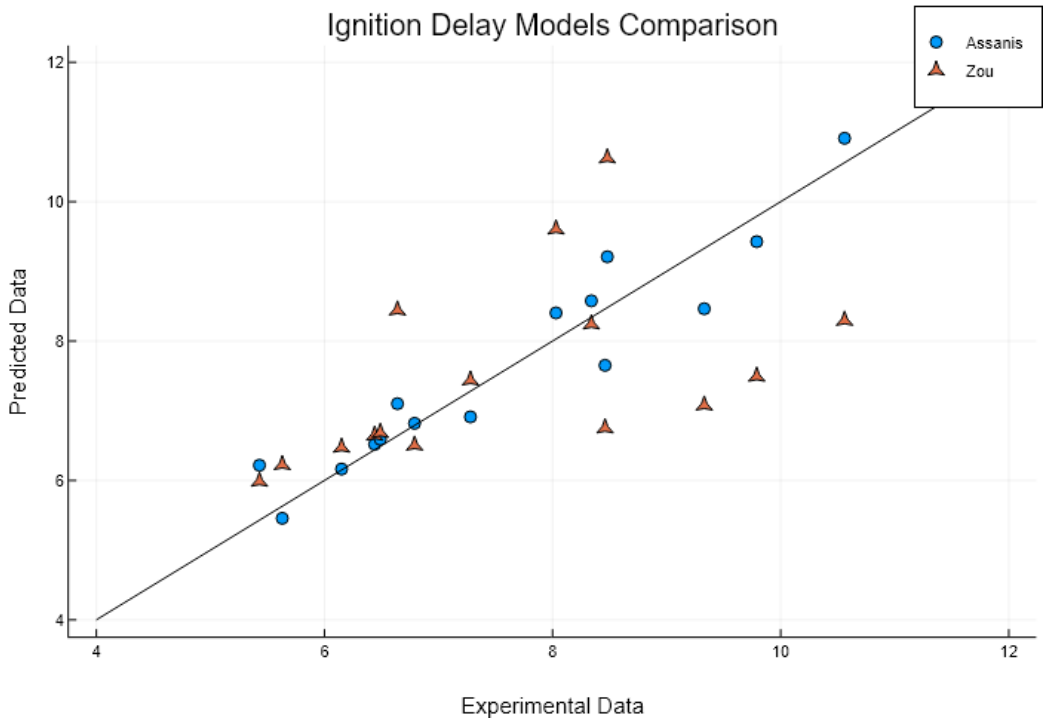

Figure 3.5: Comparison of Ignition Delay Models

Finally, the ignition delay model that was selected is the Assanis' due to the better results and it is:

$$\phi_{id,Assanis} = A \cdot \phi_{pD}^{k} \cdot p^{n} \cdot exp\left(\frac{E_A}{\bar{R} \cdot T}\right) \cdot (6 \cdot N)^{s} \cdot (-t_{inj})^{i}$$

$$\phi_{pD} = \frac{\frac{m_{diesel}}{m_{O_2}}}{\left(\frac{m_{diesel}}{m_{O_2}}\right)_{stoich}}$$

The calibrated coefficients are presented in Appendix.

3.7 Wiebe Function Fit

The next stage of the combustion model development, is the fit of Wiebe Function with experimental data for the purpose of finding the wiebe function parameters based on the experimental apparatus. Wiebe functions give the Fuel Burnt Mass fraction and their derivative give the Burn Mass Fraction Rate, as mentioned in section 2.5.2.

It is mentioned that double and triple wiebe function is the simultaneous appliance of two and three single wiebe functions respectively, adding the parameter λ (Amplitude Correction Factor) that determines the contribution of each branch. Single Wiebe function is (equation 2.37):

$$x_b(\theta) = 1 - exp\left[-a\left(\frac{\theta - \theta_{ign}}{\Delta\theta}\right)^{m+1}\right]$$

and Triple Wiebe Function, that is selected to be used, is (2.41):

$$\begin{aligned} x_b(\theta) = \lambda_1 &\left(1 - exp\left[-a\left(\frac{\theta - \theta_{ign}}{\Delta\theta_1}\right)^{m_1+1}\right]\right) \\ +\lambda_2 &\left(1 - exp\left[-a\left(\frac{\theta - \theta_{ign}}{\Delta\theta_2}\right)^{m_2+1}\right]\right) \\ +\lambda_3 &\left(1 - exp\left[-a\left(\frac{\theta - \theta_{ign}}{\Delta\theta_3}\right)^{m_3+1}\right]\right) \end{aligned}$$

As a result, the wiebe parameters that have to be determined are:

$$\alpha, \Delta\theta_1, \Delta\theta_2, \Delta\theta_3, m_1, m_2, m_3, \lambda_1, \lambda_2, \lambda_3$$

The Amplitude Correction Factors are connected based on equation 2.40 and thus:

$$\lambda_1 + \lambda_2 + \lambda_3 = 1$$

The parameter θ_{ign} is the time of start of combustion and is determined using the Ignition Delay Model and the Injection Time.

3.7.1 Start of Combustion

In wiebe function, it is necessary the defining of Start of Combustion and it is obtained by the HRR data. The method that the SOC in each test is the same with the method that presented in section 3.6.1. As SOC, it is assumed the crank angle where the HRR from negative to positive.

3.7.2 Heat Release Rate Data Processing

The experimental data give the Heat Release Rate (HRR) in J/CA of the total engine. Due to the fact that the HRR data are results of an experiment,

it is certain that would exist irregularities and errors. Thus, in order to reduce this phenomenon, the data are smoothed with a spline and the all the negative values and the values before the Start of Combustion are become zero. In addition, the HRR data have to be divided with the total cylinder fuel heating value in order to be transformed in Burnt Mass Fraction Rate (equation 2.18).

$$\frac{dx_b(\phi)}{dt} \cdot \eta_{comb} = \frac{\frac{dQ(\phi)}{dt}}{m_{fuel} \cdot LHV}$$

The total cylinder fuel heating value can be calculated using the equations 2.9,2.10 and 2.19.

$$v = \frac{n}{30K} \ , \quad m_{cyl} = \frac{\dot{m_B}}{z \cdot v}$$

$$m_{fuel} = m_{dies} + m_{meth}$$

$$LHV = \frac{m_{dies} * LHV_{dies} + m_{meth} * LHV_{meth}}{m_{dies} + m_{meth}}$$

In this way, the processed experimental results are ready to be in inserted in the fitting procedure.

3.7.3 Combustion Efficiency, a

In this work, the combustion efficiency a that is used in the wiebe function, is assumed to be constant due to computational convenience and because it does not affect the accuracy of the results. Particularly, is assumed that 99.9 % of the fuel has been burnt, hence $x_d = 0.999$ and as a result, from the equation 2.39:

$$a = -ln(1 - x_d) \rightarrow a = 6.908$$

It is also presupposed that the combustion efficiency is the same, regardless the degree of wiebe function that will be used and equal for all branches of wiebe function.

3.7.4 Single Wiebe Function

First it is fitted wiebe function (equation 2.37). Thus, the final coefficients are obtained and a sample result of the estimated wiebe function and its derivative are presented below.

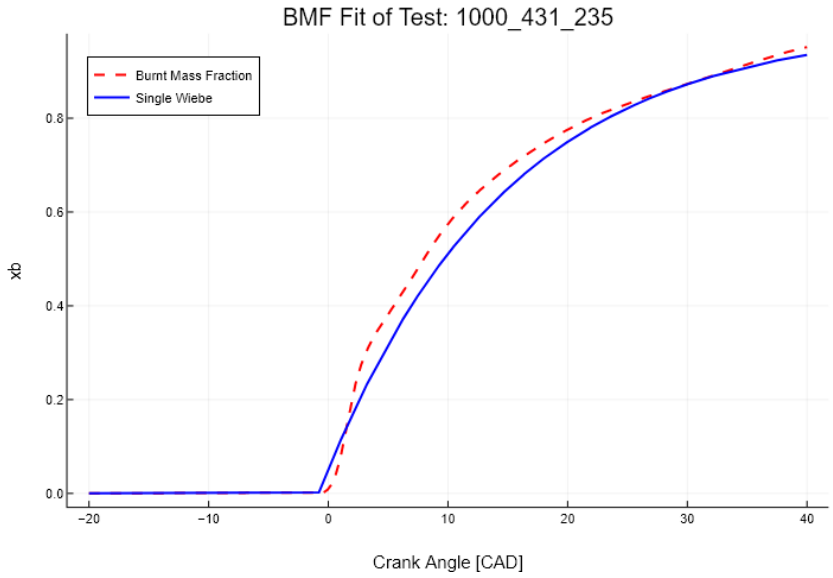

(a) Burnt Mass Fraction

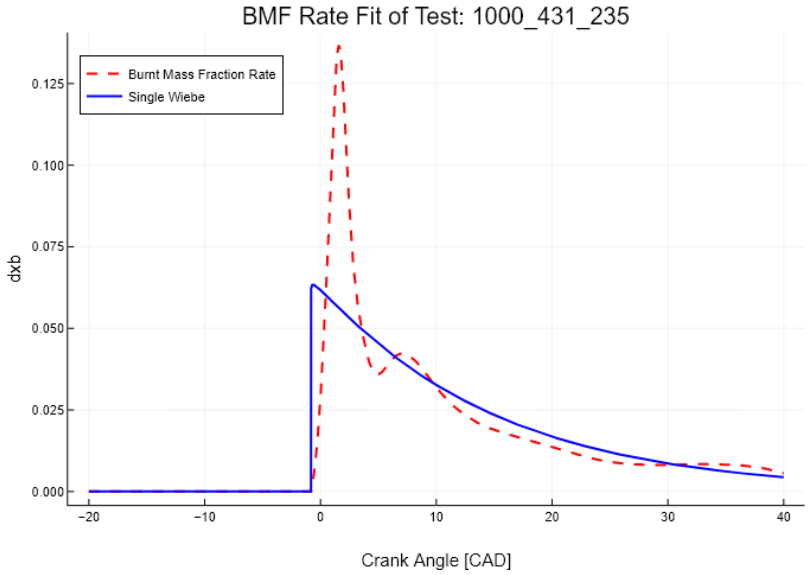

(b) Burnt Mass Fraction Rate

Figure 3.6: Single Wiebe Function Fit

As it is obvious, the result can't be accepted due to the complexity of the Heat Release Rate curve. Therefore, it is necessary to increase the degree of wiebe function in order to improve the results.

3.7.5 Double Wiebe Function

For more accuracy, Double Wiebe Function (equation 2.41) was also fitted. Although, the coefficients that have to be determined are more, the results are better.

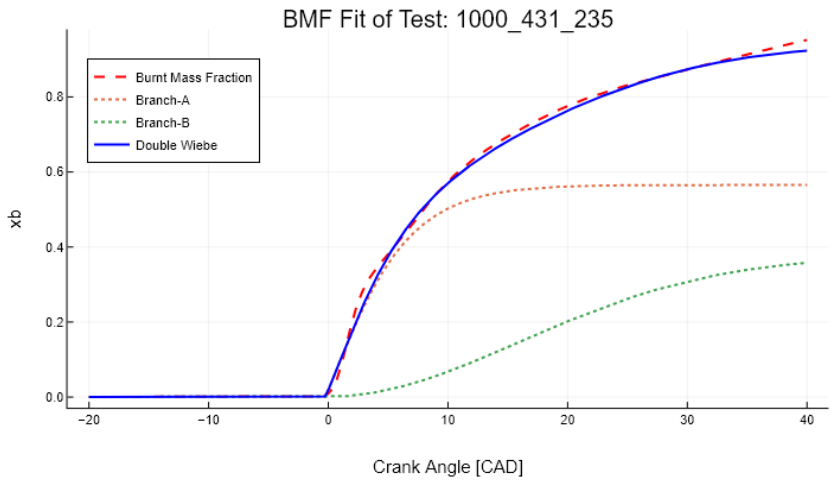

(a) Burnt Mass Fraction

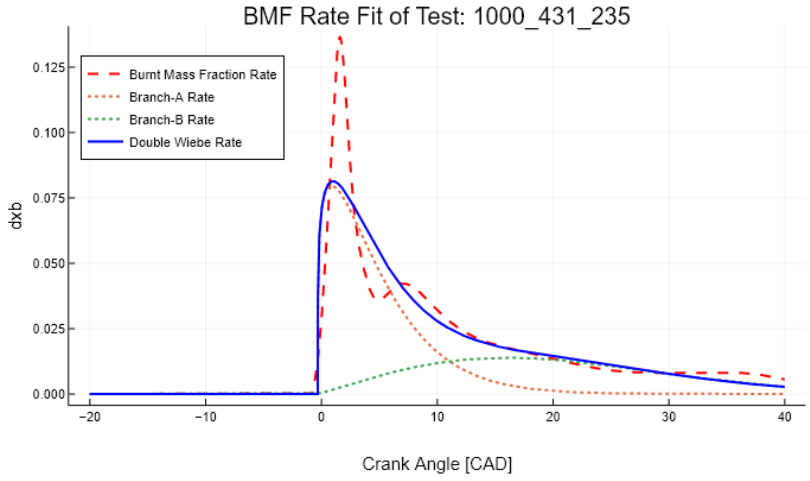

(b) Burnt Mass Fraction Rate

Figure 3.7: Double Wiebe Function Fit

However, it seems that the accuracy of Double Wiebe is not satisfying because it can't model the second phase of combustion which is the combustion of methanol. Thus, more complexity have to be added for better results.

3.7.6 Triple Wiebe Function

Triple Wiebe Function (equation 2.41) was also investigated. In this occasion, the complexity of the function is considerable, the coefficients that have to be determined are even more, but the results are the best better comparing with Single and Double Wiebe Function Fitting.

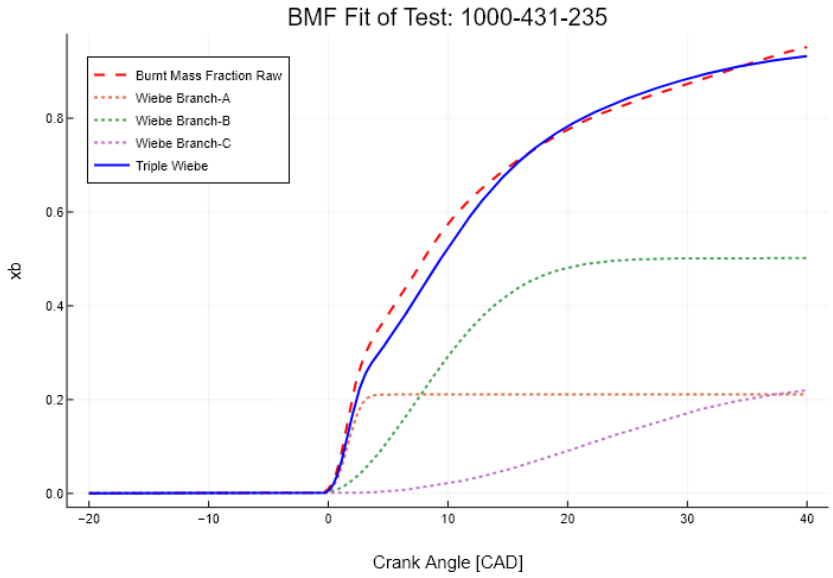

(a) Burnt Mass Fraction

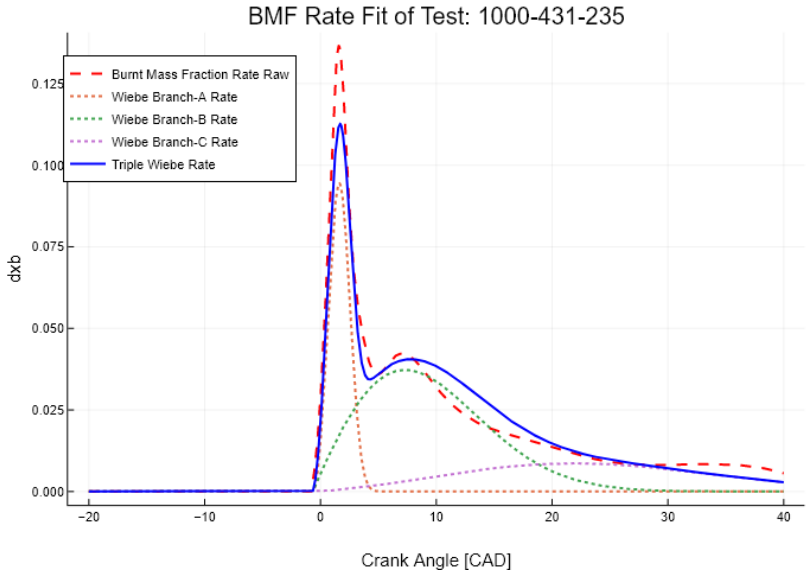

(b) Burnt Mass Fraction Rate

Figure 3.8: Triple Wiebe Function Fit

Triple Wiebe Function seem to model all phases of combustion adequately and as a result it was finally selected for the combustion model.

3.7.7 Wiebe Fitting Conclusions

As mentioned earlier, in order to achieve more accuracy in the combustion model, Triple Wiebe Function was selected, even though the complexity is high and the parameters are many.

It is mentioned that the combustion efficiency η_{comb} it is considered as Wiebe Parameter.

All things considered, and after fitting the wiebe functions, the Wiebe Parameters were defined and are presented in Appendix.

3.8 Wiebe Parameters Models

The wiebe parameters that were determined in the previous stage have not constant values and as a result a method has to be found in order to be possible their accurate estimation.

Some parameters have almost constant values regardless the experiment condition. These parameters are:

$$\Delta\theta_1 \ , \ \ m_1 \ , \ \ m_3 \ , \ \ \lambda_{33}$$

In most parameters Lasso Regression was used, which was described in section 2.6 in order to find polynomial equations that best predict each wiebe parameter. These equations have as inputs the speed, the diesel, methanol and air consumption, the injection time and the ignition time. After some trials, it was selected the degree of polynomials that gives accepted results and at the same time keeps the complexity of these equations at low levels. The parameters which are predicted with good precision are:

$$\Delta\theta_2 \ , \ \ \Delta\theta_3 \ , \ \ m_2 \tag{3.11}$$

The function that predicts the above parameters is:

$$RegressonModel = A \cdot N + B \cdot \phi_{dies} + C \cdot \phi_{meth} + D \cdot \theta_{inj} + E \cdot \phi_{id} + F \tag{3.12}$$

The Amplitude Correction Factor of the premixed phase of the combustion λ_{31} is calculated based on the equation 2.43 with some modifications for better results.

$$\lambda_1 = 1 - \frac{a \cdot \phi_{diesel}^{b_1} \cdot (1 - \phi_{methanol})^{b_2}}{\left(\frac{\theta_{ign} - \theta_{inj}}{6 \cdot N}\right)^c} \tag{3.13}$$

The coefficients a, b_1, b_2, c were determined and are presented in Appendix.

Thus, the Amplitude Correction Factor λ_{32} can be determined by equation 2.40:

$$\lambda_2 = 1 - \lambda_1 - \lambda_3 \tag{3.14}$$

The combustion efficiency can be modeled by an expression:

$$\eta_{comb} = 100 \cdot (1 - exp(-(a \cdot \phi_{diesel}^{b} \cdot (1 - \phi_{methanol})^{c} \cdot (N/1000)^{d} \cdot (\theta_{ign} - \theta_{inj})^{e}))) \tag{3.15}$$

where a, b, c, d and e are calibrating parameters.
In the above expressions, ϕ_{diesel} and $\phi_{methanol}$ is the equivalence ratio of diesel and methanol respectively, θ_{ign} is the ignition time in CAD, θ_{inj} is the injection time in CAD,ϕ_{id} is the ignition delay in CAD, and N is the engine's speed in RPM.
All calibrated coefficients of the above model are presented in Appendix.

3.9 Pressure Estimation Model

The final step of the combustion model, after have been estimated the Gross Heat Release Rate by the Wiebe Function Model, is to calculate the in-cylinder pressure.

3.9.1 Heat Loss Rate Model

In order to be found the Net Heat Release Rate, it has to be calculated the Heal Loss Rate using the method that described in section 2.3.2 and the equation 2.23.

$$\frac{dQ_h}{dt} = h_c A_w (T - T_w)$$

As mentioned earlier, the heat that is transferred to the cylinder walls is due to convection and radiation but in this work it is assumed that radiation effect is neglected.

For this method, it is declared that the lubricant temperature is assumed to be equal to 100^oC and the reference state is the intake valve close, where the combustion chamber is isolated.

3.9.2 Heat Release Rate Analysis

As the Heat Loss Rate have been calculated, and knowing the Gross Heat Release Rate from the Wiebe Function Model, using the equation 2.20, the Net Heat Release Rate $dQ_n dt$ can be found.

$$\frac{dQ_n}{dt} = \frac{dQ_{ch}}{dt} - \frac{dQ_{ht}}{dt}$$

where dQ_{ch}/dt is the gross heat release rate and dQ_{ht}/dt is the heat loss rate. The following figure shows how the Gross Heat Release Rate is analyzed in Net Heat Release Rate and Heat Loss Rate, based on the Heat Loss Rate model that presented earlier.

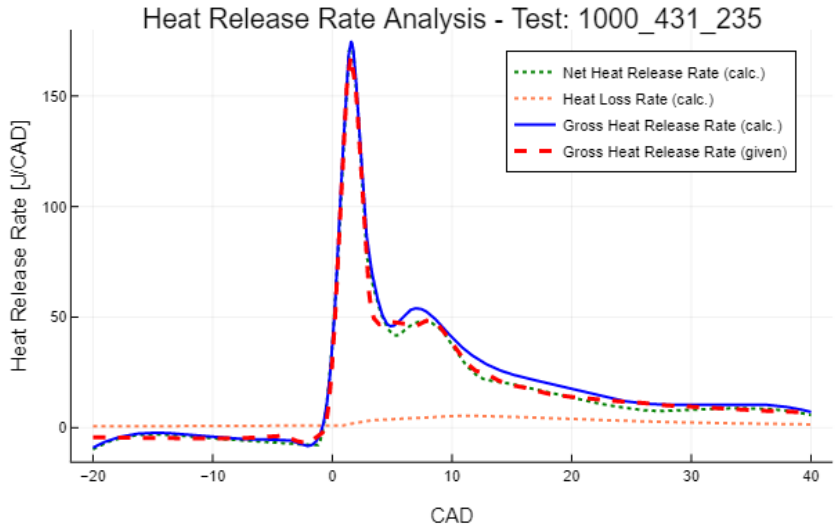

Figure 3.9: HRR Analysis

In this respect, from the Net Heat Release Expression (equation 2.21), using the equation 2.6 and using the derivative definition, can be found the in-cylinder pressure.

$$\frac{dQ_n}{dt} = \frac{\gamma}{\gamma - 1} p \frac{dV}{dt} - \frac{1}{\gamma - 1} V \frac{dp}{dt}$$

The value of the ratio of specific heats,γ, as mentioned earlier, is considered to be constant.

3.9.3 Pressure Estimation Model Conclusions

As a result, the in-cylinder pressure is calculated and the combustion model is ready.

A sample pressure after the initial wiebe function fit is presented below.

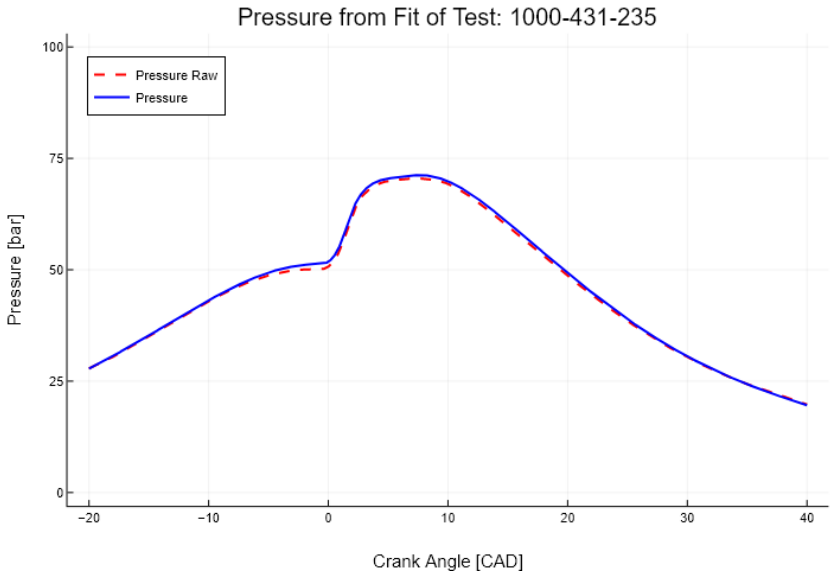

Figure 3.10: Sample of Pressure Estimation

Chapter 4

Results and Validation

In this chapter, the experimental data which were used, the results of the combustion model and some intermediate steps of the model development are presented.

4.1 Initial Wiebe Function Fitting

Initially, in order to find the Wiebe Parameters, a fit of Wiebe Function with Experimental Data was necessary. Below, a sample result from initial Wiebe Function Fitting is presented.

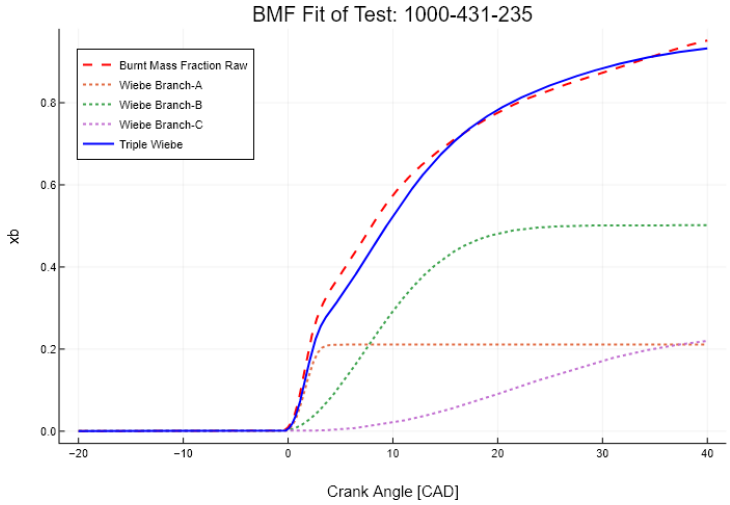

(a) Burned Mass Fraction

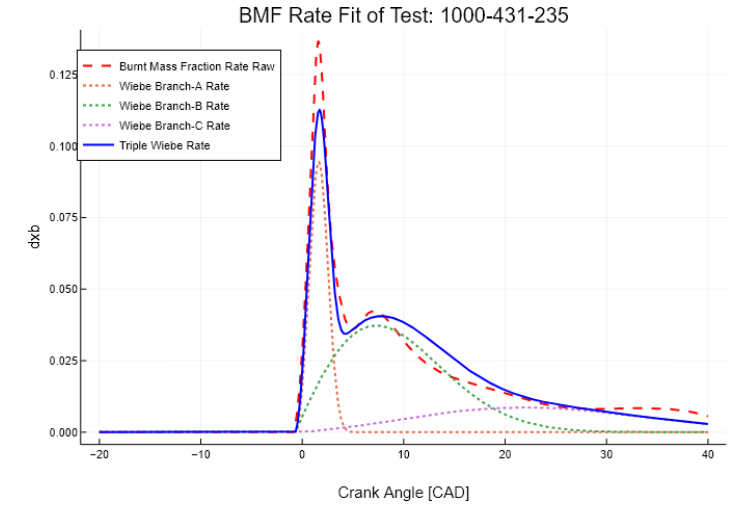

(b) Burned Mass Fraction Rate

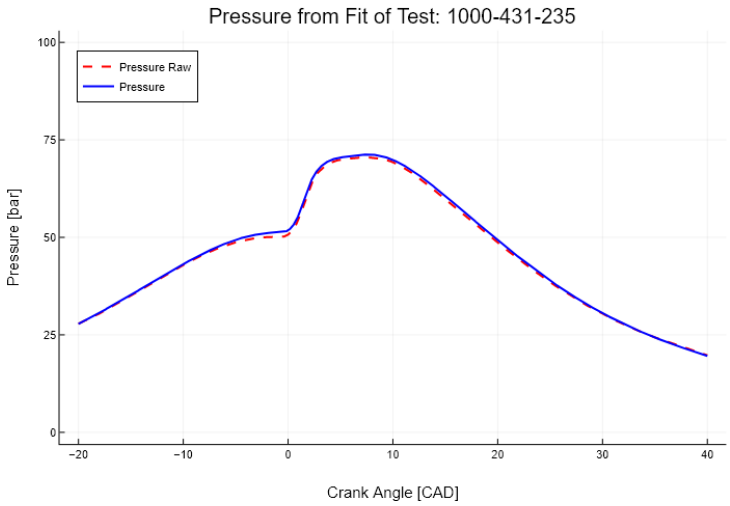

(c) Pressure

Figure 4.1: Results from Initial Wiebe Fit of Test 1000-431-235

This sample fitting result shows that the accuracy of the initial Wiebe Function Fitting is satisfying. The fitted Burned Mass Fraction curve almost coincide with the Burned Mass Fraction Rate of experimental data, except a small declination at the pilot fuel combustion phase. The Burned Mass Fraction Rate is also fitted very well. The fitted curve describe almost precisely the duration both of the pilot fuel combustion and the main fuel combustion. However, the local maxima of the pilot combustion phase is not predicted accurately, hence the small declination in the Burned Mass Fraction curve. The combustion of the main fuel is fitted well with some small declination and the local maxima of the main fuel combustion is estimated well. The third combustion phase is the post-combustion where rest fuel in the chamber is burned. The results of this phase of combustion modeling are acceptable. The most important is that each single wiebe function branch (all three composes the Triple Wiebe Function), model the three phases of combustion. Thus the change of one parameter e.g. the methanol consumption, which primarily contributes in the main combustion branch (2nd brach), will affect primarily this branch, contributing in the model's accuracy. As far as pressure curve concerned, the initial wiebe function fitting seem to overestimate the pressure by experimental data. This may be due to the assumption of the ratio of specific heats which was assumed to be constant, or due to the Heat Loss Rate model which is a semi-empirical approach. In general, the initial wiebe fitting give satisfactory results and the estimations are acceptable. After the initial wiebe fitting, the Wiebe Parameters are determined and in a next stage, the modeling of these parameters is taken place.
More results from the initial wiebe function fitting are presented in Appendix.

The Correlation Coefficients R^2 of the Initial Wiebe Fits for Burned Mass Fraction, Burned Mass Fraction Rate and Pressure are presented in the following table.

Initial Wiebe Fitting R^2			
Test Name	BMF	BMF Rate	Pressure
1000-537-0	0.9959	0.8774	0.9998
1000-431-235	0.9965	0.9588	0.9987
1000-334-417	0.9993	0.9592	0.9992
1000-235-709	0.9948	0.9518	0.9998
1000-875-0	0.9934	0.9402	0.9973
1000-603-552	0.9981	0.946	0.9979
1000-476-770	0.9984	0.9444	0.9969
1300-351-0	0.9997	0.9509	0.9871
1300-351-369	0.9992	0.9516	0.9929
1300-351-738	0.9979	0.9354	0.994
1300-351-1580	0.9966	0.9258	0.9995
1300-772-0	0.9994	0.9496	0.9959
1300-772-441	0.9962	0.9813	0.9978
1300-772-659	0.9968	0.9692	0.9996
1300-772-866	0.9989	0.9166	0.9996

Table 4.1: R^2 of Initial Wiebe Function Fitting Results

4.2 Wiebe Parameters Fitting

In this stage, the fit of the Wiebe Parameters is taken place, which come from the initial Wiebe Function Fitting. Several parameters were assumed to be constant in order to make the combustion model more simple and in the same time keep the model's precision in high levels. As is is obvious by the following figures, the wiebe parameters can be predicted with good accuracy. However, these results depend highly by the ignition delay as it is one parameter that affect the prediction. In this respect, the parameters estimation depend on the prediction of the ignition delay which comes from a semi-empirical model too. However, the results seem to be very satisfying except the combustion efficiency which has the more poor precision. After the estimation of these parameters in combination with the ignition delay prediction, Triple Wiebe Function can be constructing which gives the Burned Mass Fraction and the Burned Mass Fraction Rate, and consequently the

Heat Release Rate and the in-Cylinder Pressure.

The errors of the wiebe parameter fitting are presented in the following table:

Wiebe Parameters Fitting Errors			
Parameter	MSE	RMSE	R^2
$\Delta\theta_2$	0.014724	0.121343	0.9989
$\Delta\theta_3$	0.113974	0.337601	0.9795
m_2	0.000328	0.018102	0.9829
λ_1	4.68E-06	0.002163	0.9987
$\eta_{comb,3}$	6.441056	2.537924	0.5365

Table 4.2: Wiebe Parameters Fitting Errors

The results from the Wiebe Parameters Fitting are presented below.

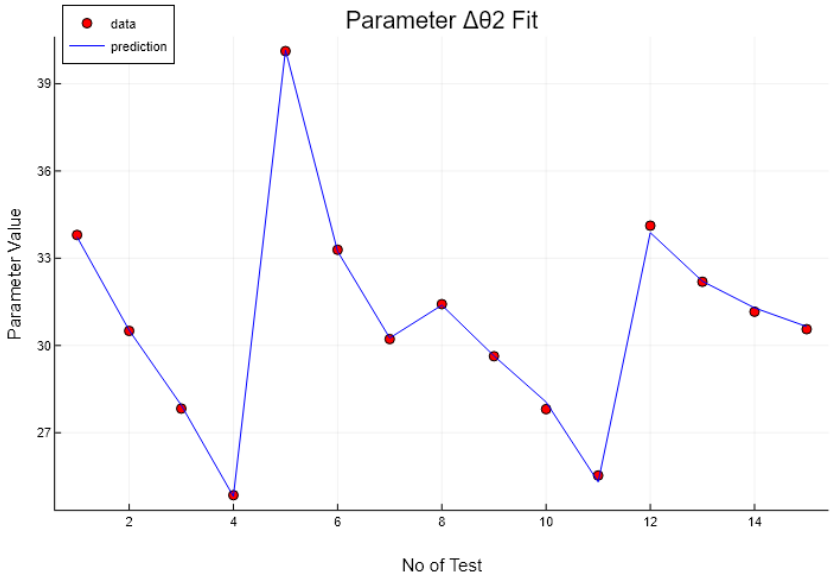

(a) Model Validation

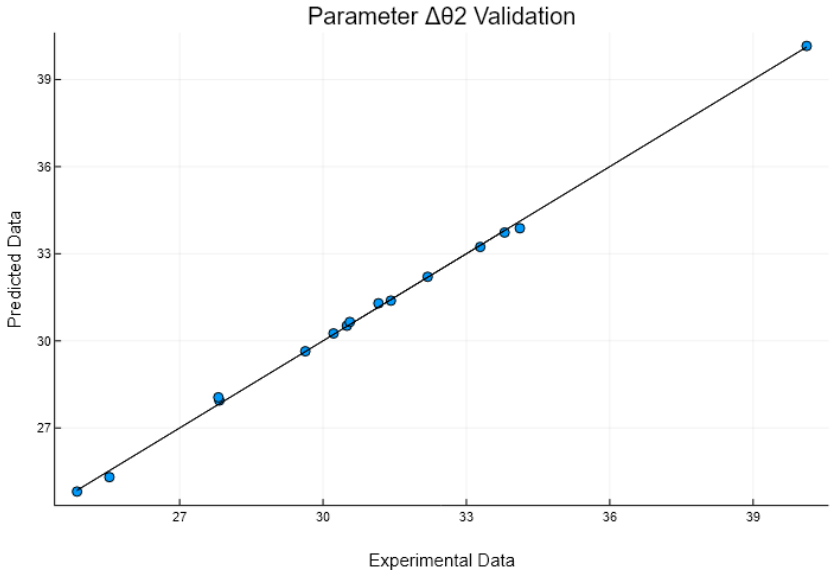

(b) Predicted vs. Experimental Data

Figure 4.2: Fit of Parameter $\Delta\theta_2$

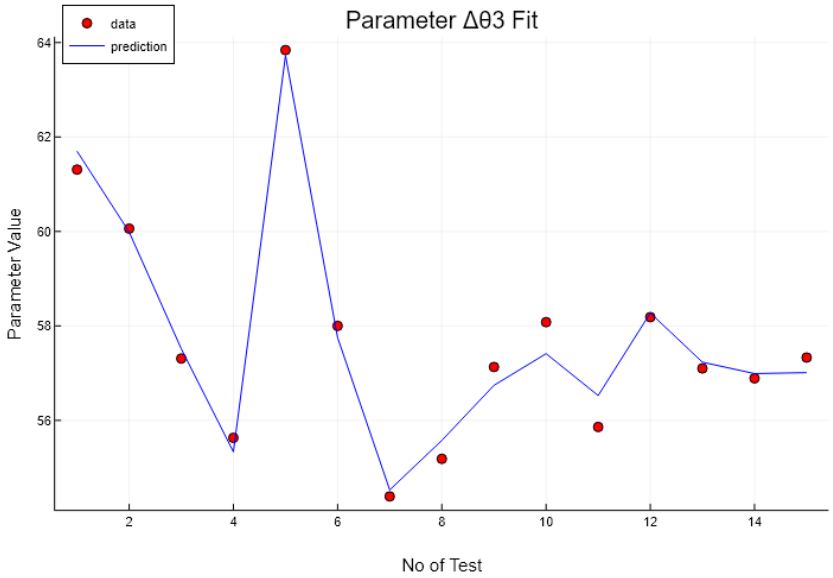

(a) Model Validation

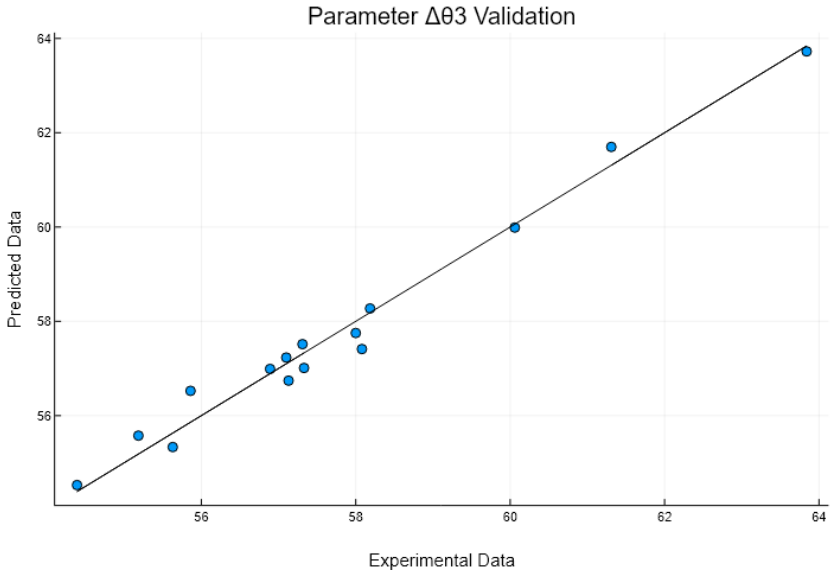

(b) Predicted vs. Experimental Data

Figure 4.3: Fit of Parameter $\Delta\theta_3$

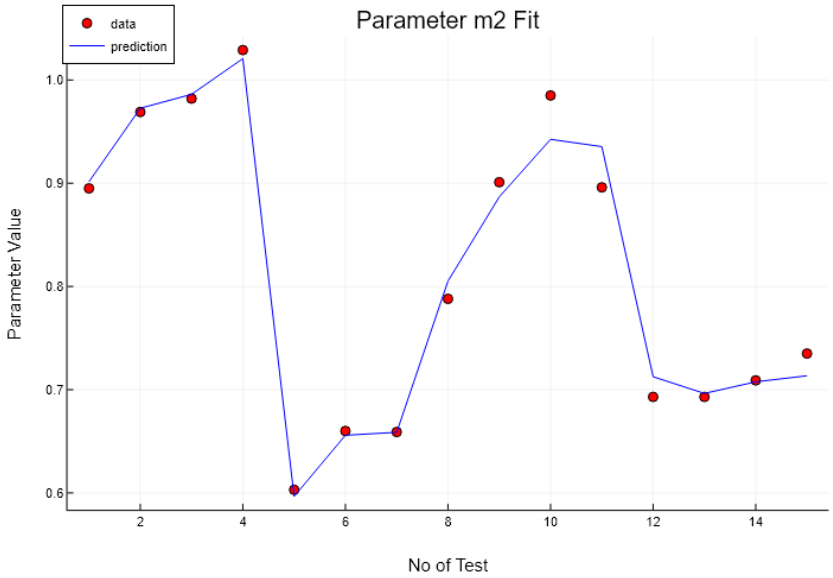

(a) Model Validation

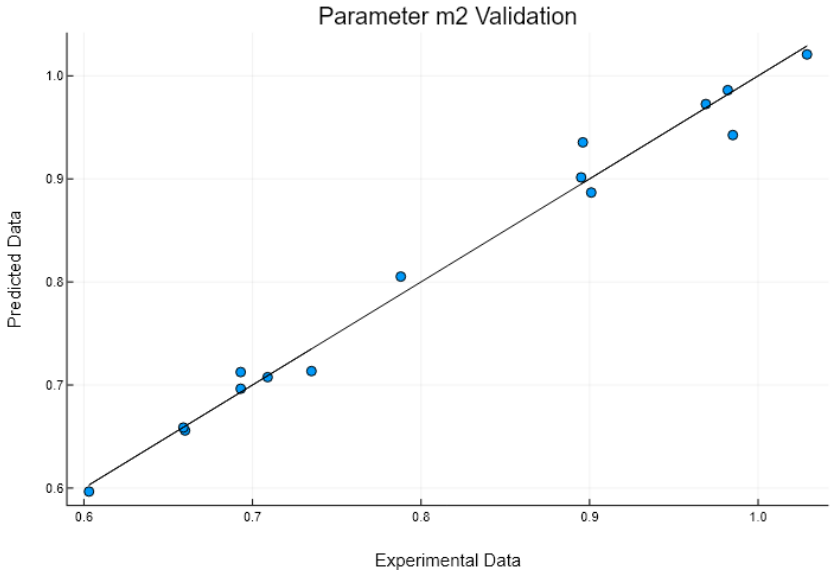

(b) Predicted vs. Experimental Data

Figure 4.4: Fit of Parameter m_2

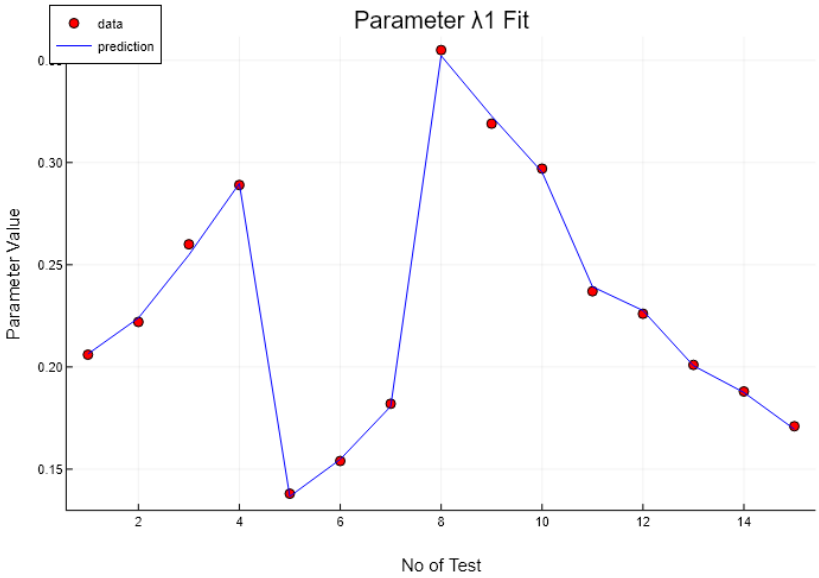

(a) Model Validation

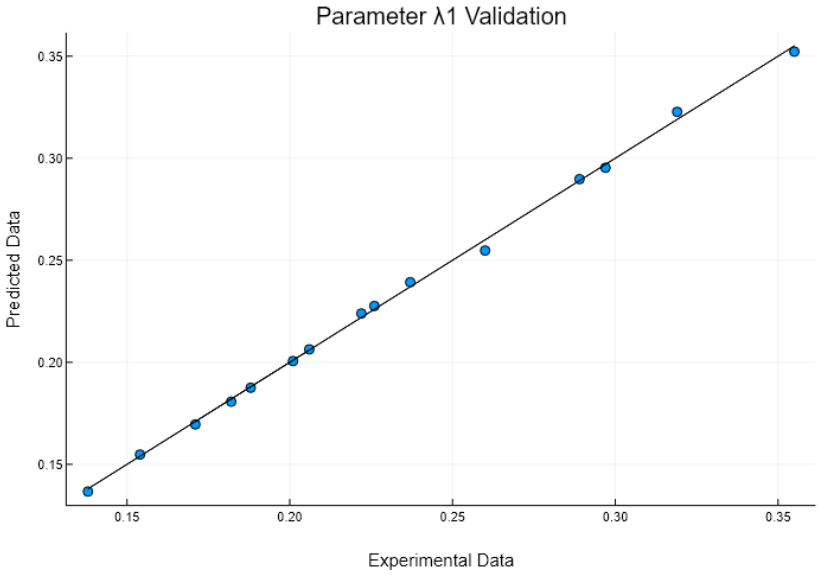

(b) Predicted vs. Experimental Data

Figure 4.5: Fit of Parameter λ_1

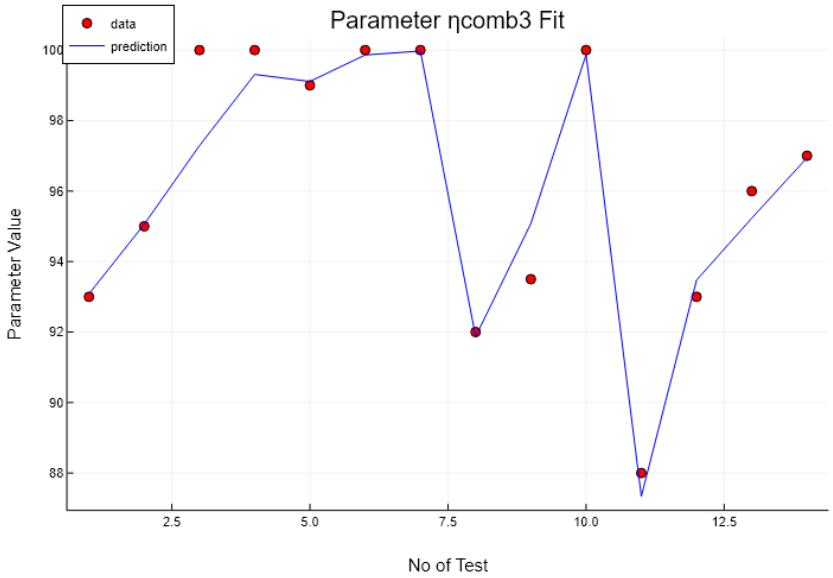

(a) Model Validation

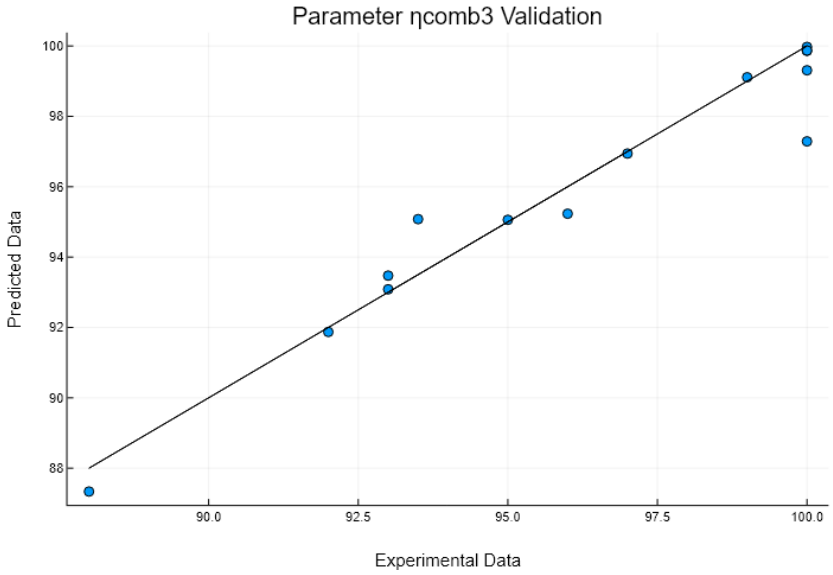

(b) Predicted vs. Experimental Data

Figure 4.6: Fit of Parameter η_{comb}

4.3 Combustion Model Validation

The complete Combustion Model has to be validated with the experimental data which were used in its construction, to ensure its accuracy.

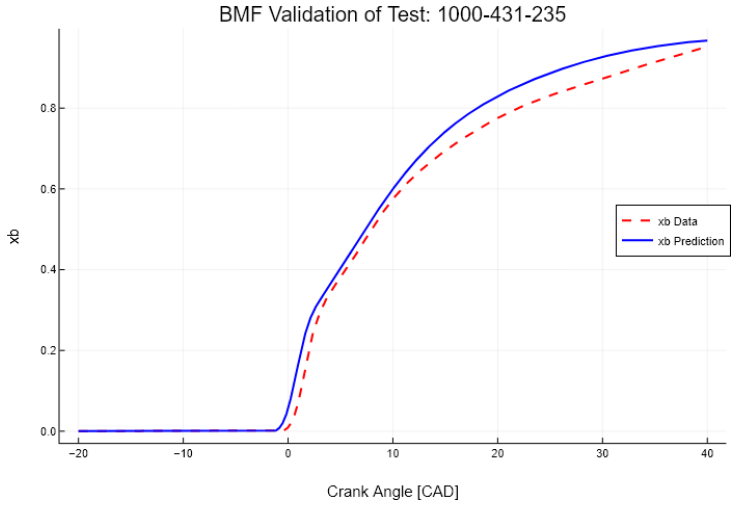

(a) Burned Mass Fraction

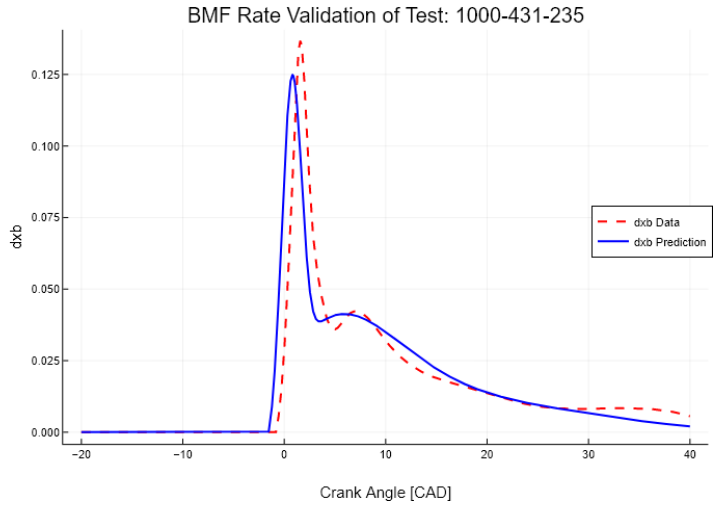

(b) Burned Mass Fraction Rate

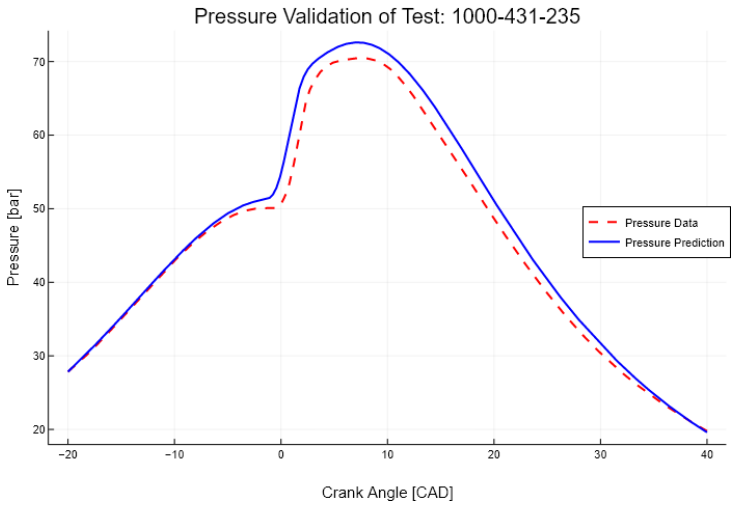

(c) Pressure

Figure 4.7: Combustion Model Validation with Test 1000-431-235

More validation figures are presented in Appendix.

The above figure shows a sample validation of the combustion model and with a first view the results are satisfying. The Burned Mass Fraction seem to be slightly overestimated and is obvious that the ignition delay prediction is slightly less than the actual ignition delay. However, the total Burned Mass Fraction is estimated accurately. In the Burned Mass Fraction Rate figure, the ignition delay underestimation is more obvious and the predicted Start of Combustion is earlier than the actual. Nevertheless, the peaks of the pilot fuel combustion phase and the main fuel combustion phase seem to be predicted more accurately than the initial wiebe function fitting which means that the model mitigates the experimental results unavoidable error. Furthermore, the duration of all three phases are estimated with good accuracy and finally give an acceptable prediction result. According to the pressure diagram, an overestimation of the experimental data is obvious, as it was in the initial wiebe function fitting. However, the change in slope of the curve seem to be predicted well and all three predictions seem to be acceptable.
The Correlation Coefficients R^2 of the Predicted Burned Mass Fraction, Burned Mass Fraction Rate and Pressure from the Combustion are presented in the following table.

Combustion Model Validation R^2			
Test Name	BMF	BMF Rate	Pressure
1000-235-709	0.9982	0.9217	0.9958
1000-334-417	0.999	0.9565	0.9972
1000-431-235	0.99	0.7598	0.9828
1000-476-770	0.9884	0.819	0.9489
1000-537-0	0.977	0.6157	0.9776
1000-603-552	0.9971	0.9005	0.9858
1000-875-0	0.9995	0.9537	0.9946
1300-351-1580	0.9984	0.8355	0.9935
1300-351-369	0.9978	0.9188	0.9863
1300-351-738	0.9919	0.9032	0.9966
1300-772-0	0.9995	0.9466	0.9934
1300-772-441	0.9987	0.9601	0.9962
1300-772-659	0.9983	0.928	0.9924
1300-772-866	0.9959	0.8804	0.987

Table 4.3: R^2 of Combustion Model Validation Results

4.4 Combustion Model Prediction outside Calibration Region

In this section, the combustion model will be compared with the 1100 RPM Data which were not used in it's calibration. This type of validation is necessary to ensure the accuracy of the model.

A sample result is presented in the following figure.

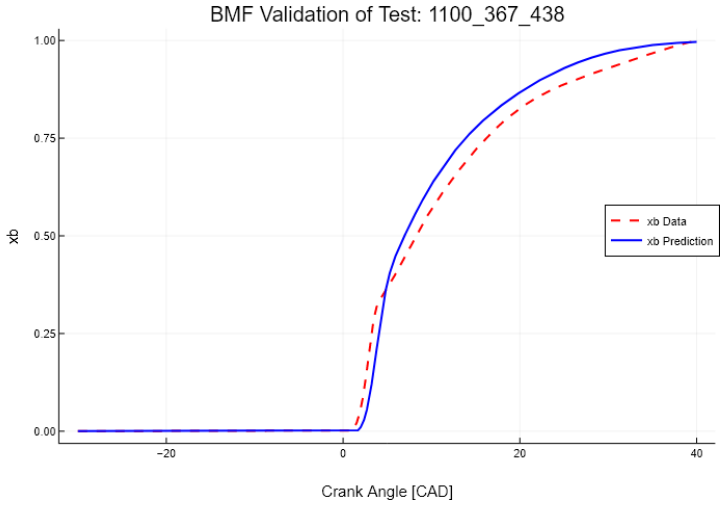

(a) Burned Mass Fraction

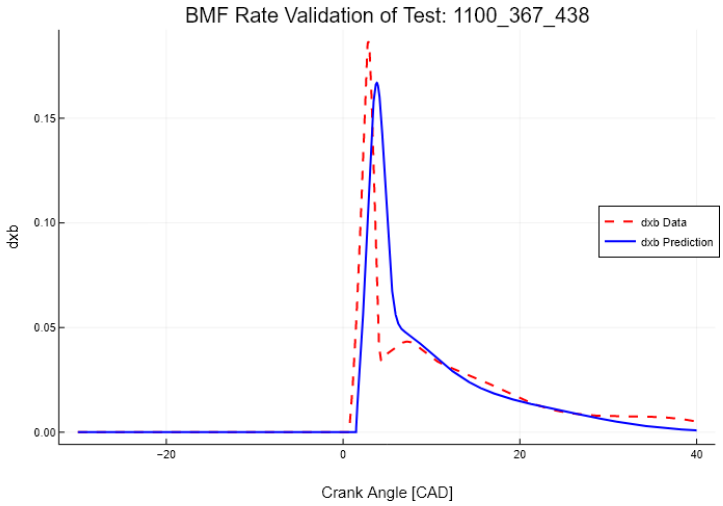

(b) Burned Mass Fraction Rate

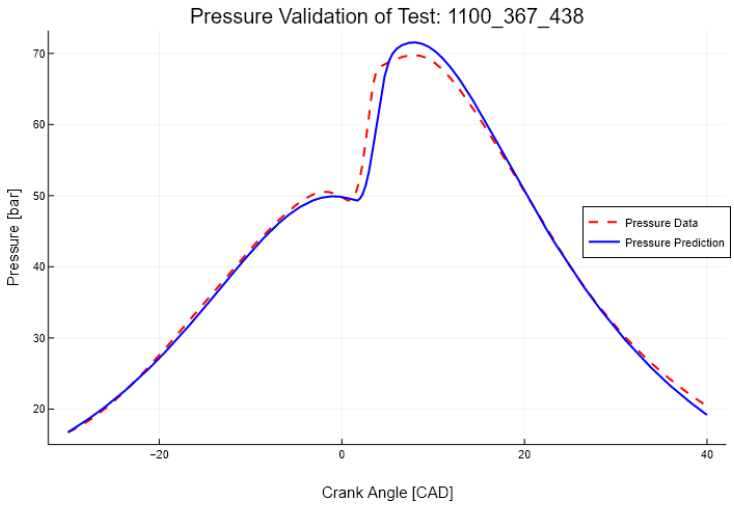

(c) Pressure

Figure 4.8: Combustion Model Validation with Test 1100-367-438

As the above figure shows, the prediction of the three curves has more declination compared with the experimental data. This is unavoidable when zero-dimensional modeling is selected due to the fact that semi-empirical approaches were used and, as mentioned in Chapter 2, there is poor estimation results outside of the calibration region. In this test, the Ignition Delay has been estimated accurately. The Burned Mass Fraction seem to be overestimated after the pilot fuel combustion phase and the total Burned Mass Fraction is higher than the actual. As far as the Burned Mass Fraction Rate concerned, in general the shape of the curve with the experimental curve is similar. The post-combustion phase seem to converge with the experimental results and the duration of three phases of combustion have been estimated accurately. However, the local maxima of the pilot diesel combustion phase has not predicted well and the main fuel combustion phase seem to be overestimated. An overestimation is taken place in pressure curve as well but the change in slope is similar with the experimental curve. In general, the results are not satisfying due to the combustion approach that selected, but the validation show some consequence of the combustion model as the duration of the combustion phases are predicted precisely and the shape of the curve is similar to the experimental data.
More Validation figures are presented in Appendix.

The Correlation Coefficients R^2 of the Predicted Burned Mass Fraction, Burned Mass Fraction Rate and Pressure from the Combustion are presented in the following table.

1100 RPM Prediction Results R^2			
Test Name	BMF	BMF Rate	Pressure
1100-233-730	0.9642	0.6394	0.9651
1100-317-538	0.988	0.63	0.9909
1100-367-438	0.9921	0.4821	0.9914
1100-620-0	0.9962	0.5268	0.9906
1100-657-152	0.9689	0.3989	0.971

Table 4.4: R^2 of Combustion Model 1100 RPM Prediction Results

4.4.1 Combustion Model Conclusions

All things considered, the combustion model seem to give acceptable results as a zero-dimensional approach was used and semi-empirical models

were calibrated with experimental data. As mentioned earlier in this work, the approach that selected does not follow the physical and chemical laws completely, as mathematical empirical expressions was used to keep the complexity of the model at low levels and simultaneously give as accurate results as possible in small time interval. In addition, the model's accuracy depends highly on the experimental data which were used in calibration. However, the results from experiments hide an unavoidable error both from the experiments themselves and from the way that they obtained. Thus, their consequence can't be absolute and as a result the combustion model can't predict them absolutely. However, the validation of the combustion model is acceptable, hence the success of this work for the purpose that has been developed.

Chapter 5

Conclusions and Future Work

5.1 Conclusion

In this diploma thesis, was constructed a combustion model for a Dual Fuel Diesel-Methanol Four-Stroke Marine Engine.

The upcoming legislations and in the same time the willing to protect the environment, have created the aim to find alternative ways to produce power and mitigate the harmful emissions from the atmosphere. In this respect, this work contributes in the search of making engines more efficient and more environmentally friendly by the investigation of methanol use in internal combustion marine engines.

Initially, was investigated the Ignition Delay and were tested some models from bibliography for the purpose of finding a method to estimate the Start of Combustion, having as known the Injection Time.

Afterwards, was used the Wiebe Function in order to find a mathematical expression which can give the Heat Release Rate of the experimental apparatus. In particular, due to the necessity of more accuracy, it was selected the Triple Wiebe function which is a combination of three Single Wiebe functions and can describe three phases of the combustion process.

Thus, with the fitting of Wiebe functions, the Wiebe Parameters were defined. As a result, were investigated some methods to predict these parameters. The basic tool for this purpose was Lasso Regression, which has the advantage of making zero the terms of a mathematical expression that don't contribute in the final result.

Subsequently, the Heat Release Rate, could be estimated completely and to extend the combustion model, was researched the in-cylinder Pressure estimation. In particular, having as known the Heat Release Rate,the calculation of the in-cylinder temperature is possible.

5.2 Future Work

This topic of research is highly attracted nowadays and many engineers are investigating alternative fuels such as methanol and a future work that can be made is the improvement of the combustion model's accuracy.

For instance, the fumigation of methanol that takes place inside the intake manifold at the injection time of methanol, cause a small decrease in the Heat Release Rate curve before the Start of Combustion.

Furthermore, Lasso Regression is a completely empirical method of approach making the calculation error is unavoidable. Thus, a method that follows the physical laws could be investigated, for the purpose of increasing the model's accuracy and subsequently having better predictions.

Finally, the Woschni Heat Transfer Model was observed to be not so accurate, especially during compression phase. Thus, a more sophisticated model should be developed for more accurate predictions.

Bibliography

[1] "Dual fuel process - engine on gas — wärtsilä." https://www.youtube.com/watch?v=6mifHJ3MkfE.

[2] G. P. Merker, C. Schwarz, G. Stiesch, and F. Otto, *Simulating Combustion, Simulation of combustion and pollutant formation for engine-development*. Berlin, Heidelberg: Springer, 2006.

[3] J. B. Heywood, *Internal Combustion Engine Fundamentals, Second Edition*. New York: McGraw-Hill Education, 2018.

[4] R. Stone, *Introduction to Internal Combustion Engines, Third Edition*. London: Palgrave Macmillan, 1999.

[5] G. Karim, *Dual-Fuel Diesel Engines*. CRC Press, 2015.

[6] L. Wei, C. Yao, Q. Wang, W. Pan, and G. Han, "Combustion and emission characteristics of a turbocharged diesel engine using high premixed ratio of methanol and diesel fuel," *Fuel*, pp. 156–163, 2015.

[7] P. Ni, X. Wang, and H. Li, "A review on regulations, current status, effects and reduction strategies of emissions for marine diesel engines," *Fuel*, p. 118477, 2020.

[8] E. Tzannatos, "Ship emissions and their externalities for greece," *Atmospheric Environment*, vol. 44, no. 18, pp. 2194–2202, 2010.

[9] M. Klagkou, "Development of a semi-empirical combustion model for a dual fuel two-stroke low-pressure marine engine," Master's thesis, National Technical University of Athens, School of Naval Architecture and Marine Engineering, Laboratory of Marine Engineering, Athens, 2019.

[10] T.-H. Joung, S.-G. Kang, J.-K. Lee, and J. Ahn, "The imo initial strategy for reducing greenhouse gas(ghg) emissions, and its follow-up actions towards 2050," *Journal of International Maritime Safety, Environmental Affairs, and Shipping*, pp. 1–7, 2020.

[11] S. Verhelst, J. W. Turner, L. Sileghem, and J. Vancoillie, "Methanol as a fuel for internal combustion engines," *Progress in Energy and Combustion Science*, pp. 43–88, 2019.

[12] "Methanex posts regional contract methanol prices for north america, europe and asia.." `https://www.methanex.com/our-business/pricing`.

[13] "Ship & bunker." `https://shipandbunker.com/`.

[14] L. Wei, C. Yao, G. Han, and W. Pan, "Effects of methanol to diesel ratio and diesel injection timing on combustion, performance and emissions of a methanol port premixed diesel engine," *Energy*, pp. 223–232, 2016.

[15] H. Wei, C. Yao, W. Pan, G. Han, Z. Dou, T. Wu, M. Liu, J. Gao, C. Chen, and J. Shi, "To meet demand of euro v emission legislation urea free for hd diesel engine with dmcc," *Fuel*, pp. 33–46, 2017.

[16] "Methanol solvent properties." `https://macro.lsu.edu/howto/solvents/methanol.htm`.

[17] Q. Wang, L. Wei, W. Pan, and C. Yao, "Investigation of operating range in a methanol fumigated diesel engine," *Fuel*, pp. 164–170, 2015.

[18] F. Černík, *Phenomenological Combustion Modelling for Optimization of Large 2-stroke Marine Engines under both Diesel and Dual Fuel Operating Conditions*. PhD thesis, Czech Technical University In Prague, Prague, 2018.

[19] C. D. Rakopoulos, *Internal Combustion Engines I (in Greek)*. Fountas Books, 2013.

[20] J. Dierickx, J. Verbiest, T. Janvier, J. Peeters, L. Sileghem, and S. Verhelst, "Retrofitting a high-speed marine engine to dual-fuel methanol-diesel operation: A comparison of multiple and single point methanol port injection," *Fuel Communications*, vol. 7, p. 100010, 2021.

[21] A. A. Hairuddin, A. Wandel, and T. Yusaf, "Effect of different heat transfer models on a diesel homogeneous charge compression ignition engine," *International Journal of Automotive and Mechanical Engineering (IJAME)*, pp. 1305–1317, 2013.

[22] "Finite heat release with heat transfer." `https://www.engr.colostate.edu/~allan/thermo/page8/page8.html`.

[23] H. S. Soyhan, H. Yasar, H. Walmsley, B. Head, G. T. Kalghatgi, and C. Sorusbay, "Evaluation of heat transfer correlations for hcci engine modeling," *Applied Thermal Engineering*, pp. 541–549, 2009.

[24] I. Glassman and R. A. Yetter, *Combustion (Fourth Edition)*. Burlington: Academic Press, 2008.

[25] H. Zou, L. Wang, S. Liu, and Y. Li, "Ignition delay of dual fuel engine operating with methanol ignited by pilot diesel," *Frontiers of Energy and Power Engineering in China*, pp. 285–290, 2008.

[26] G. Prakash, A. Ramesh, and A. B. Shaik, "An approach for estimation of ignition delay in a dual fuel engine," *SAE Transactions*, vol. 108, pp. 399–405, 1999.

[27] J. Ghojel, "Review of the development and applications of the wiebe function: A tribute to the contribution of ivan wiebe to engine research," *International Journal of Engine Research*, p. 297, 2010.

[28] G.-L. Xu, C.-D. Yao, and C. J. Rutland, "Simulations of diesel–methanol dual-fuel engine combustion with large eddy simulation and reynolds-averaged navier–stokes model," *International Journal of Engine Research*, pp. 751–769, 2014.

[29] S. Xu, D. Anderson, M. Hoffman, R. Prucka, and Z. Filipi, "A phenomenological combustion analysis of a dual-fuel natural-gas diesel engine," *Proceedings of the Institution of Mechanical Engineers, Part D: Journal of Automobile Engineering*, 2016.

[30] "Lasso regression: Simple definition." `https://www.statisticshowto.com/lasso-regression/`.

[31] D. Assanis, Z. Filipi, S. B. Fiveland, and M. Syrimis, "A predictive ignition delay correlation under steady-state and transient operation of a direct injection diesel engine," *Journal of Engineering for Gas Turbines and Power-transactions of The Asme*, pp. 450–457, 2003.

Appendix A

Fuel Properties

In some stages of the combustion model development, they are necessary the Molecular Weights MW of some substances which were taken either bibliography [24],[14] or were calculated.

$$\begin{aligned} MW_{O_2} &= 32 \ \ g/mol \\ MW_{N_2} &= 28 \ \ g/mol \\ MW_{CO_2} &= 44 \ \ g/mol \\ MW_{H_2O} &= 18 \ \ g/mol \end{aligned} \tag{A.1}$$

The two fuels that are examined are Diesel and Methanol. Their characteristics are presented in the following table:

Properties	Diesel	Methanol
Molecular Formula	$C_{12}H_{23}$	CH_3OH
Air Mass to Fuel Mass in Stoichiometric Ratio	14.7	6.45
Lower Heating Value [MJ/kg]	42.5	19.7
Heat of Evaportation [kJ/kg]	260	1178
Cetane Number	51	<5
Molecular Weight [g/mol]	167	32
Auto-Ignition Temperature [oC]	316	464

Table A.1: Diesel & Methanol Characteristics

Appendix B

Models Coefficients

In this chapter, the coefficients of the Wiebe Parameters Models are presented.

The coefficients of Ignition Delay Model:

$$\phi_{id,Assanis} = A \cdot \phi_{pD}^{k} \cdot p^{n} \cdot exp\left(\frac{E_A}{\bar{R} \cdot T}\right) \cdot (6 \cdot N)^{s} \cdot (-t_{inj})^{i} \tag{B.1}$$

are presented in the following table:

Ignition Delay Model Coefficients					
	A	k	n	s	i
ϕ_{id}	13.76012	-0.43286	2.32167	-1.36243	0.330571

Table B.1: Ignition Delay Model Coefficients

The coefficients of Regression Model Function:

$$RegressionModel = A \cdot N + B \cdot \phi_{dies} + C \cdot \phi_{meth} + D \cdot \theta_{inj} + E \cdot \phi_{id} + F \tag{B.2}$$

are presented in the following table:

Regression Models Coefficients						
	A	B	C	D	E	F
$\Delta\theta_2$	0.016901	32.67363	-9.8774	-1.28055	-0.84231	1.453678
$\Delta\theta_3$	0.084558	53.66582	-25.2596	-3.21518	3.301775	-98.87
m_2	0.002868	0.224808	-1.35966	-0.07938	0.185996	-4.40086

Table B.2: Regression Models Coefficients

The Amplitude Correction Factor of the premixed phase of the combustion λ_{31} is calculated based on the equation:

$$\lambda_{31} = 1 - \frac{a_w \cdot \phi_{diesel}^{b_{1,w}} \cdot (1 - \phi_{methanol})^{b_{2,w}}}{\left(\frac{\theta_{ign} - \theta_{inj}}{6 \cdot N}\right)^{c_w}} \tag{B.3}$$

and the calibrated coefficients are mentioned in the following table:

Premixed Combustion Phase Model Coefficients				
	a	b1	b2	c
λ_1	1.937052	0.258295	-0.43954	-0.08813

Table B.3: Premixed Combustion Phase Model Coefficients

The combustion efficiency can be predicted using the equation 3.15

$$\eta_{comb} = 100 \cdot (1 - exp(-(a \cdot \phi_{diesel}^{b} \cdot (1 - \phi_{methanol})^{c} \cdot (N/1000)^{d} \cdot (\theta_{ign} - \theta_{inj})^{e})))$$

The calibrating parameters are:

Combustion Efficiency Models Coefficients					
	a	b	c	d	e
η_{comb}	489.6996	-0.07934	-5.86916	-4.79951	-2.48556

Table B.4: Combustion Efficiency Model Coefficients

Appendix C

Initial Wiebe Function Fit

In this chapter, the rest results from the Initial Wiebe Function Fit are presented.

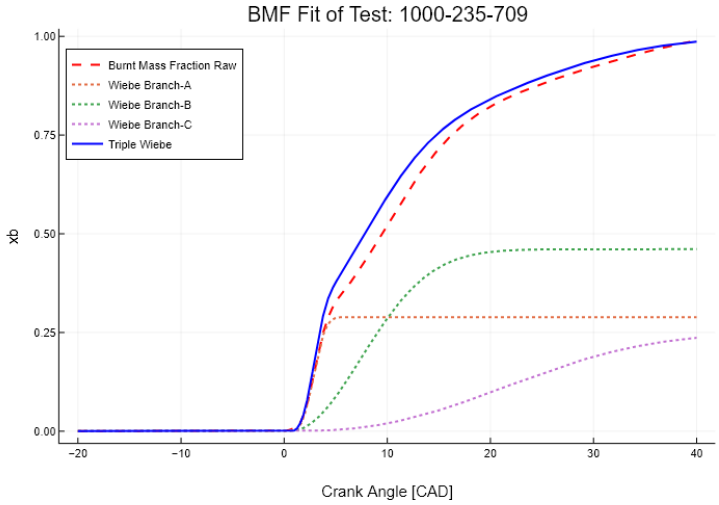

(a) Burned Mass Fraction

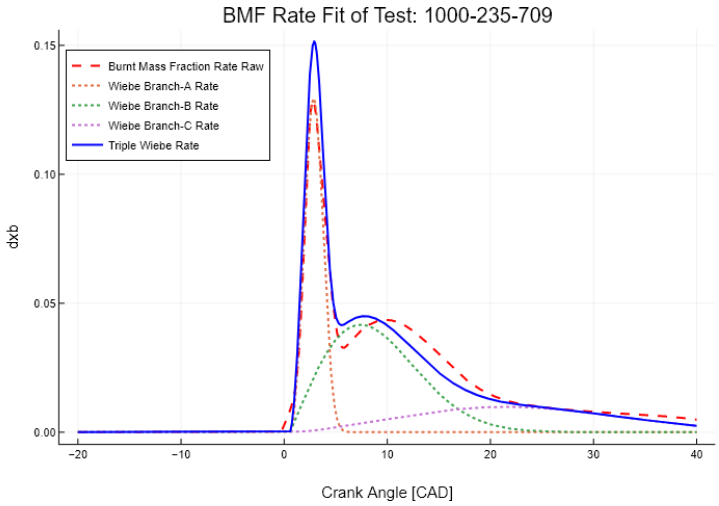

(b) Burned Mass Fraction Rate

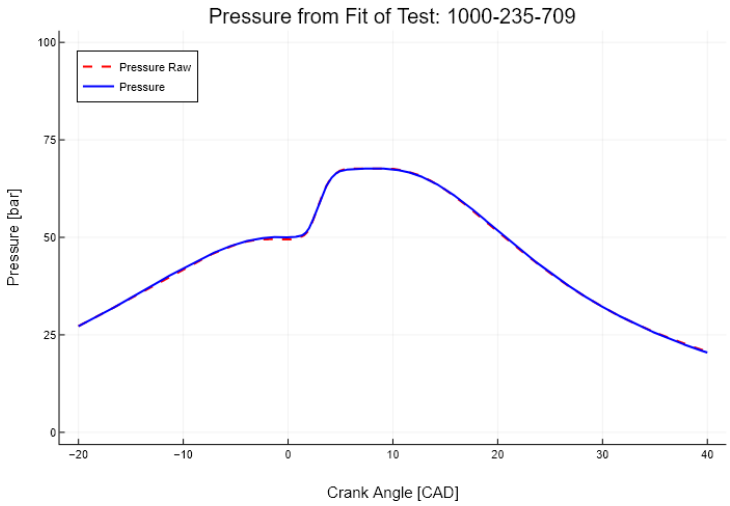

(c) Pressure

Figure C.1: Results from Initial Wiebe Fit of Test 1000-235-709

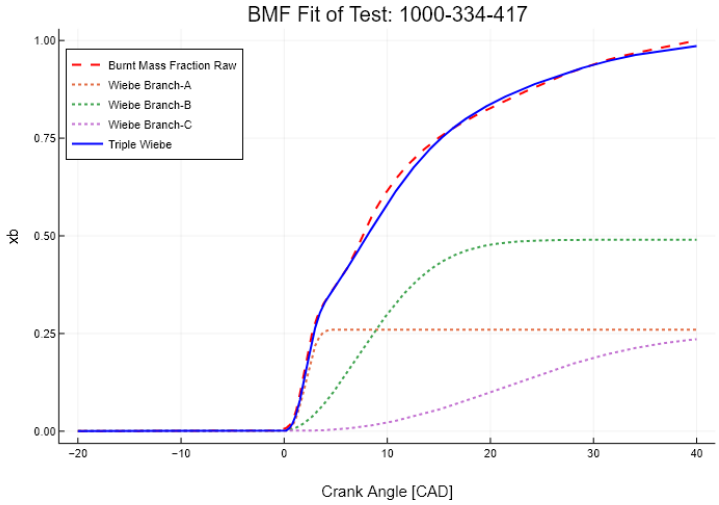

(a) Burned Mass Fraction

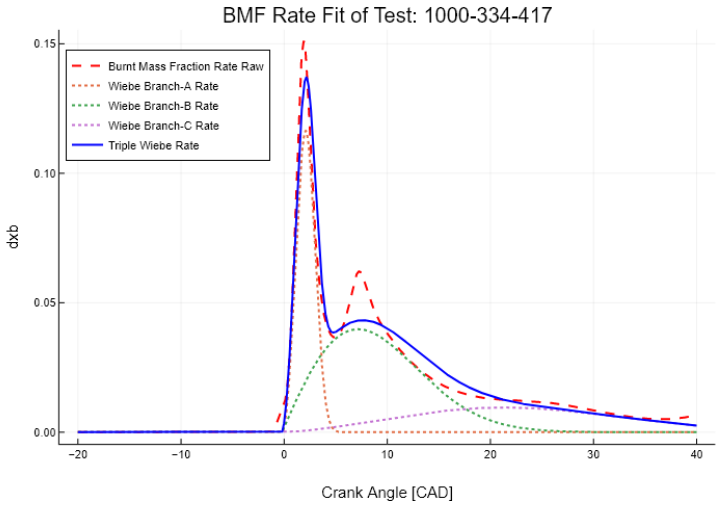

(b) Burned Mass Fraction Rate

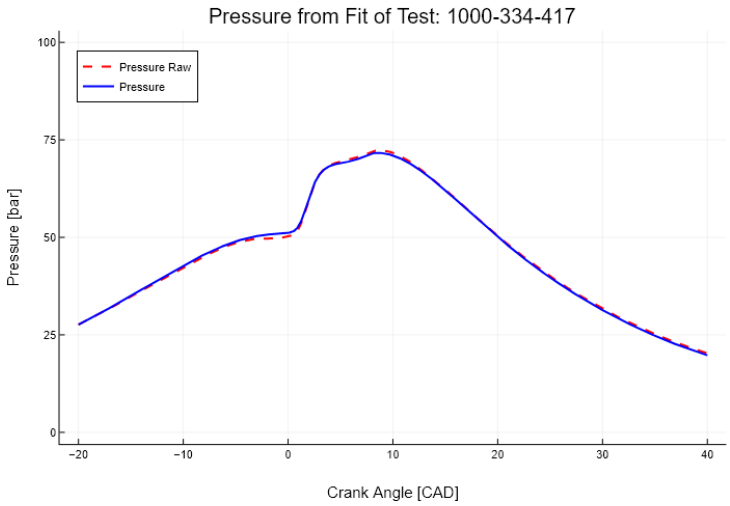

(c) Pressure

Figure C.2: Results from Initial Wiebe Fit of Test 1000-334-417

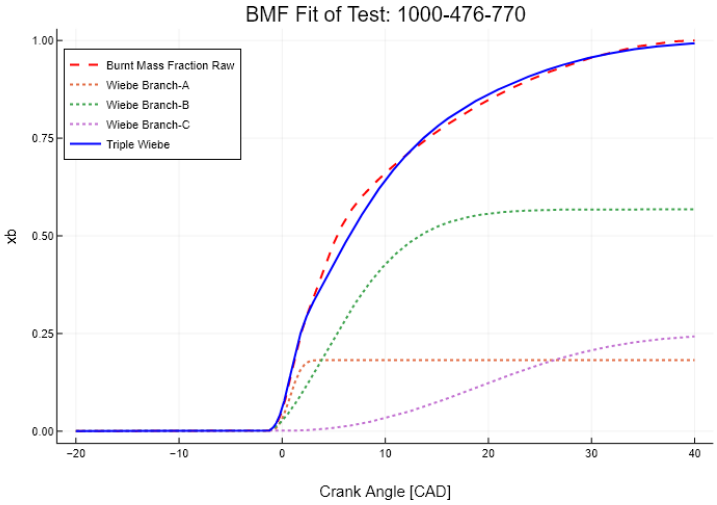

(a) Burned Mass Fraction

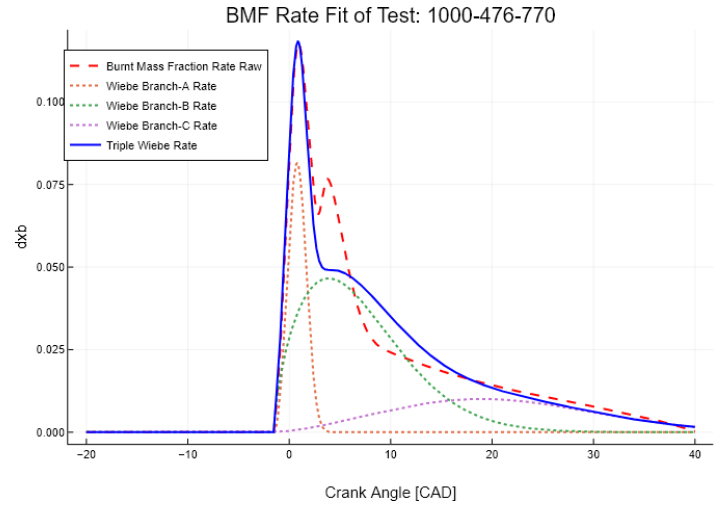

(b) Burned Mass Fraction Rate

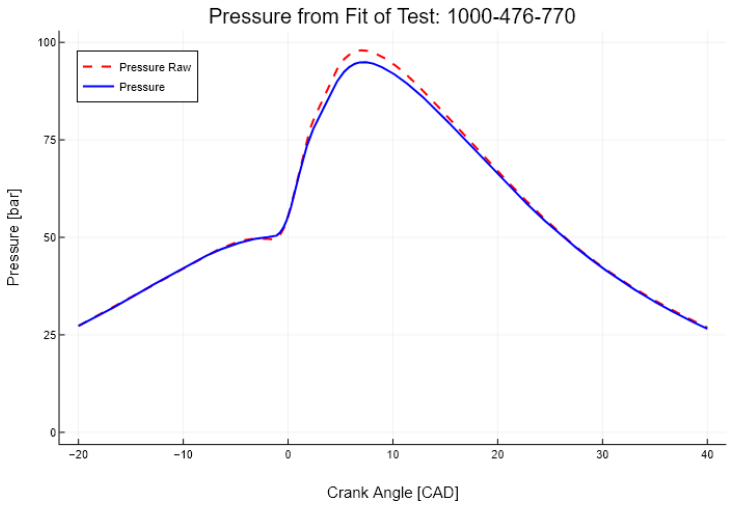

(c) Pressure

Figure C.3: Results from Initial Wiebe Fit of Test 1000-476-770

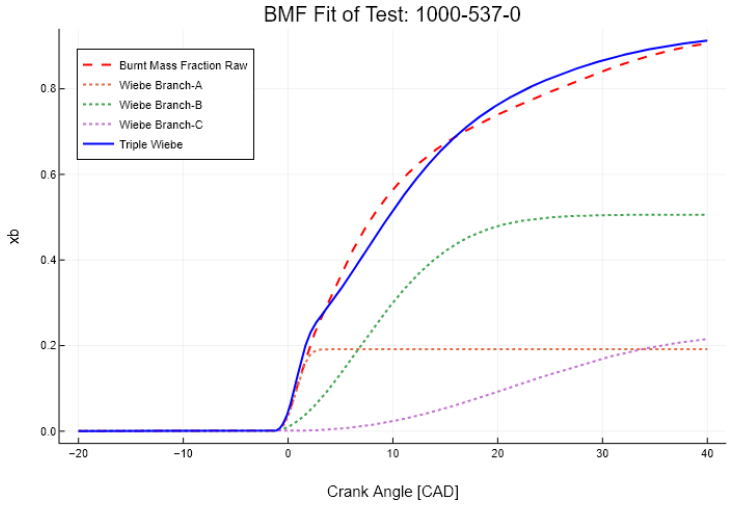

(a) Burned Mass Fraction

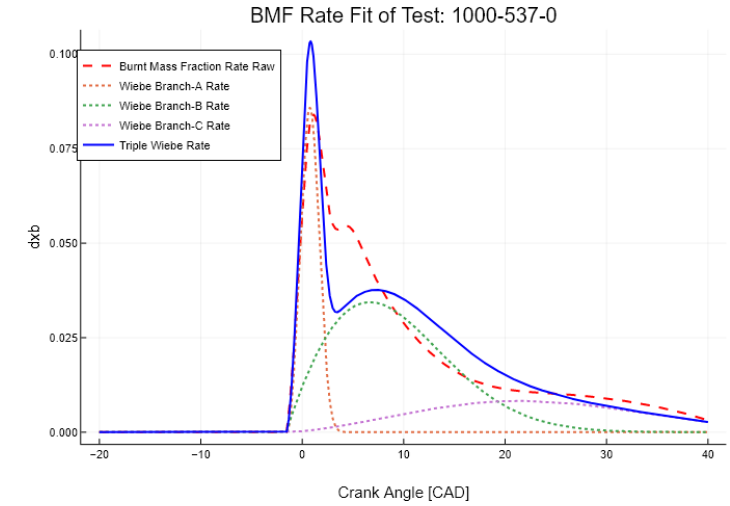

(b) Burned Mass Fraction Rate

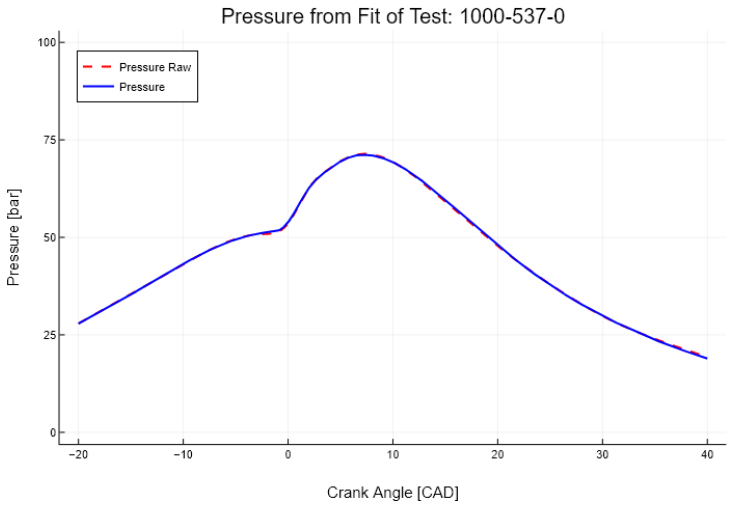

(c) Pressure

Figure C.4: Results from Initial Wiebe Fit of Test 1000-537-0

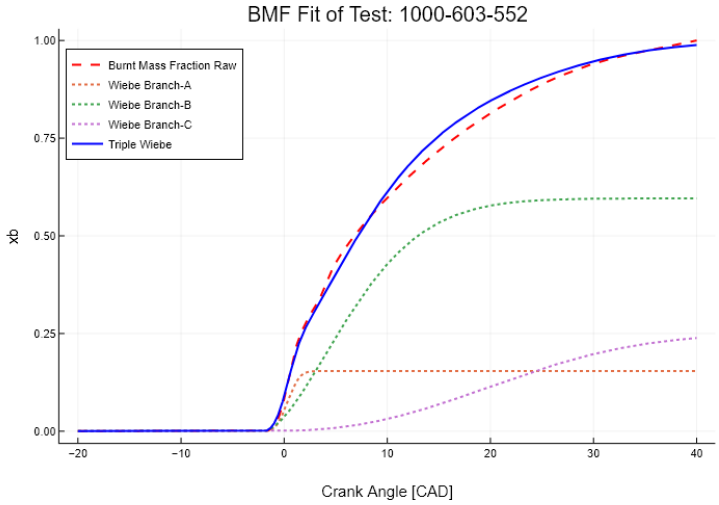

(a) Burned Mass Fraction

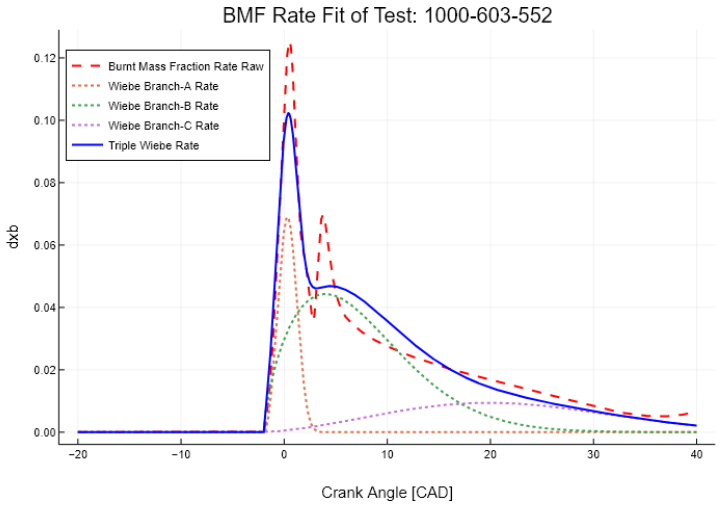

(b) Burned Mass Fraction Rate

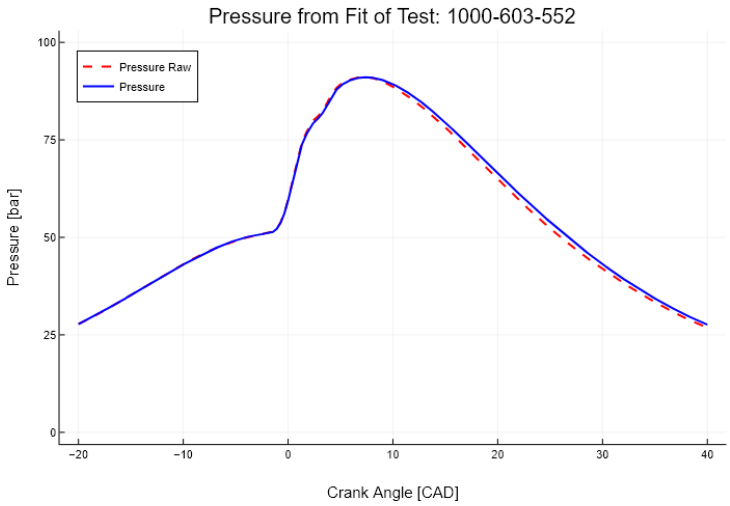

(c) Pressure

Figure C.5: Results from Initial Wiebe Fit of Test 1000-603-552

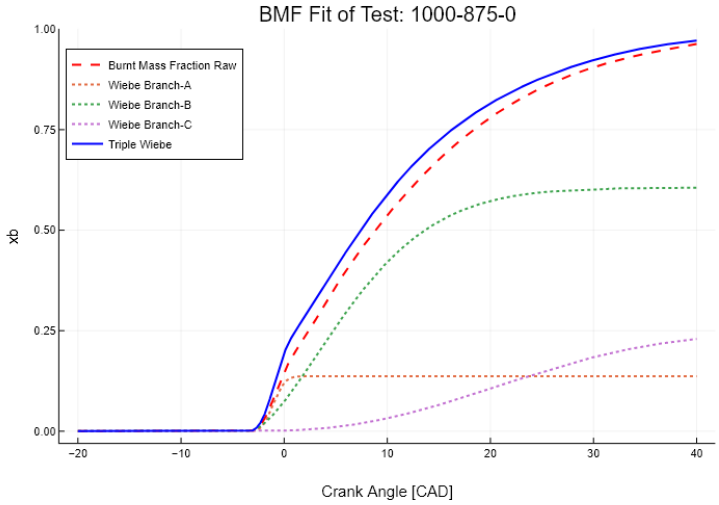

(a) Burned Mass Fraction

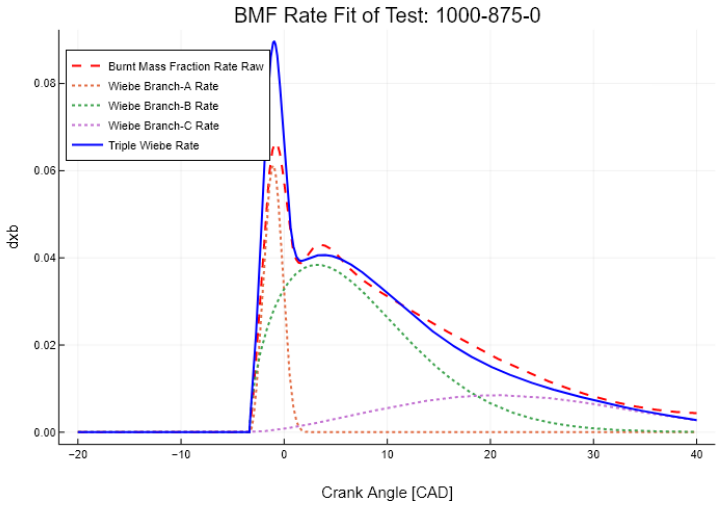

(b) Burned Mass Fraction Rate

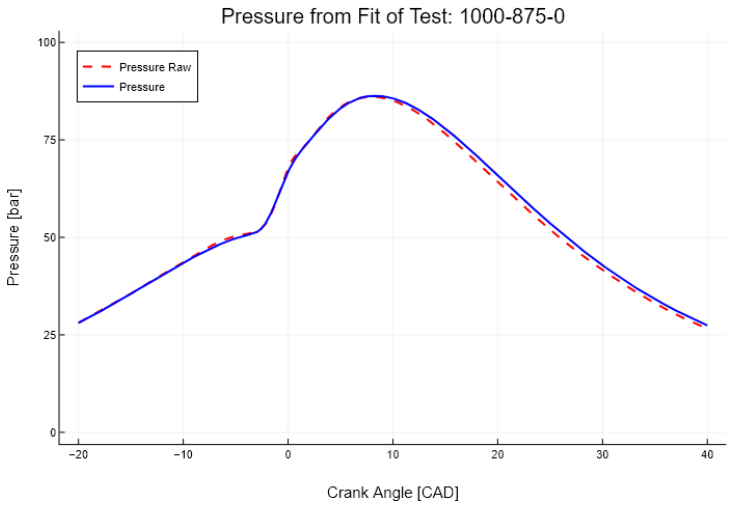

(c) Pressure

Figure C.6: Results from Initial Wiebe Fit of Test 1000-875-0

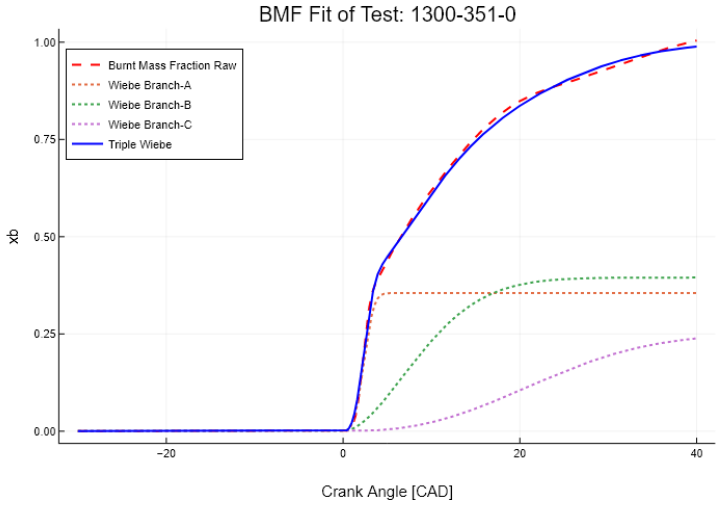

(a) Burned Mass Fraction

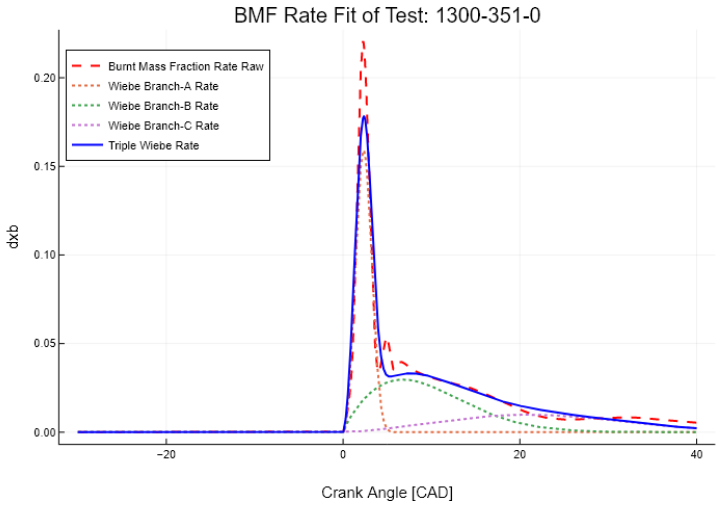

(b) Burned Mass Fraction Rate

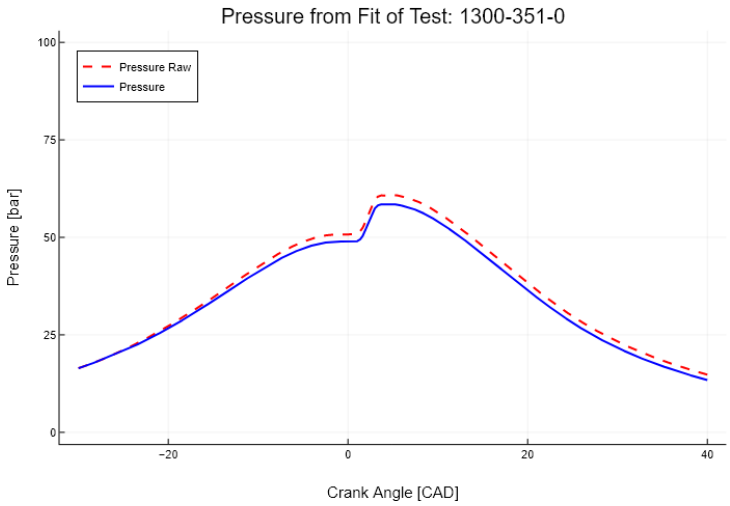

(c) Pressure

Figure C.7: Results from Initial Wiebe Fit of Test 1300-351-0

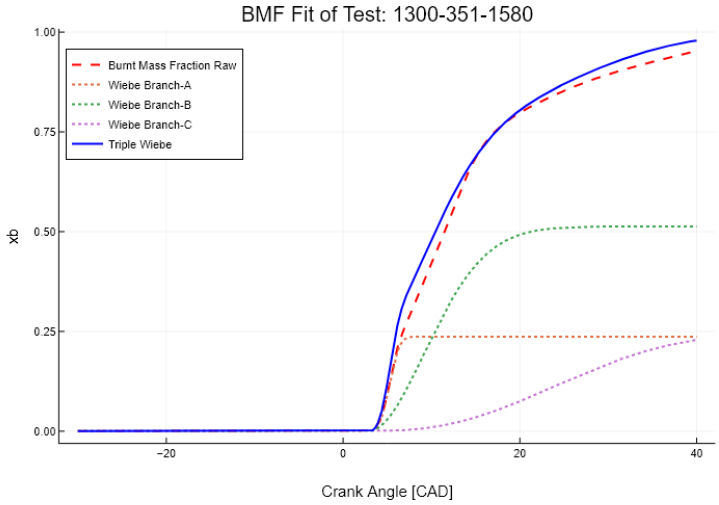

(a) Burned Mass Fraction

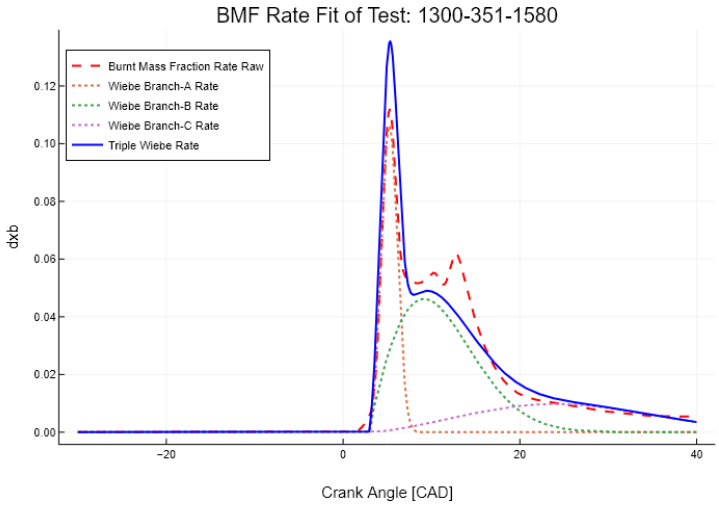

(b) Burned Mass Fraction Rate

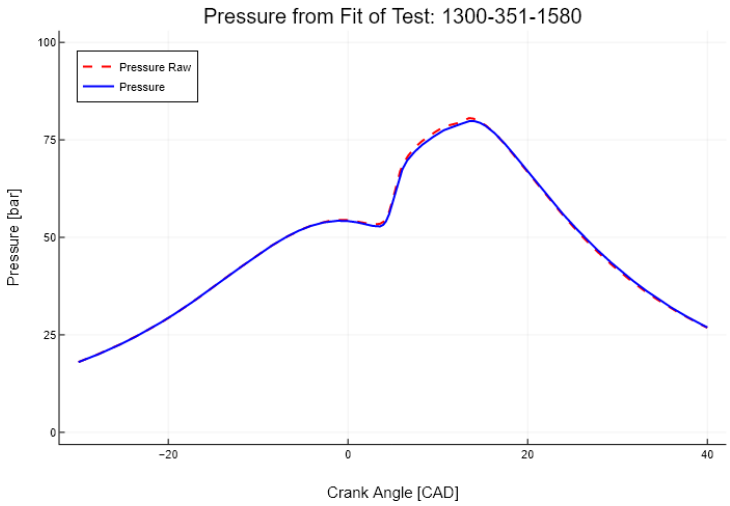

(c) Pressure

Figure C.8: Results from Initial Wiebe Fit of Test 1300-351-1580

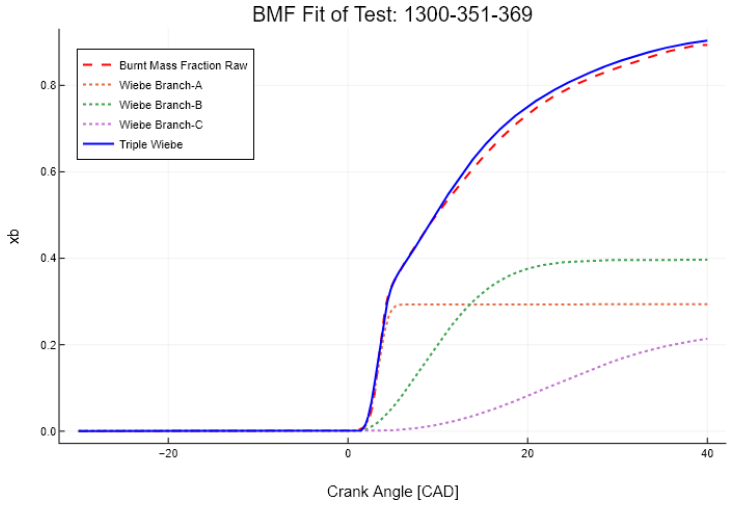

(a) Burned Mass Fraction

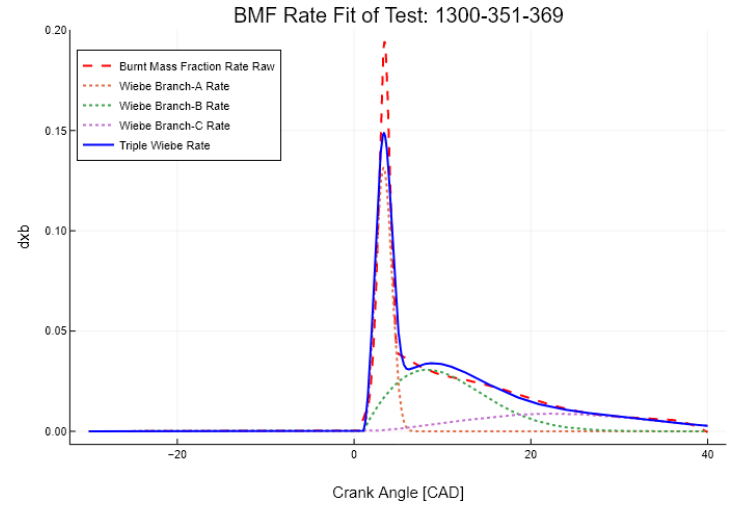

(b) Burned Mass Fraction Rate

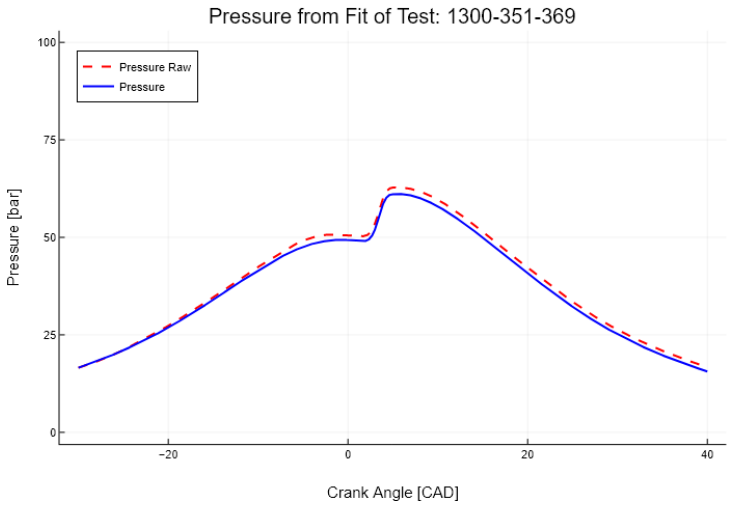

(c) Pressure

Figure C.9: Results from Initial Wiebe Fit of Test 1300-351-369

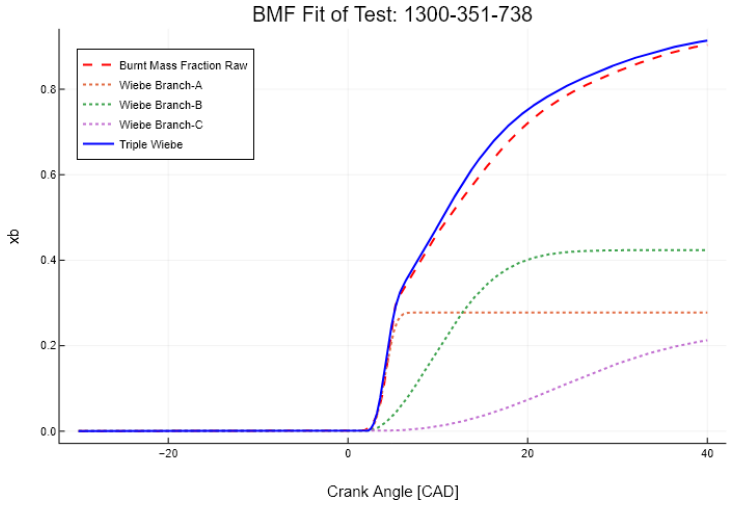

(a) Burned Mass Fraction

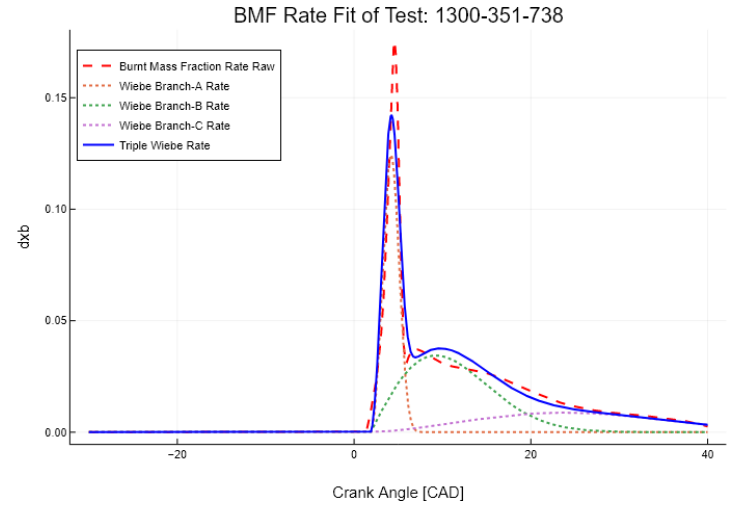

(b) Burned Mass Fraction Rate

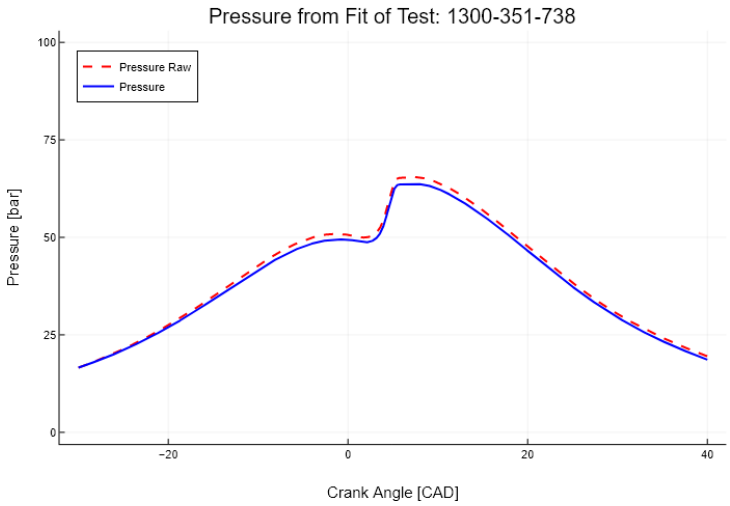

(c) Pressure

Figure C.10: Results from Initial Wiebe Fit of Test 1300-351-738

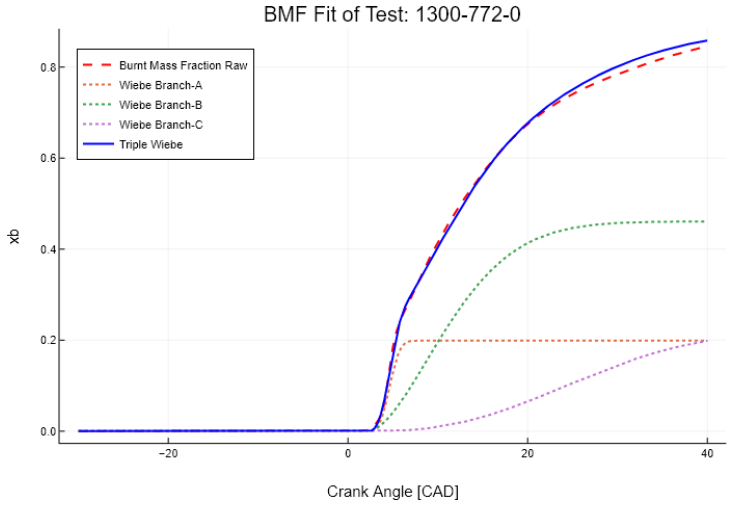

(a) Burned Mass Fraction

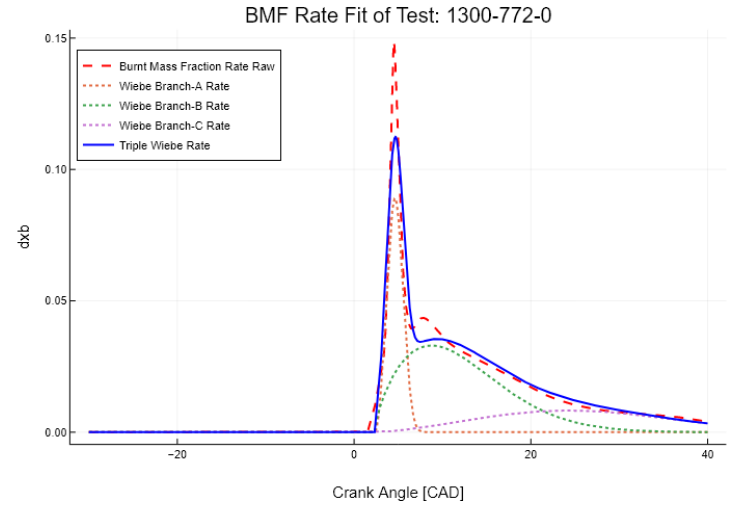

(b) Burned Mass Fraction Rate

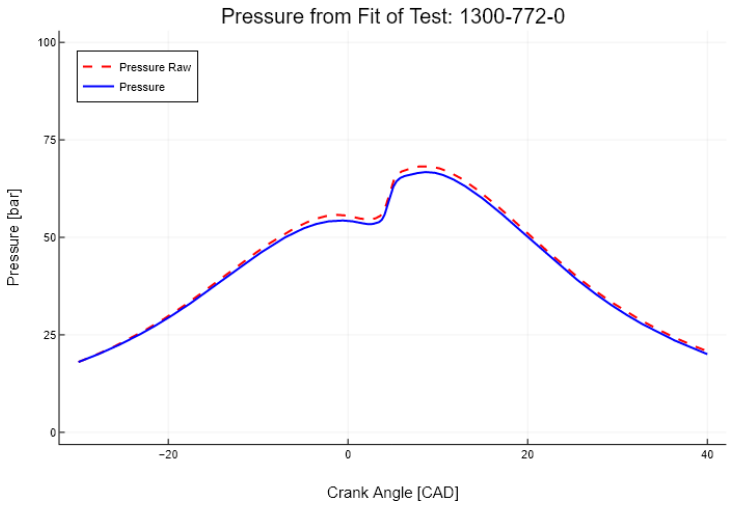

(c) Pressure

Figure C.11: Results from Initial Wiebe Fit of Test 1300-772-0

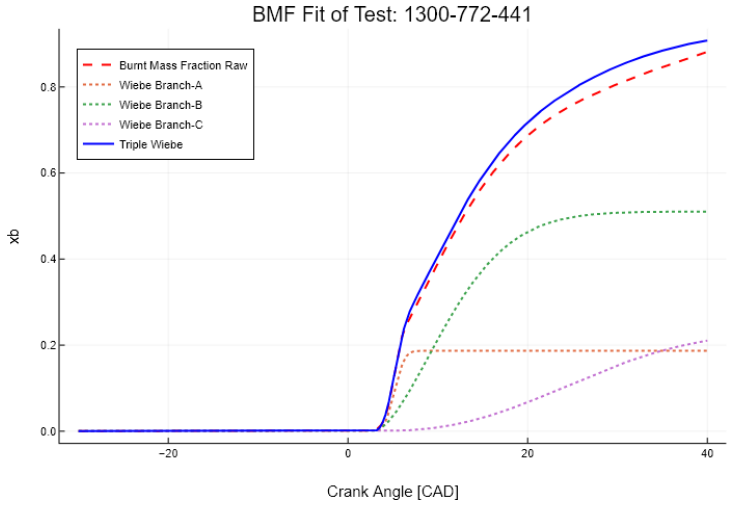

(a) Burned Mass Fraction

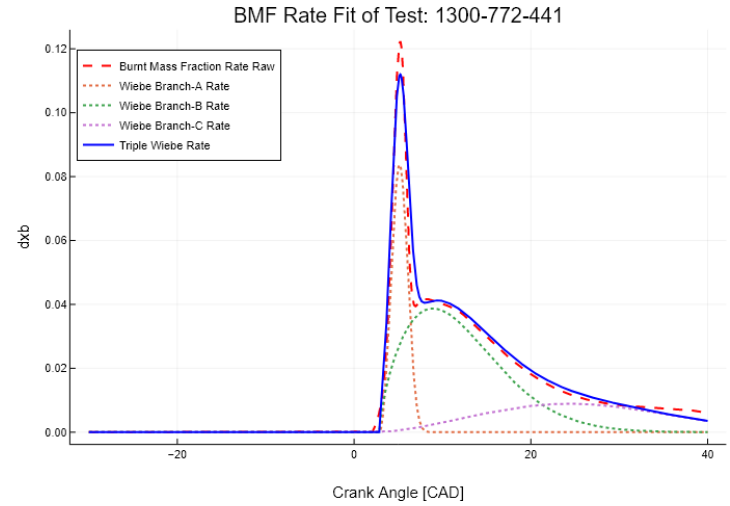

(b) Burned Mass Fraction Rate

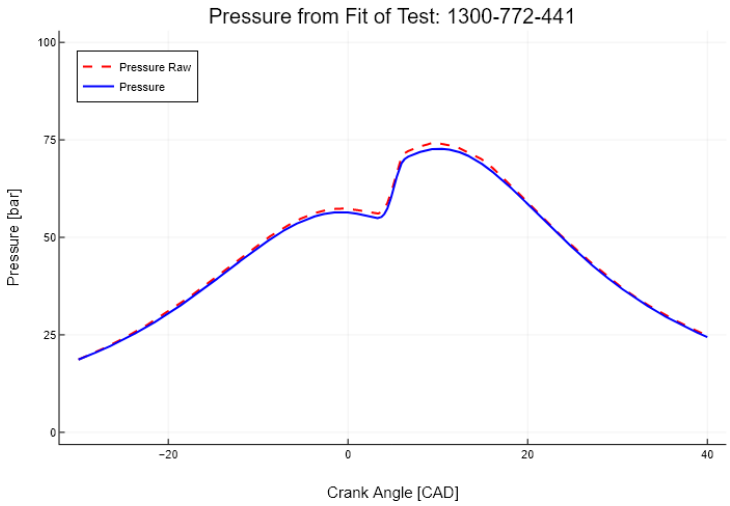

(c) Pressure

Figure C.12: Results from Initial Wiebe Fit of Test 1300-772-441

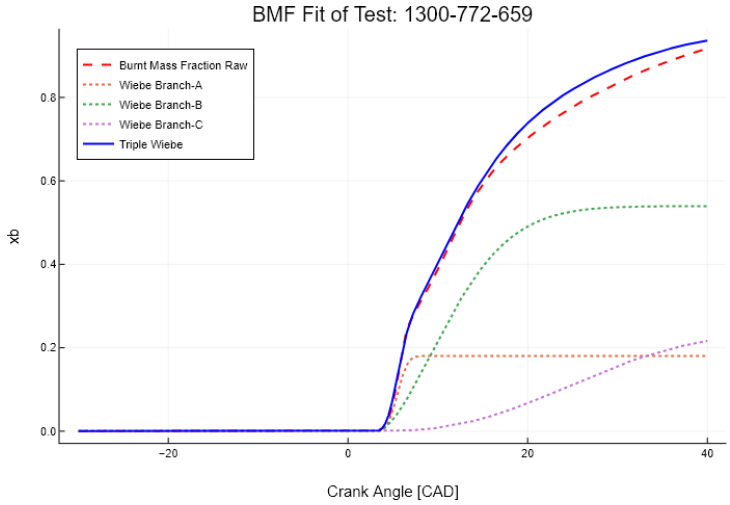

(a) Burned Mass Fraction

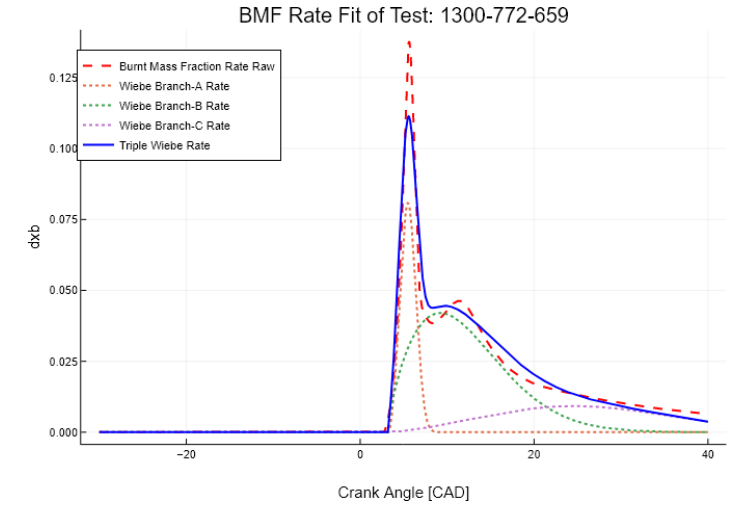

(b) Burned Mass Fraction Rate

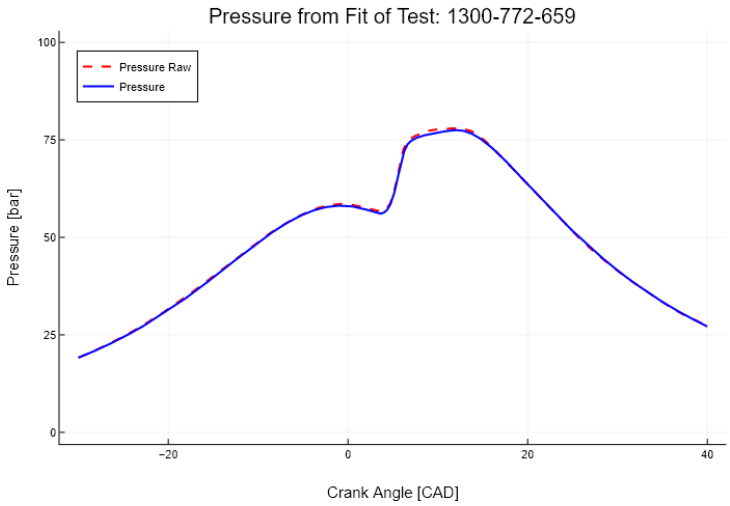

(c) Pressure

Figure C.13: Results from Initial Wiebe Fit of Test 1300-772-659

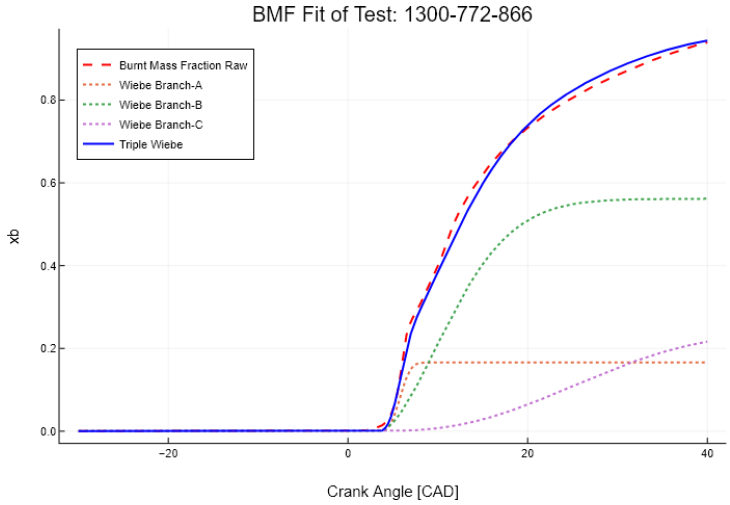

(a) Burned Mass Fraction

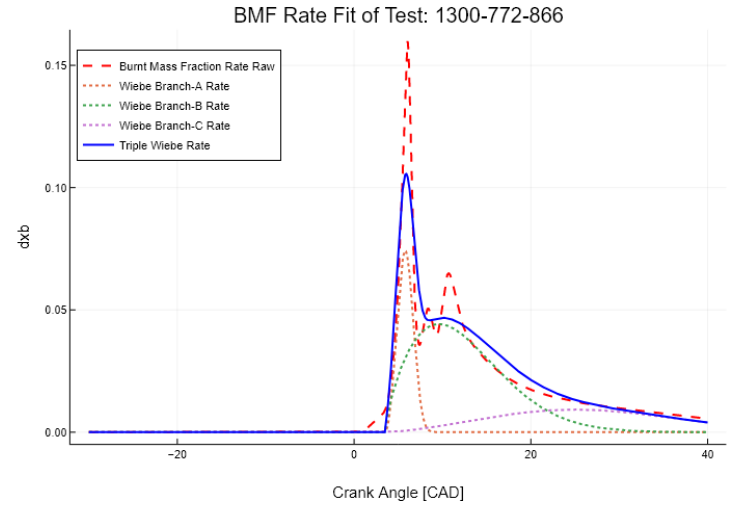

(b) Burned Mass Fraction Rate

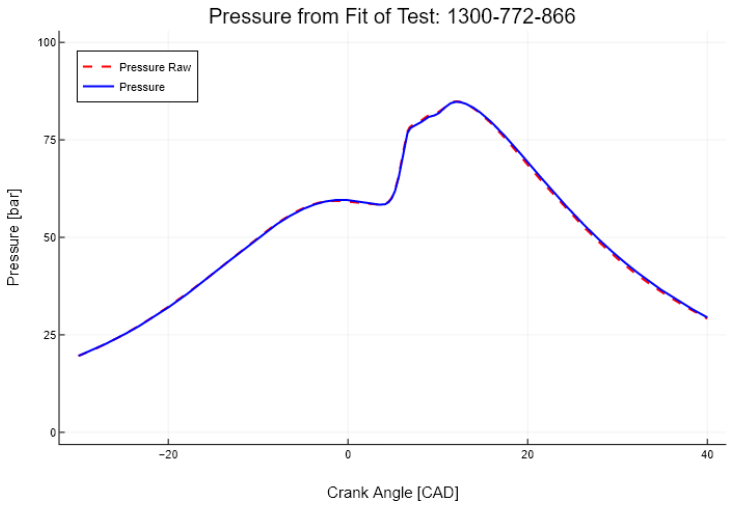

(c) Pressure

Figure C.14: Results from Initial Wiebe Fit of Test 1300-772-866

Appendix D

Final Wiebe Parameters

The Wiebe Parameters that comes from the initial wiebe function fit are exhibited in the following tables.

Wiebe Parameters of 1000 RPM Experiments							
Test Name	1000-537-0	1000-431-235	1000-334-417	1000-235-709	1000-875-0	1000-603-552	1000-476-770
BMEP [Mpa]	0.35	0.35	0.35	0.35	0.662	0.662	0.662
Speed [RPM]	1000	1000	1000	1000	1000	1000	1000
Torque [Nm]	198.86	198.86	198.86	198.86	381.97	381.97	381.97
Power [kW]	20.83	20.83	20.83	20.83	40.00	40.00	40.00
Diesel Consumption [kg/h]	5.37	4.31	3.34	2.35	8.7444	6.03	4.76
Methanol Consumption [kg/h]	0	2.35	4.17	7.09	0	5.52	7.695
Air Consumption [kg/h]	266	266	266	266	287.9	287.9	287.9
Injection Time [CAD]	-10	-10	-10	-10	-10	-10	-10
Φ Diesel	0.30	0.24	0.18	0.13	0.45	0.31	0.24
Φ Methanol	0.00	0.06	0.10	0.17	0.00	0.12	0.17
Fuel Consumption [kg/h]	5.37	6.66	7.51	9.44	8.74	11.55	12.46
θ_{ign}	-1.54	-0.67	-0.21	0.56	-3.36	-1.97	-1.52
α	6.908	6.908	6.908	6.908	6.908	6.908	6.908
$\Delta\theta_1$	5	5	5	5	5	5	5
$\Delta\theta_2$	33.8	30.5	27.83	24.853	40.12	33.29	30.22
$\Delta\theta_2$	61.31	60.06	57.31	55.63	63.84	58	54.39
m_1	2	2	2	2	2	2	2
m_2	0.895	0.969	0.982	1.029	0.603	0.66	0.659
m_3	1.5	1.5	1.5	1.5	1.5	1.5	1.5
λ_1	0.206	0.222	0.26	0.289	0.138	0.154	0.182
λ_2	0.544	0.528	0.49	0.461	0.612	0.596	0.568
λ_3	0.25	0.25	0.25	0.25	0.25	0.25	0.25
η_comb	93	95	100	100	99	100	100

Table D.1: Wiebe Parameters of 1000 RPM Experiments from Wiebe Function Fitting

Wiebe Parameters of 1300 RPM Experiments								
Test Name	1300-351-0	1300-351-369	1300-351-738	1300-351-1580	1300-772-0	1300-772-441	1300-772-659	1300-772-866
BMEP [Mpa]	0.028	0.142	0.258	0.569	0.285	0.45	0.54087	0.6
Speed [RPM]	1300	1300	1300	1300	1300	1300	1300	1300
Torque [Nm]	15.92	80.74	146.70	323.55	162.06	255.88	307.55	341.17
Power [kW]	2.17	10.99	19.97	44.05	22.06	34.83	41.87	46.45
Diesel Consumption [kg/h]	3.51	3.51	3.51	3.51	7.72	7.72	7.72	7.72
Methanol Consumption [kg/h]	0	3.69	7.38	15.8	0	4.41	6.59	8.66
Air Consumption [kg/h]	300	307	316	341	338	352	361	362
Injection Time [CAD]	-5.4	-5.4	-5.4	-5.4	-3.3	-3.3	-3.3	-3.3
Φ Diesel	0.17	0.17	0.16	0.15	0.34	0.32	0.31	0.31
Φ Methanol	0.00	0.08	0.15	0.30	0.00	0.08	0.12	0.15
Fuel Consumption [kg/h]	3.51	7.20	10.89	19.31	7.72	12.13	14.31	16.38
θ_{ign}	0.03	1.04	1.88	2.94	2.33	2.85	3.19	3.49
α	6.908	6.908	6.908	6.908	6.908	6.908	6.908	6.908
$\Delta\theta_1$	5	5	5	5	5	5	5	5
$\Delta\theta_2$	31.42	29.63	27.81	25.53	34.119	32.19	31.16	30.56
$\Delta\theta_2$	55.185	57.13	58.08	55.86	58.1854	57.1	56.89	57.33
m_1	2	2	2	2	2	2	2	2
m_2	0.788	0.901	0.985	0.896	0.693	0.693	0.709	0.735
m_3	1.5	1.5	1.5	1.5	1.5	1.5	1.5	1.5
λ_1	0.355	0.319	0.297	0.237	0.226	0.201	0.188	0.171
λ_2	0.395	0.431	0.238	0.513	0.524	0.549	0.562	0.579
λ_3	0.25	0.25	0.465	0.25	0.25	0.25	0.25	0.25
η_comb	100	92	93.5	100	88	93	96	97

Table D.2: Wiebe Parameters of 1000 RPM Experiments from Wiebe Function Fitting

Appendix E

Combustion Model Validation

In this chapter, the rest figures from the Combustion Model Validation are presented.

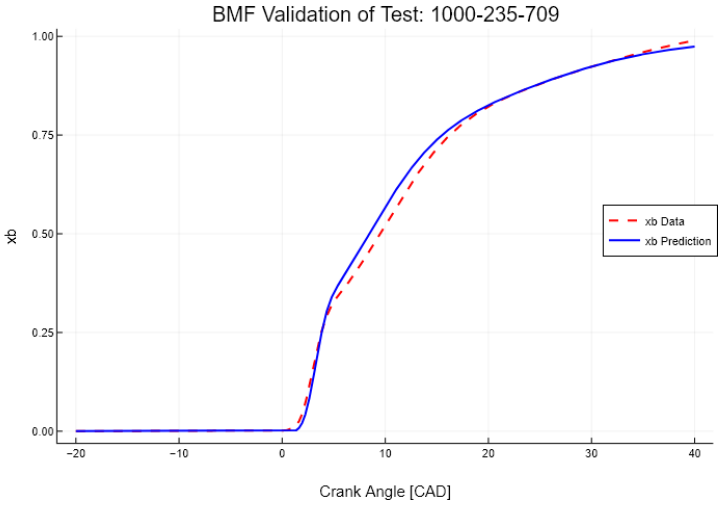

(a) Burned Mass Fraction

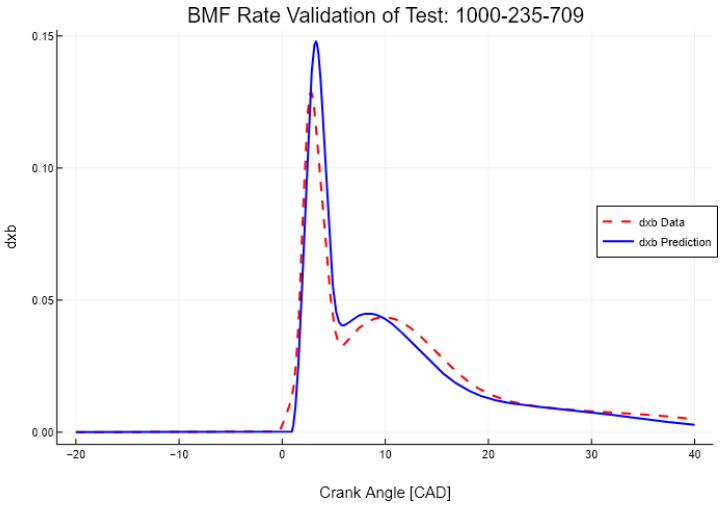

(b) Burned Mass Fraction Rate

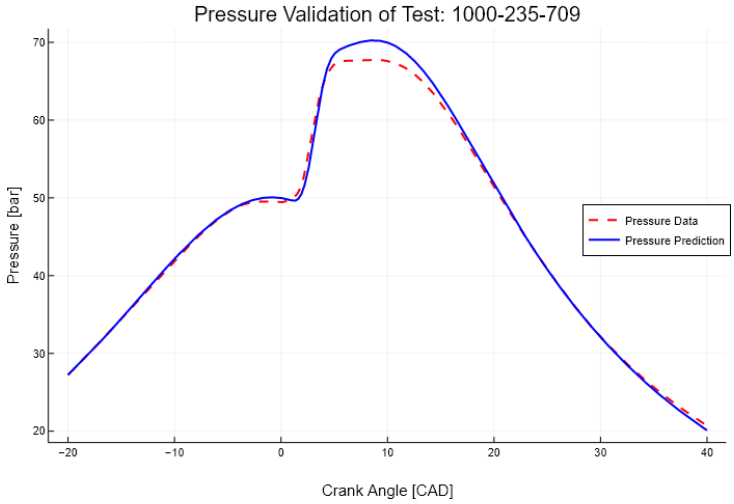

(c) Pressure

Figure E.1: Combustion Model Validation with Test 1000-235-709

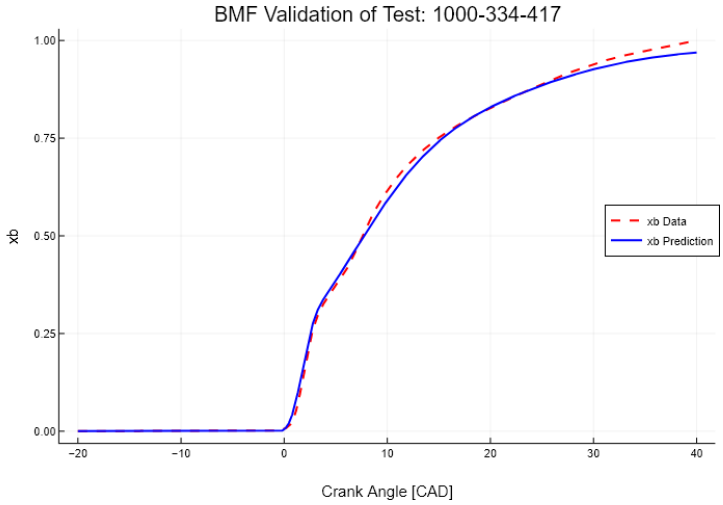

(a) Burned Mass Fraction

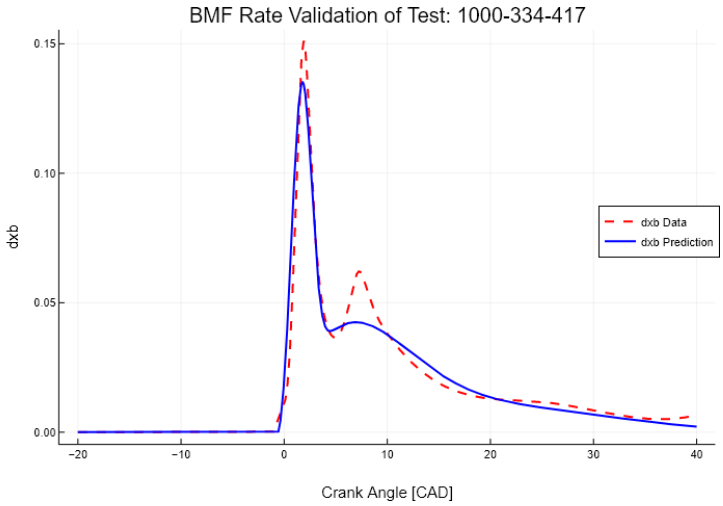

(b) Burned Mass Fraction Rate

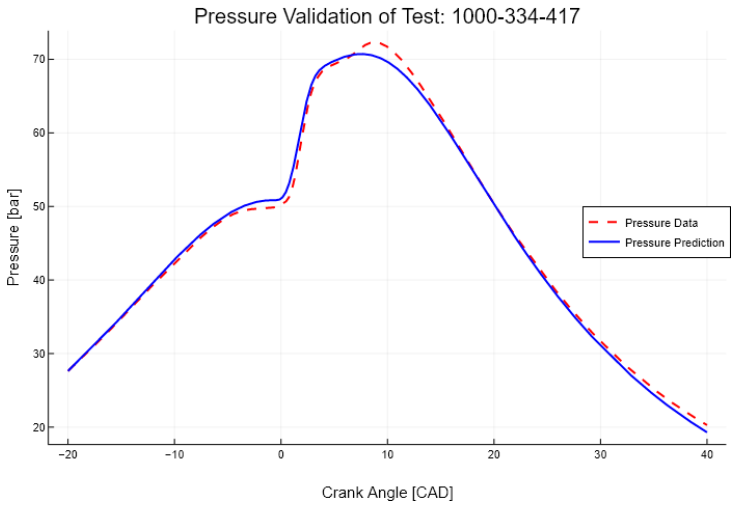

(c) Pressure

Figure E.2: Combustion Model Validation with Test 1000-334-417

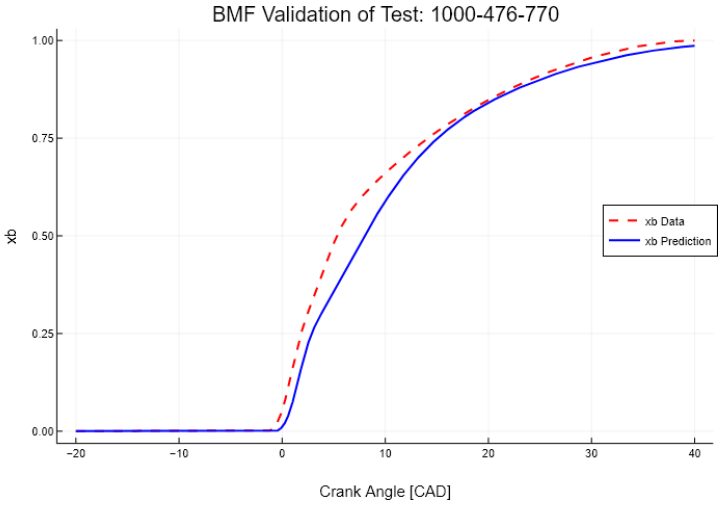

(a) Burned Mass Fraction

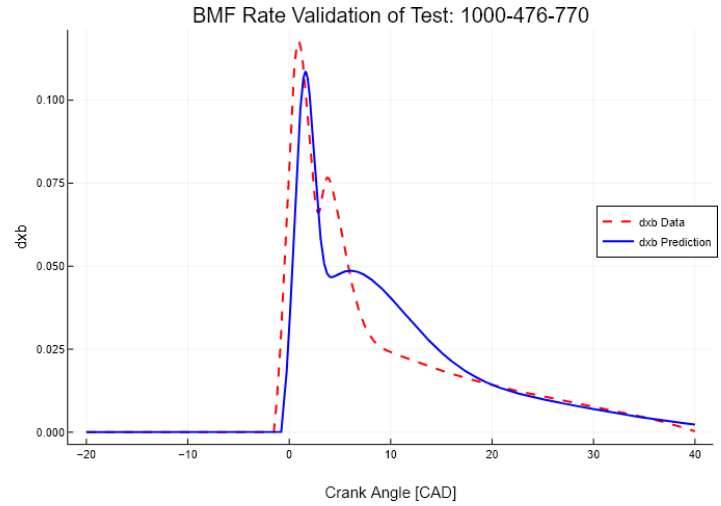

(b) Burned Mass Fraction Rate

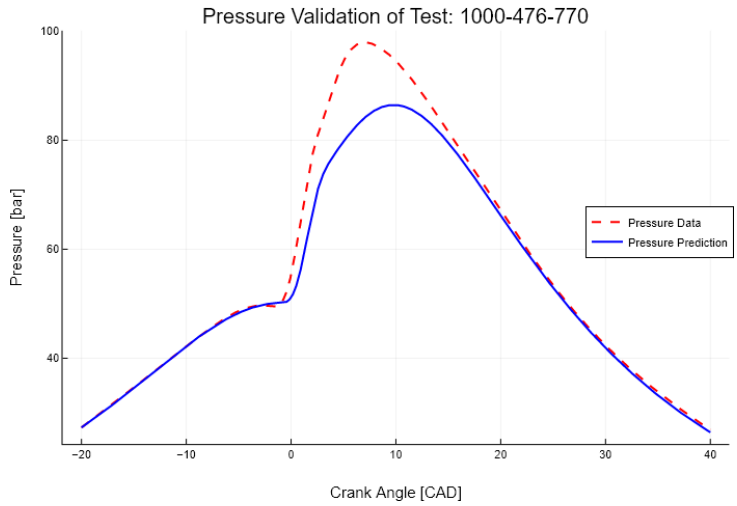

(c) Pressure

Figure E.3: Combustion Model Validation with Test 1000-476-770

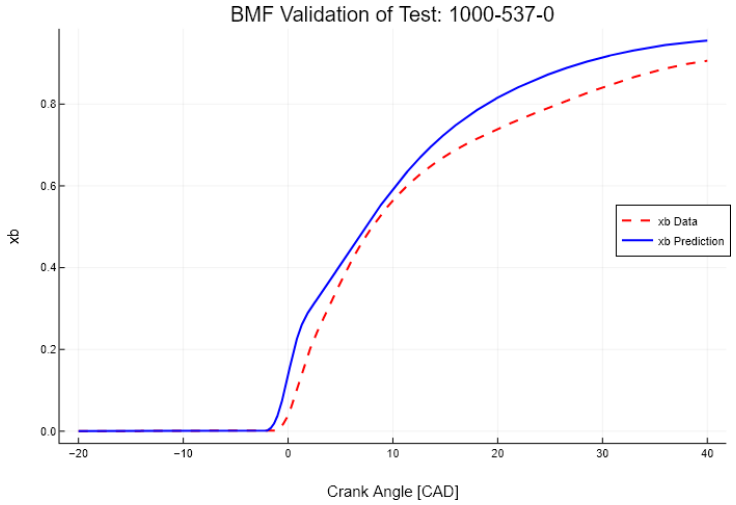

(a) Burned Mass Fraction

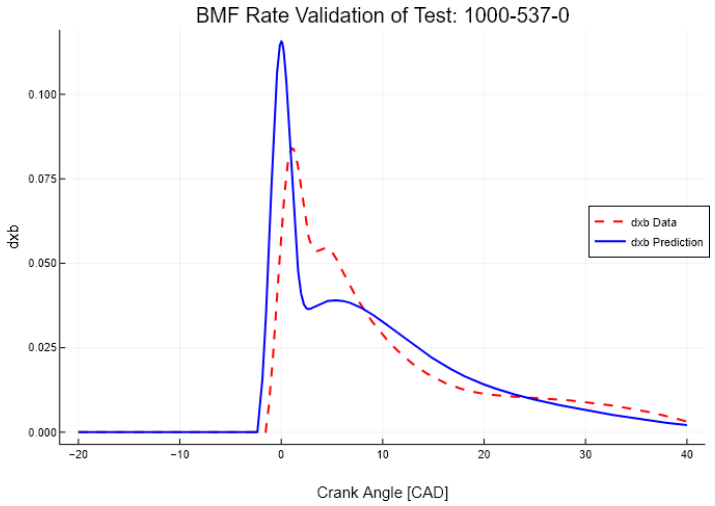

(b) Burned Mass Fraction Rate

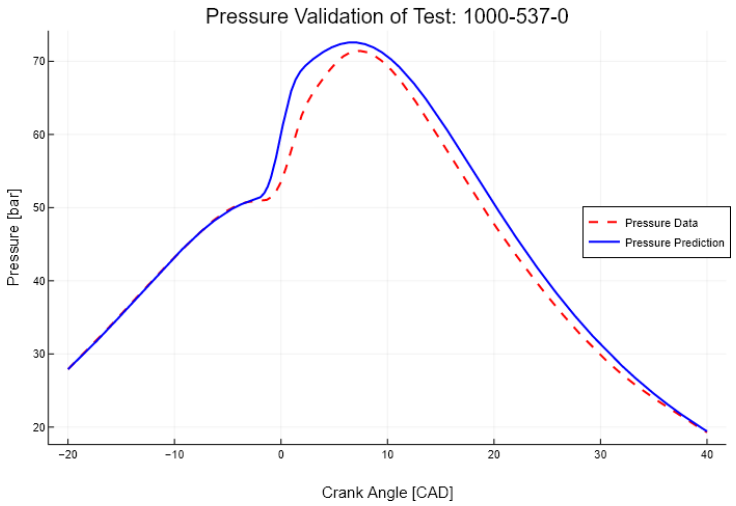

(c) Pressure

Figure E.4: Combustion Model Validation with Test 1000-537-0

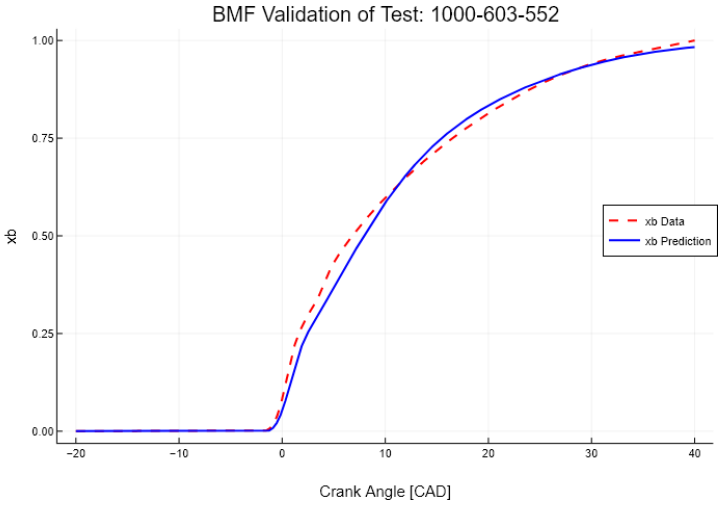

(a) Burned Mass Fraction

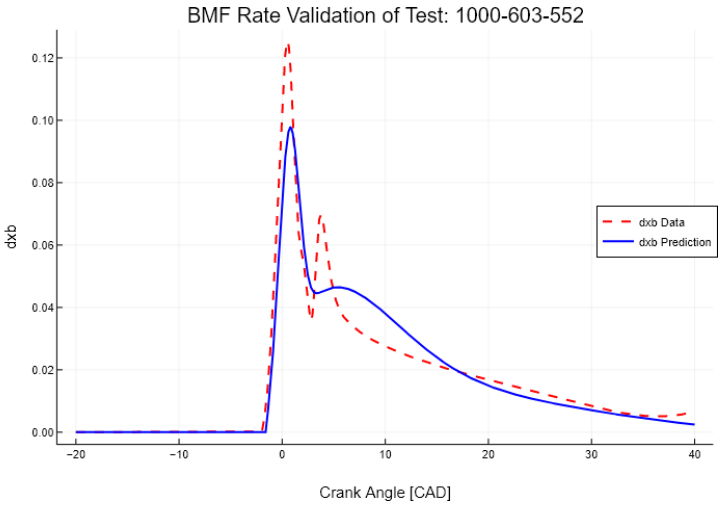

(b) Burned Mass Fraction Rate

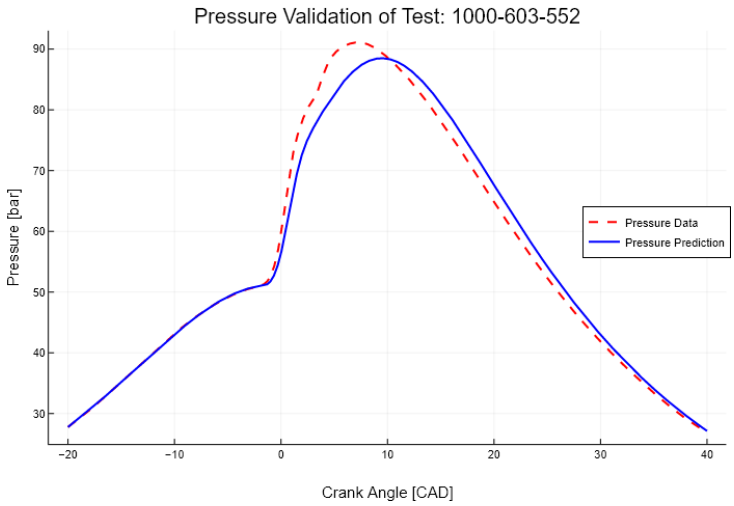

(c) Pressure

Figure E.5: Combustion Model Validation with Test 1000-603-552

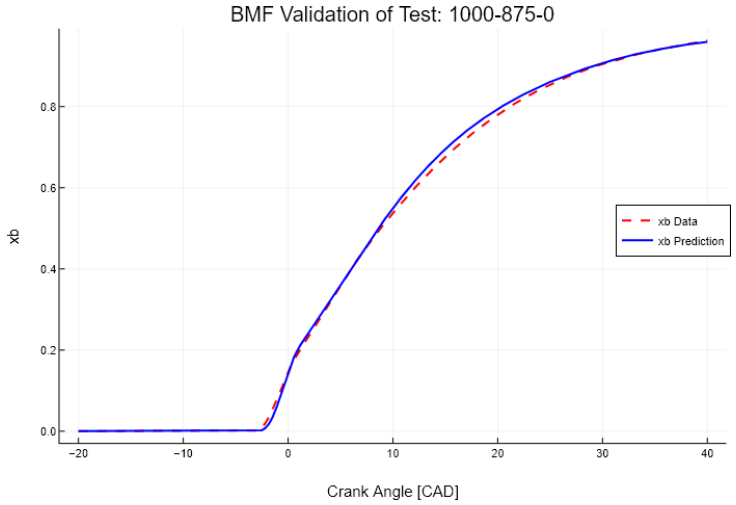

(a) Burned Mass Fraction

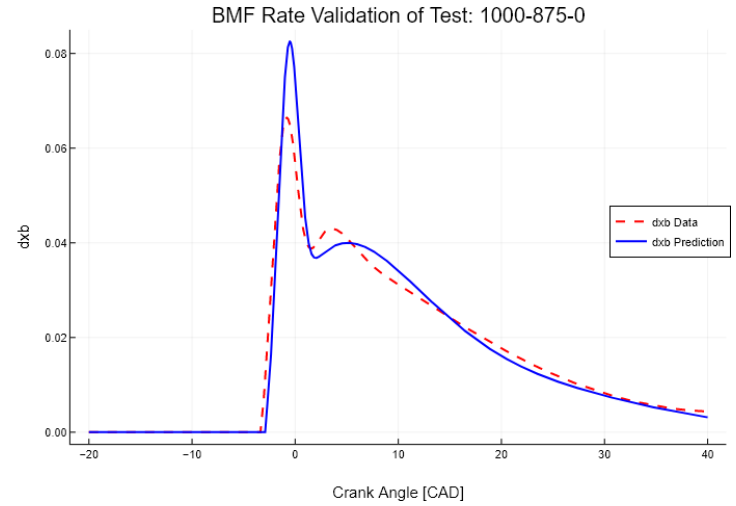

(b) Burned Mass Fraction Rate

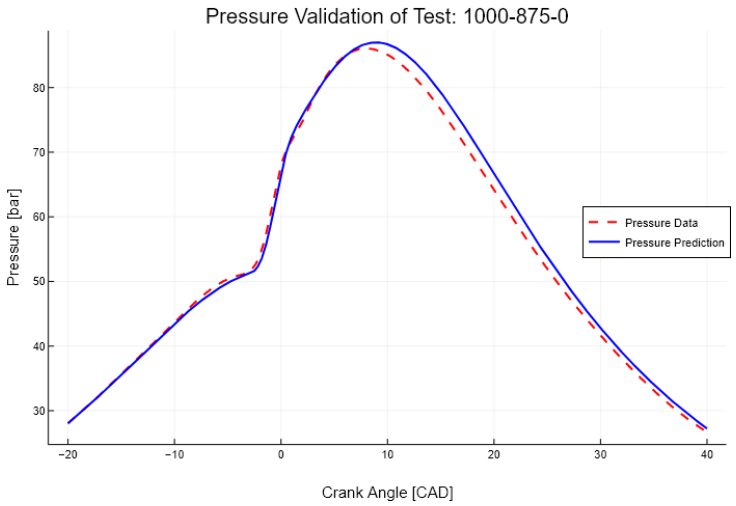

(c) Pressure

Figure E.6: Combustion Model Validation with Test 1000-875-0

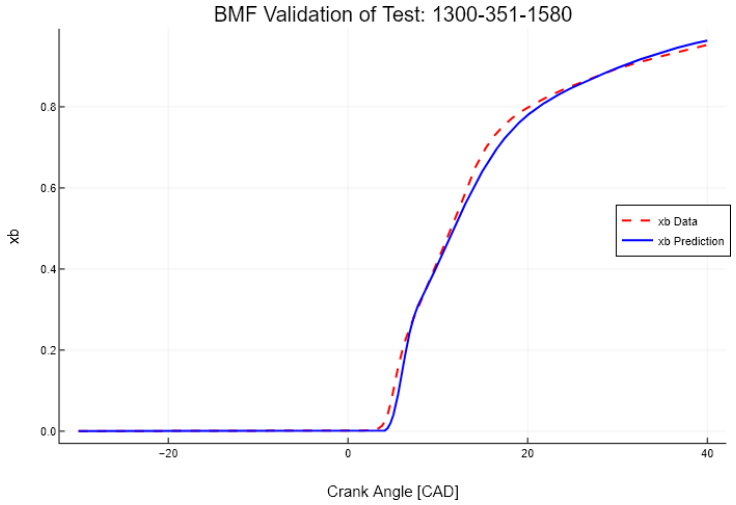

(a) Burned Mass Fraction

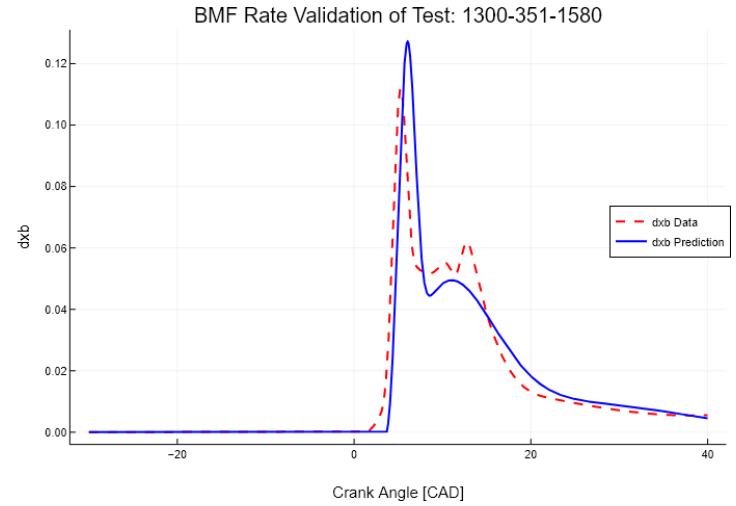

(b) Burned Mass Fraction Rate

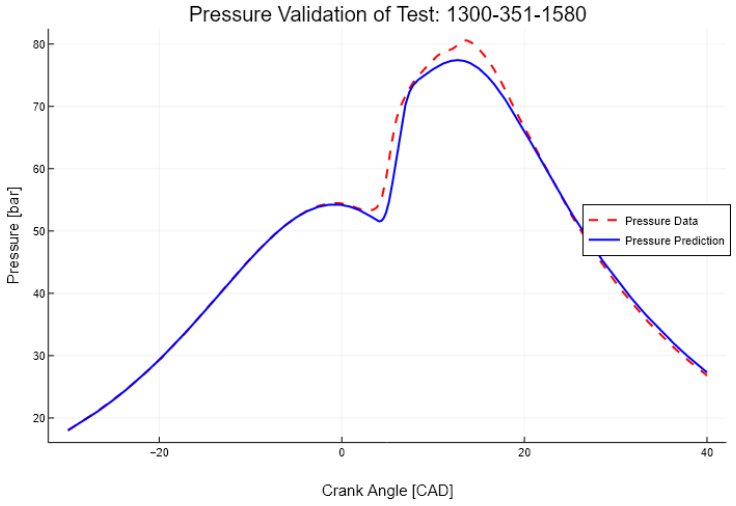

(c) Pressure

Figure E.7: Combustion Model Validation with Test 1300-351-1580

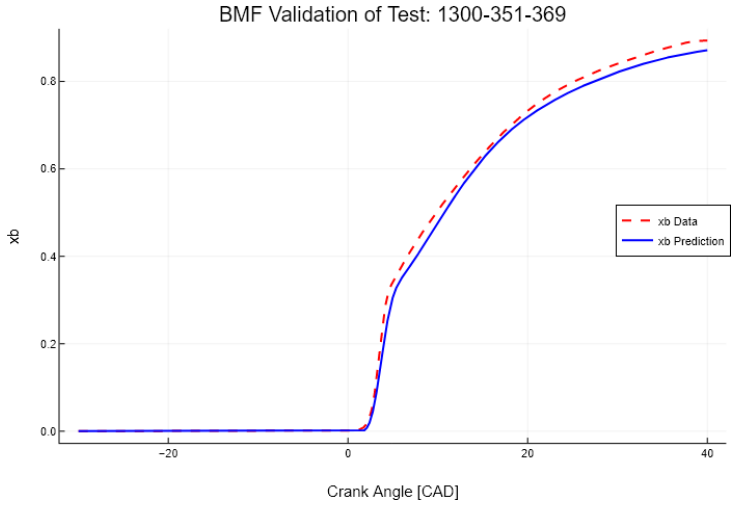

(a) Burned Mass Fraction

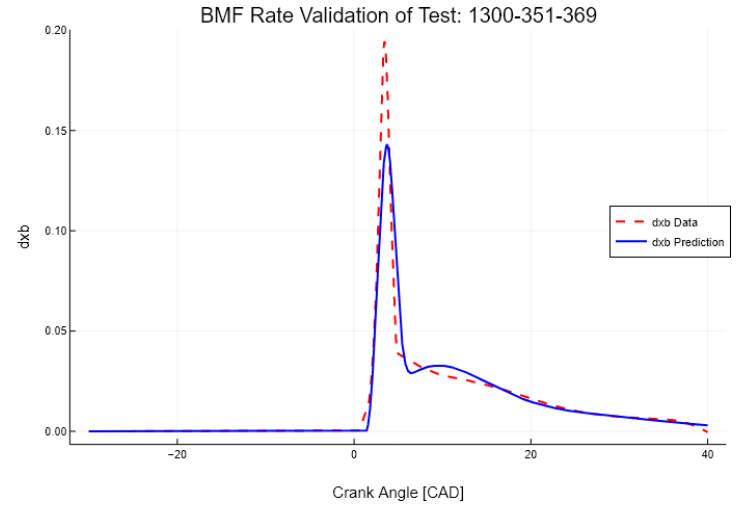

(b) Burned Mass Fraction Rate

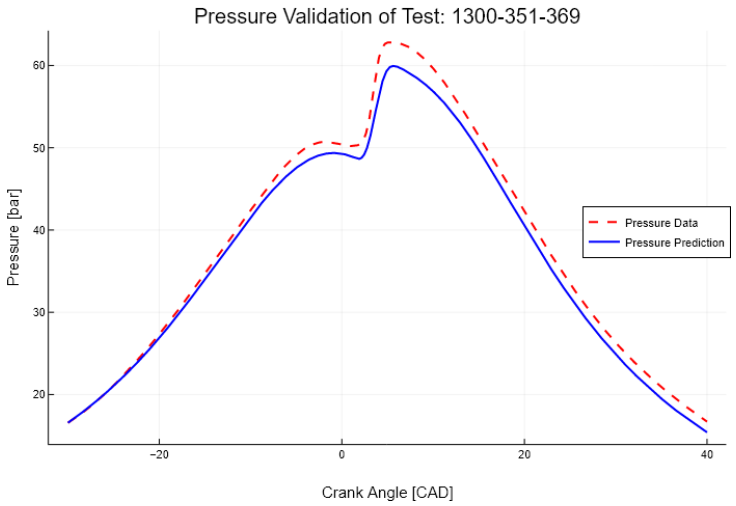

(c) Pressure

Figure E.8: Combustion Model Validation with Test 1300-351-369

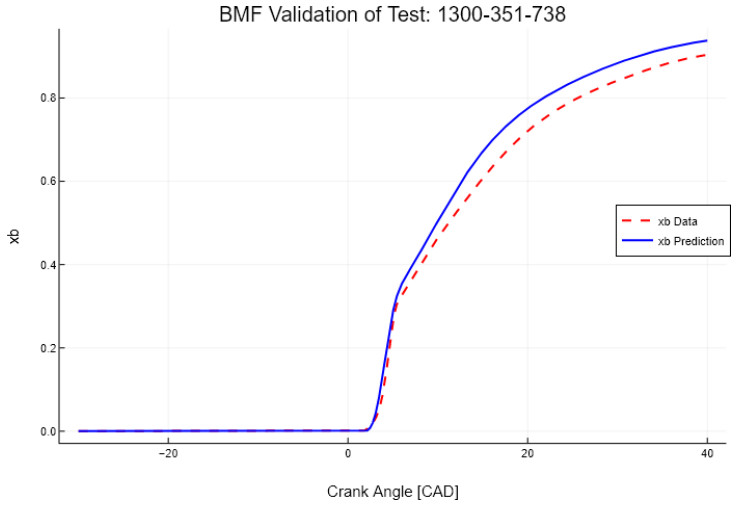

(a) Burned Mass Fraction

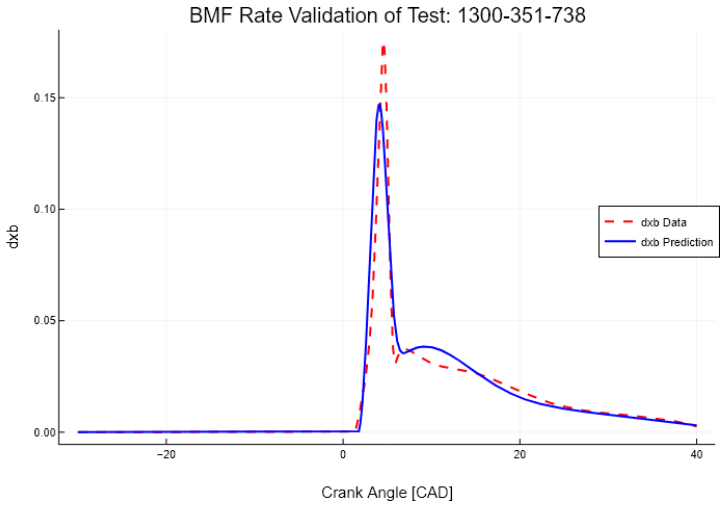

(b) Burned Mass Fraction Rate

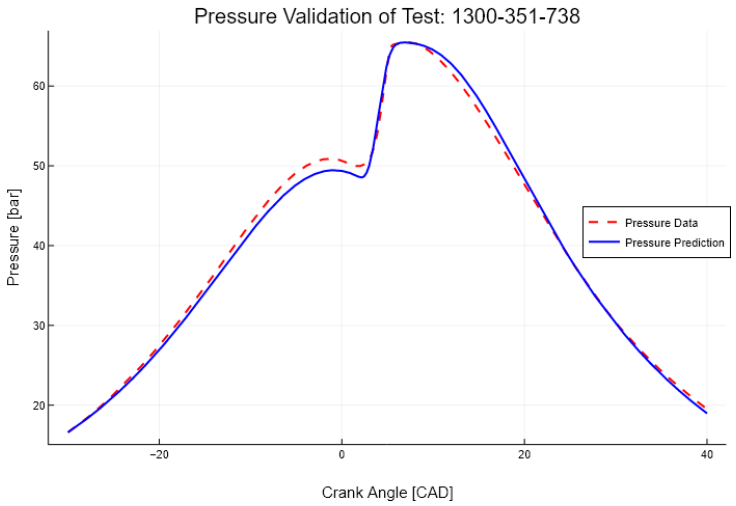

(c) Pressure

Figure E.9: Combustion Model Validation with Test 1300-351-738

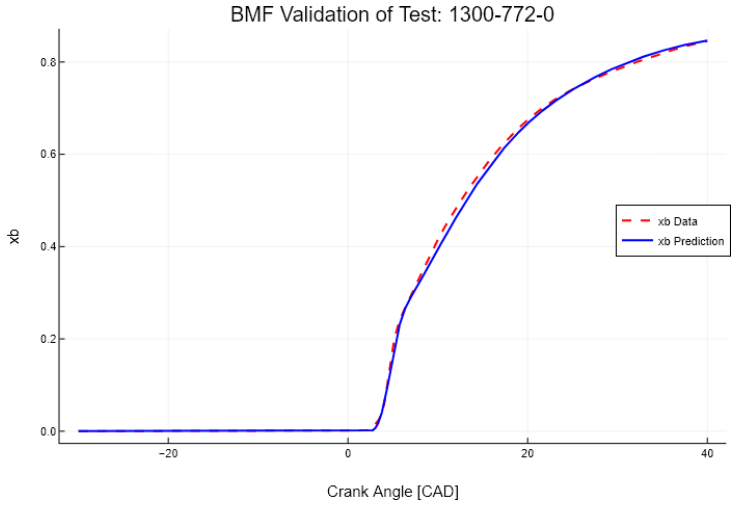

(a) Burned Mass Fraction

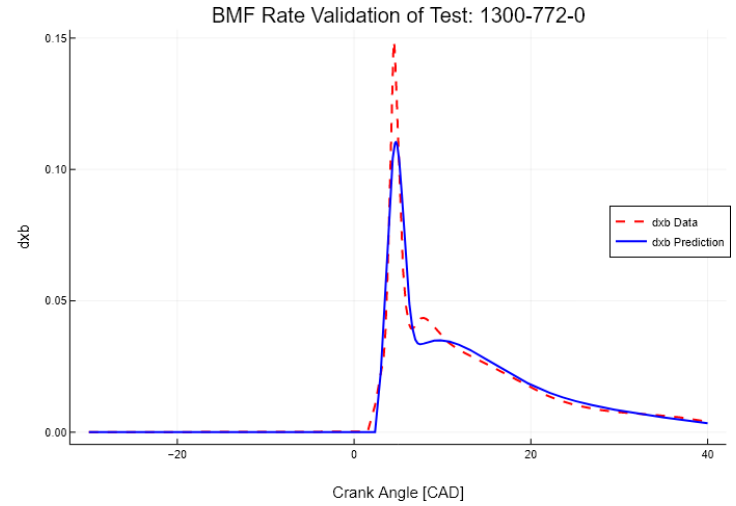

(b) Burned Mass Fraction Rate

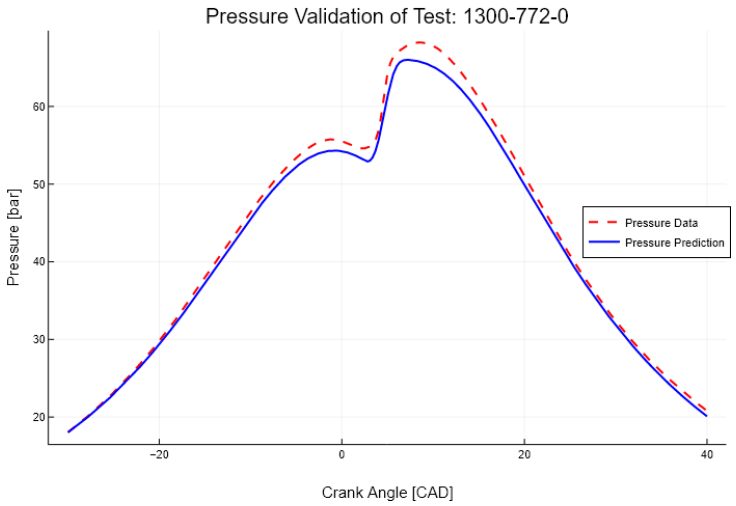

(c) Pressure

Figure E.10: Combustion Model Validation with Test 1300-772-0

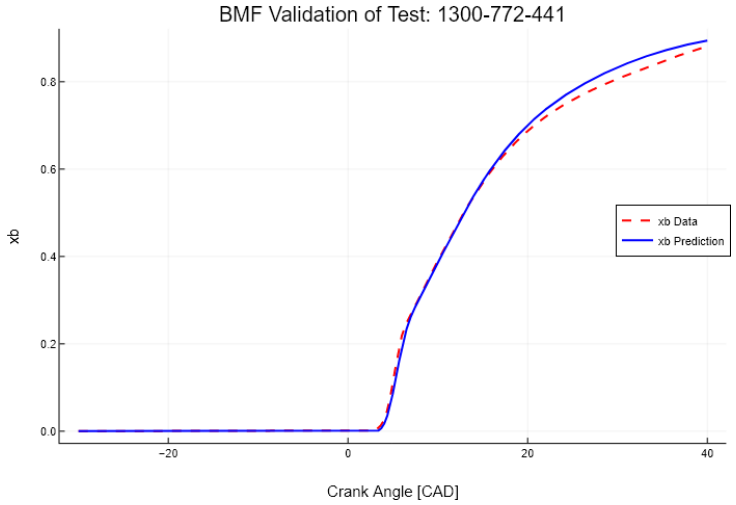

(a) Burned Mass Fraction

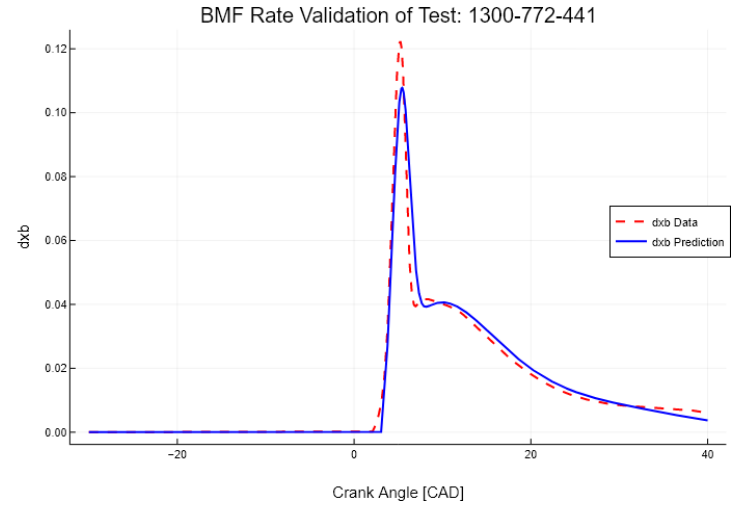

(b) Burned Mass Fraction Rate

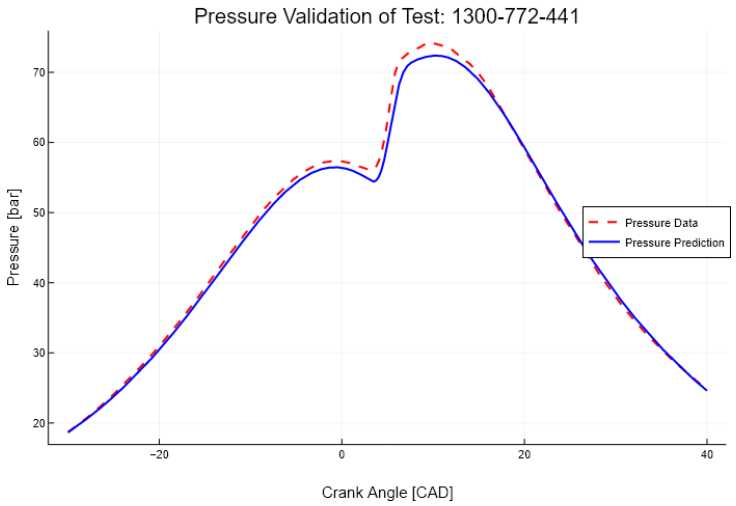

(c) Pressure

Figure E.11: Combustion Model Validation with Test 1300-772-441

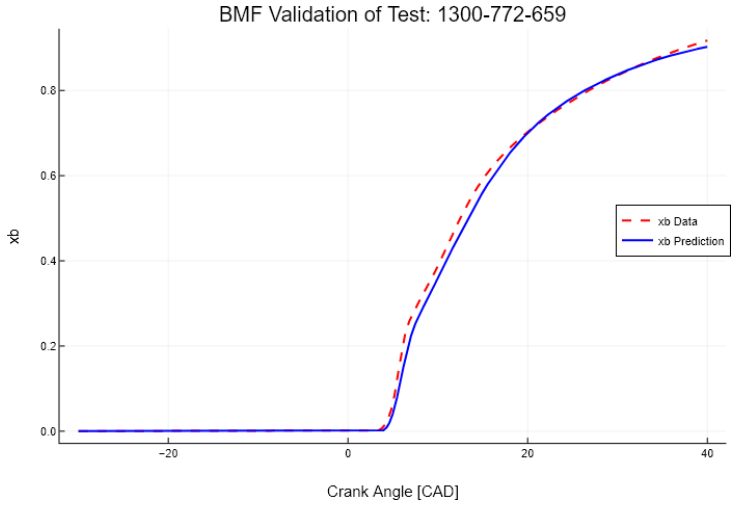

(a) Burned Mass Fraction

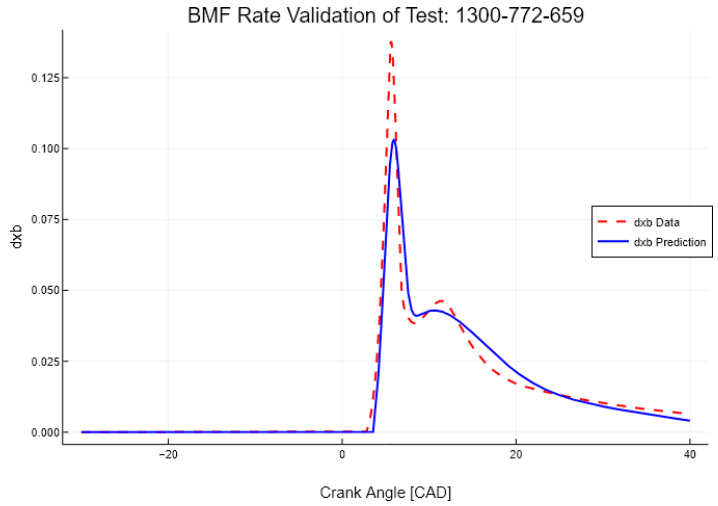

(b) Burned Mass Fraction Rate

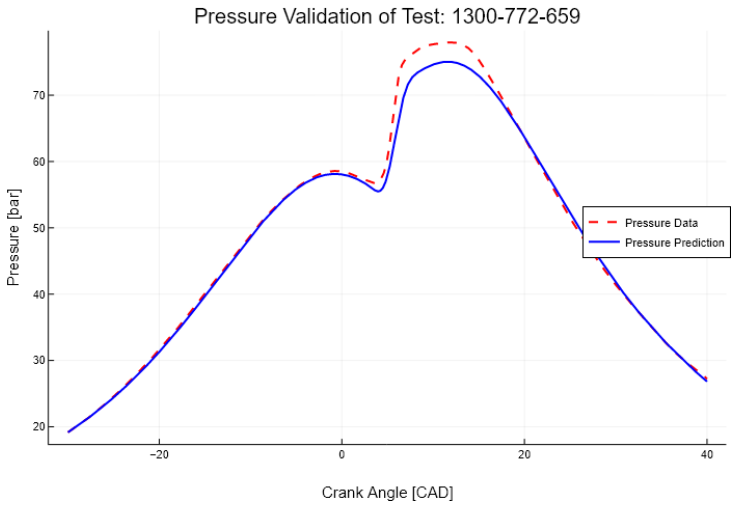

(c) Pressure

Figure E.12: Combustion Model Validation with Test 1300-772-659

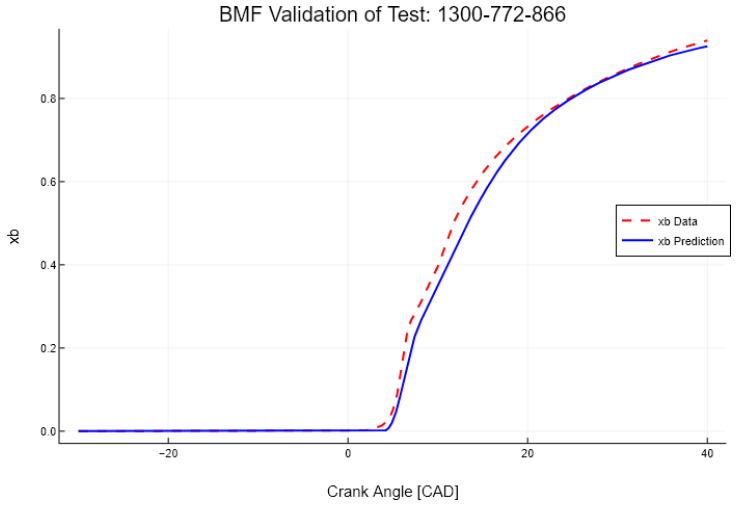

(a) Burned Mass Fraction

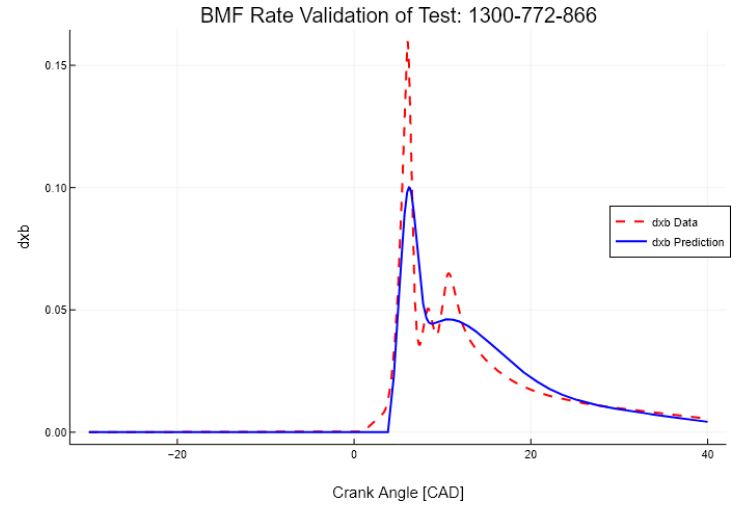

(b) Burned Mass Fraction Rate

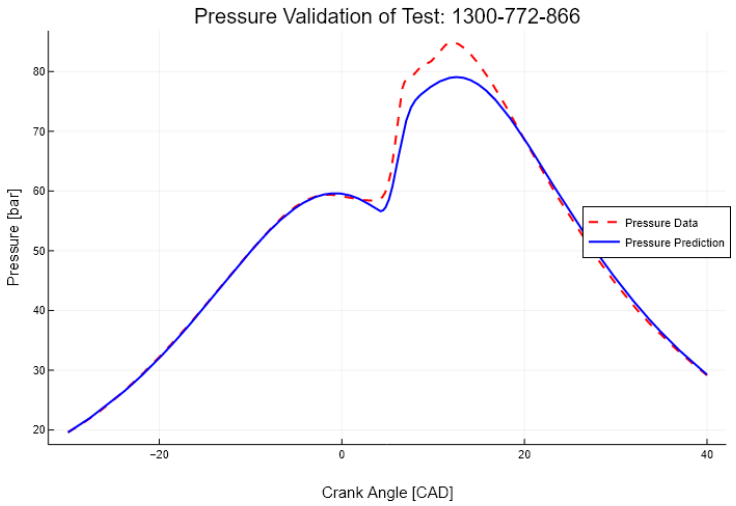

(c) Pressure

Figure E.13: Combustion Model Validation with Test 1300-772-866

Appendix F

Combustion Model Validation

In this chapter, the rest figures from the Combustion Model Validation with non calibrating data are presented.

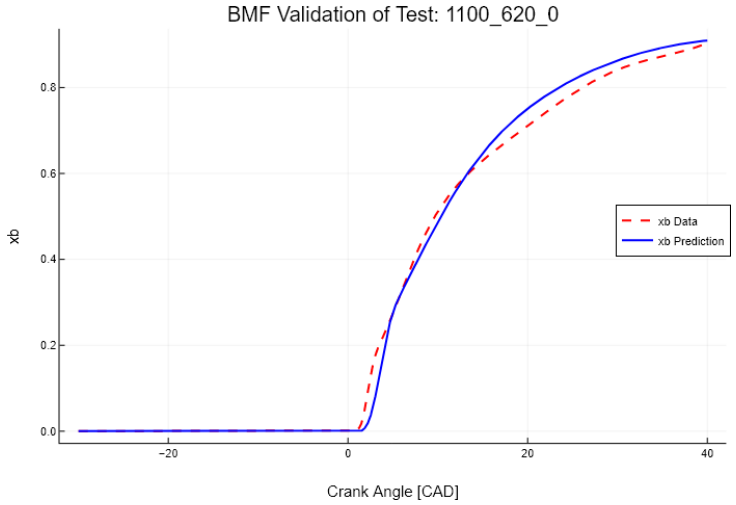

(a) Burned Mass Fraction

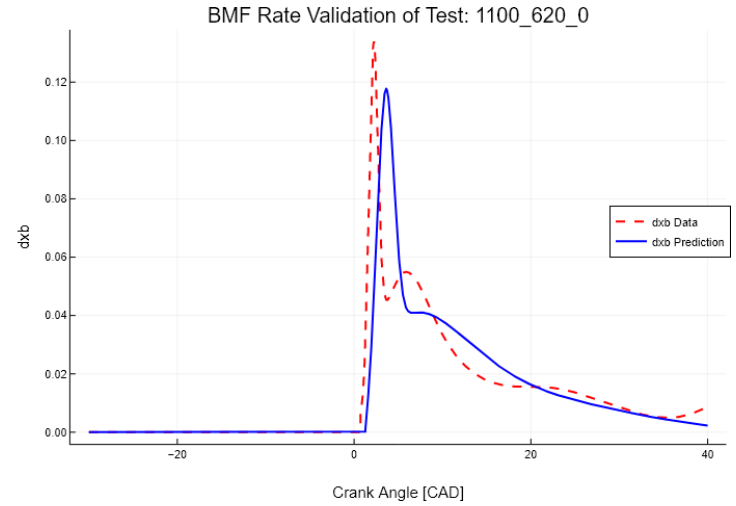

(b) Burned Mass Fraction Rate

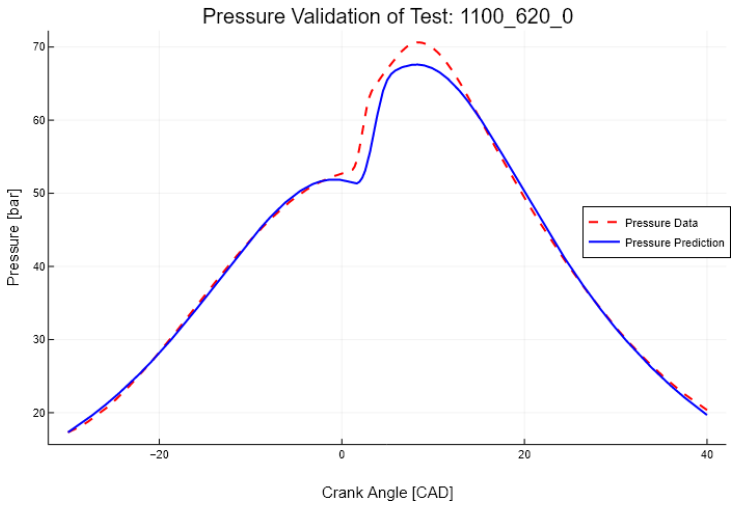

(c) Pressure

Figure F.1: Combustion Model Validation with Test 1100-620-0

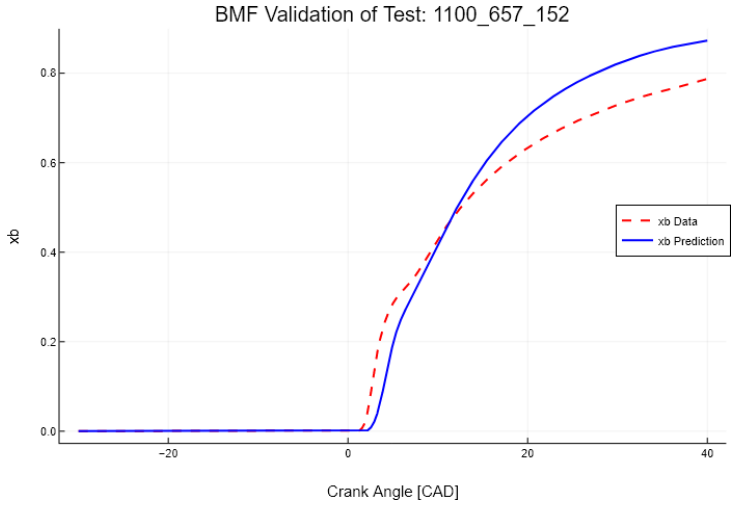

(a) Burned Mass Fraction

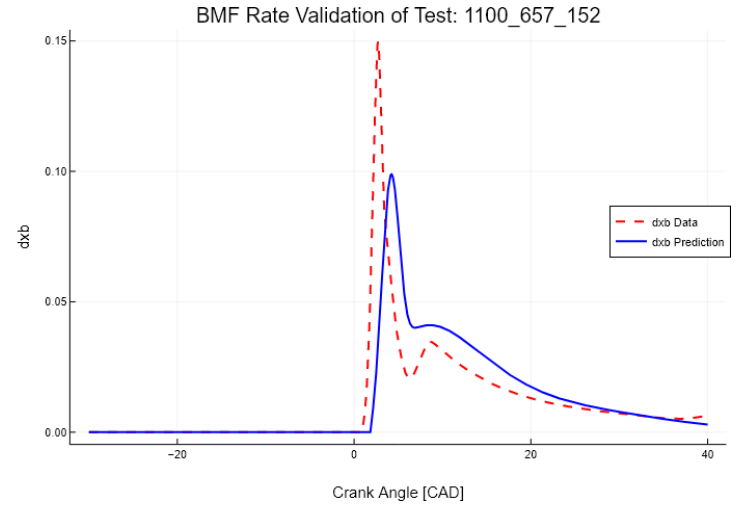

(b) Burned Mass Fraction Rate

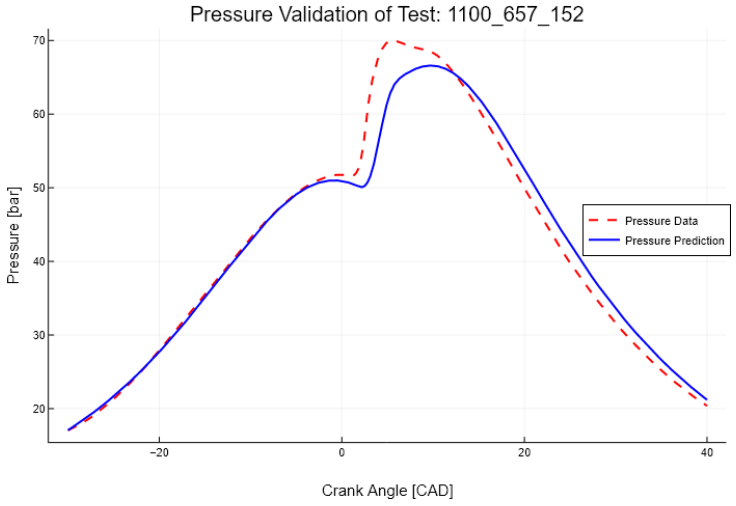

(c) Pressure

Figure F.2: Combustion Model Validation with Test 1100-657-152

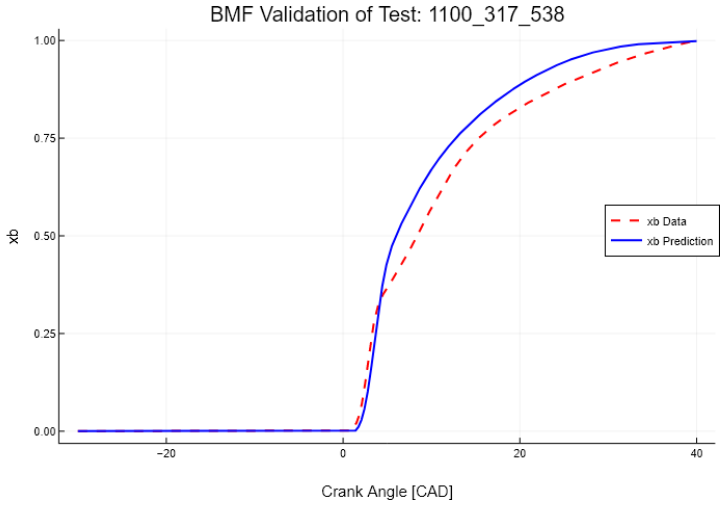

(a) Burned Mass Fraction

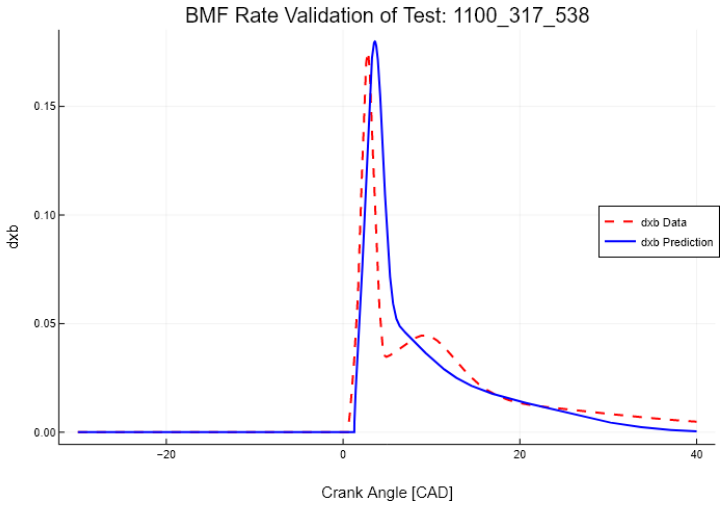

(b) Burned Mass Fraction Rate

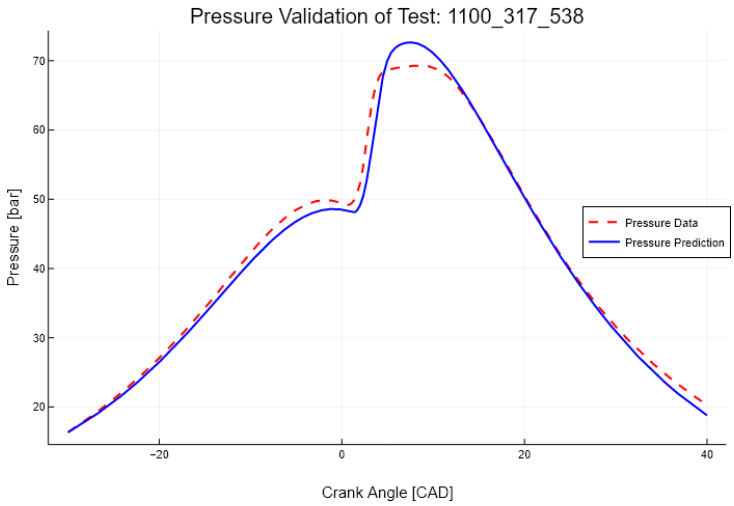

(c) Pressure

Figure F.3: Combustion Model Validation with Test 1100-317-538

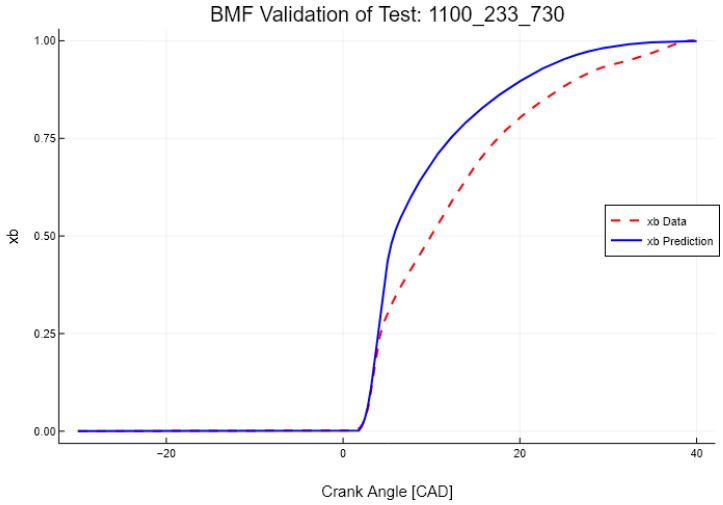

(a) Burned Mass Fraction

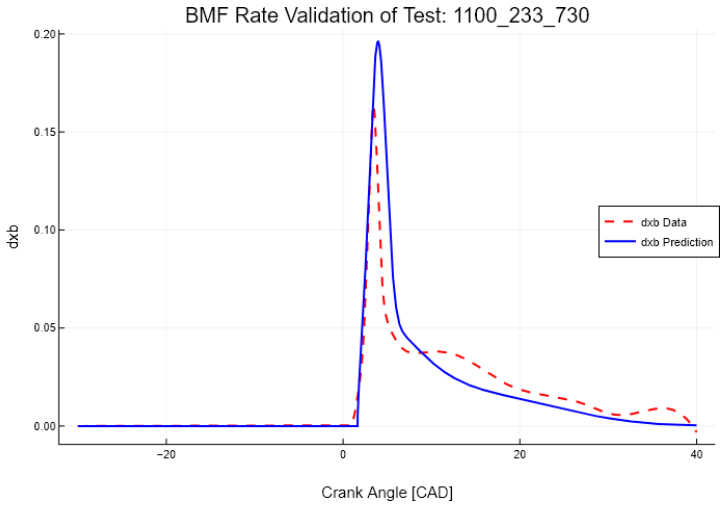

(b) Burned Mass Fraction Rate

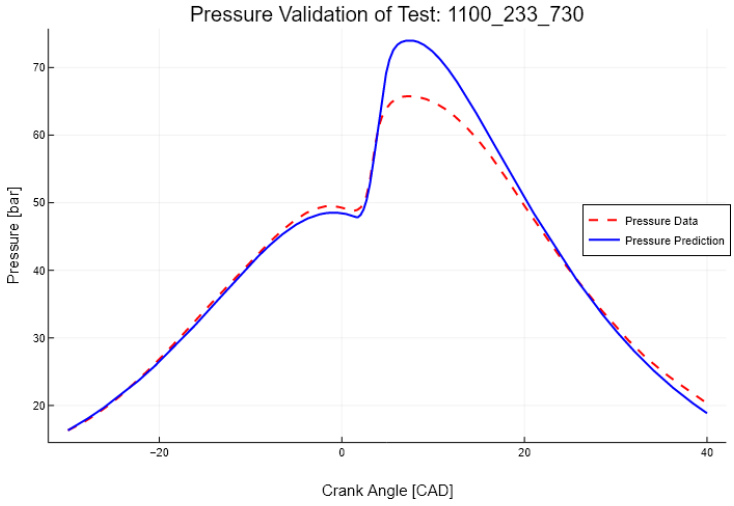

(c) Pressure

Figure F.4: Combustion Model Validation with Test 1100-233-730